INTERNATIONAL JOURNAL OF AVIATION SCIENCE AND TECHNOLOGY
IJAST
www.ijast.org

International Journal of Aviation Science and Technology

Volume 4, Issue 2, December 2023

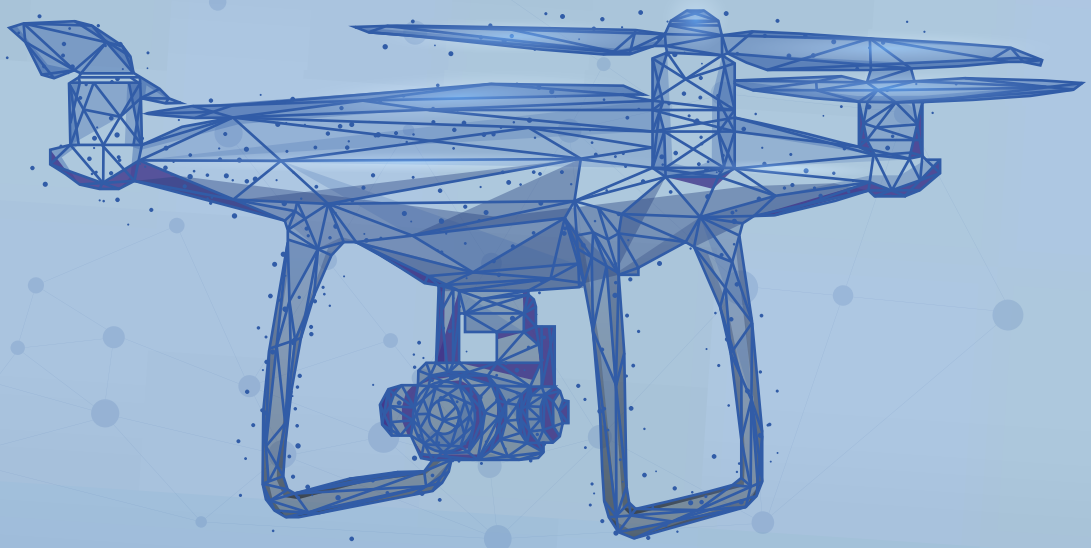

e-ISSN: 2687-525X
INTERNATIONAL SUSTAINABLE AVIATION AND ENERGY RESEARCH SOCIETY
SARES
www.sares.org

International Journal of Aviation Science and Technology

Publisher : SARES
International Sustainable Aviation and Energy Research Society
License holder : Prof. Dr. T. Hikmet Karakoç (President, SARES)
Address : Research and Application Center of Civil Aviation, Research Centers Building, Eskisehir Technical University, Eskisehir, Türkiye

e-ISSN : 2687-525X
DOI : 10.23890/IJAST
web : www.ijast.org
submission : DergiPark-IJAST
e-mail : ijast@sares.org
Copyright : SARES Society

The IJAST journal is being published with the contribution of "Research and Application Center of Civil Aviation, Eskisehir Technical University."

Index

International Journal of Aviation Science and Technology

Research Article

Investigation on the Airworthiness of a Novel Tri-Rotor Configuration for a Fixed Wing VTOL Aircraft

António Arco[1*], José Lobo Do Vale[2], Sean Bazzocchi[3], Afzal Suleman[4]

[1] *University of Lisbon, Lisbon, Portugal*
antonio.arco@tecnico.ulisboa.pt - 0000-0002-1403-4645
[2] *University of Victoria, British Columbia, Canada*
oselobodovale.cfar@gmail.com - 0000-0002-0360-9570
[3] *University of Victoria, British Columbia, Canada*
sean.bazzocchi@gmail.com - 0000-0001-9776-0695
[4] *University of Victoria, British Columbia, Canada*
suleman@uvic.ca - 0000-0001-8936-7340

Abstract

In this paper, a novel tri-rotor configuration is proposed with the goal of granting vertical take-off and landing capabilities to a future concept of tiltrotor, fixed-wing, aircraft while minimizing the overall mass of the propulsive system and the amount of aerodynamic drag developed during horizontal flight. The novelty of the presented configuration is related not only to the thrust vectoring capabilities of all three rotors but also to the constraints surrounding the action of the rear rotor, which will be required to provide thrust during both vertical and horizontal flight stages while drawing power from an internal combustion engine fixed inside the aircraft's fuselage. Another distinctive feature of the proposed configuration is related to the 20/80 thrust distribution which exists between the front and rear rotors respectively in vertical flight, unlike the more conventional approach of having all three rotors evenly loaded. The proposed rotorcraft configuration was then translated into a test vehicle which was subjected to several stages of ground and flight testing, with the ultimate goal of evaluating the airworthiness of this multi-rotor configuration as a concept. This process also encompasses the development of a custom flight control firmware in PX4, required to operate not only this vehicle but also any other multi-rotor or Vertical Take-Off and Landing system with such configuration. Finally, a frequency-response based system identification technique is applied to the collected flight data as to obtain a suitable flight dynamics model for future autopilot tuning

Keywords

Unmanned Aerial Vehicle
Vertical Take-Off and Landing
Tilt-rotor
Tri-rotor
System Identification

Time Scale of Article

Received 9 May 2023
Revised to 6 November 2023
Accepted 10 November 2023
Online date 30 December 2023

1. Introduction

One of the most prominent topics within the current aerospace engineering paradigm revolves around the development of hybrid aircraft concepts which combine the horizontal flight speed and efficiency of fixed-wing (FW) vehicles with the flexibility of executing Vertical Take-Off and Landing (VTOL) and steady hovering manoeuvres, attributes that were, until recently, reserved for rotary wing vehicles such as helicopters and multicopters. As the topic of Urban Air Mobility gains momentum, and with a growing interest, especially by the military, in unmanned aircraft which incorporate the aforementioned characteristics, investigation into the development of novel configurations of VTOL aircraft designs presents an unprecedented level of relevance.

*: Corresponding Author António Arco, antonio.arco@tecnico.ulisboa.pt
DOI: 10.23890/IJAST.vm04is02.0201

Several possible platforms of hybrid (FW+VTOL) aircraft have been proposed over the years through concepts for both manned and unmanned aviation. The multiple suggested configurations can, in general, be grouped in two broad categories (Saeed et al., 2018): tail-sitters and convertiplanes. Tail-sitters usually present a fixed propulsion system, i.e., without thrust vectoring capabilities, relying on a complete change of the airframe's orientation throughout the different mission segments. As so, aircraft of this kind usually take-off and land with the airframe in a vertical stance and then, to achieve forward flight, execute a complete tilting maneuver of the aircraft's body. On the other hand, the usually called convertiplanes maintain their airframe orientation throughout the mission (usually horizontal or at a pitch angle within the flight envelope of the aircraft), relying on propulsion systems with thrust vectoring capabilities (e.g.: tilt-rotor, tilt-wing, tilt-prop) or separate, segregated systems to deal with the vertical and horizontal flight stages of the mission as happens with Lift+Cruise configurations (Goetzendorf-Grabowski et al., 2020).

The multi-rotor propulsive system configuration proposed in this paper is the result of a series of design constraints which were imposed during the conceptual design of the new, canard configuration, fixed-wing, unmanned aerial vehicle (UAV) for which such a system is being devised (Fig. 1). The main requirement and motivation for this investigation is that the vehicle should be capable of performing VTOL manoeuvres, as well as being able to hover steadily upon request. With respect to the categorization presented above, this vehicle shall be classified as a convertiplane.

The propulsive system was conceptualized in a way that the two front rotors are to be powered by electric motors, with the frontal arms on which these are mounted retrieving into the fuselage of the aircraft during horizontal flight to optimize the aerodynamic efficiency of the vehicle (note that the design of the fixed-wing aircraft is out of the scope of this work and has already been explored previously in Pedro et al., 2021). The front rotors are meant to operate only in the vertical flight stages and are responsible for generating, in nominal flight conditions, around 10% of the total vertical thrust required to hover (i.e., enough thrust to balance 10% of the total aircraft's weight each). The third, rear tilting rotor, which will provide thrust in both the vertical and horizontal stints of the aircraft's mission should, in its term, be powered by an internal combustion engine. This engine is to be fixed inside the aircraft's fuselage, in such a way that the rear rotor, responsible for generating enough thrust to balance the remaining 80% of the vehicle's weight in vertical flight, shall assume a tilt-shaft configuration. To achieve this, a tilting 90° gearbox system will be used. The tilting axis of said gearbox shall be aligned with the motor's output shaft (gearbox's input shaft) in order to allow for the proper transmission of power between motor and propeller regardless of the angle assumed by the propeller shaft.

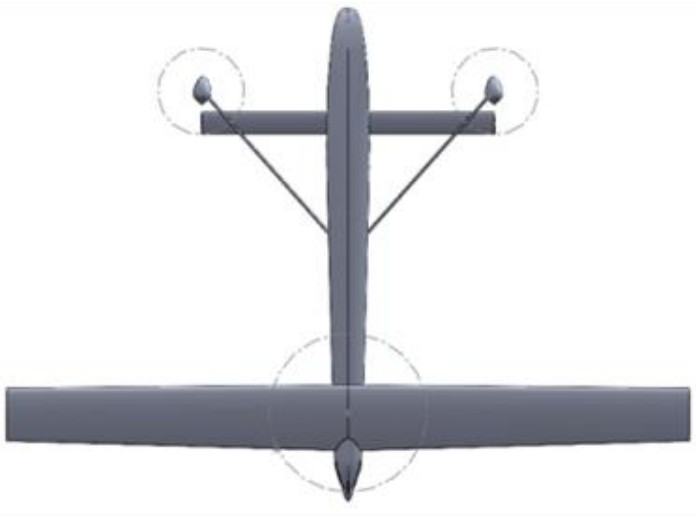

Fig. 1. Preliminary CAD model of the VTOL UAV first conceptualized in Pedro et al., 2021.

When dealing with a multi-rotor configuration where the number of propellers is not even, and thus propeller pairing cannot be accomplished, a problem arises regarding the balance of the drag torques developed by each rotating propeller. While in multi-rotors with an even number of propellers these are usually paired between them (same number of vertically pointing propellers rotating clockwise as counterclockwise) yielding that a balance of torques along the yaw axis is achievable as long as the rotational speed of any given clockwise rotor is matched to the one of a counterclockwise one. Furthermore, in such cases, these rotational speeds can be manipulated by the flight controller, as is often, to manoeuvre the aircraft in yaw. Tri-rotor configurations however, having an uneven number of rotors, must achieve yaw stability through other means, the most common one being thrust vectoring. This approach requires that one of the rotors (usually the aft one in a y configuration) is capable of tilting laterally, thus developing a lateral thrust component and an associated torque along the yaw axis (Salazar-Cruz & Escareño, 2009; Mohamed & Lanzon, 2012; Papachristos & Tzes, 2012; Gu et al., 2021). However, in the proposed configuration, the aft rotor shaft will already be required to tilt between the initial vertical stance and a longitudinal orientation during the forward flight stages. As so, it was decided that the yaw attitude should be managed by a similar thrust vectoring approach but performed by the two frontal rotors. These will thus tilt along the longitudinal axis of the frontal arms of the tri-rotor simultaneously, which allows to minimize the tilting angle that is required from each front rotor to achieve the necessary equilibrium of torques in yaw. Furthermore, the sense of rotation of the

frontal rotors (counterclockwise) shall be opposite to the one of the rear one (clockwise) as shown in Figure 2. This will allow to minimize the natural torque imbalance and consequently the lateral thrust vector needed to achieve equilibrium, the tilting angle of the frontal rotors (assuming that the required vertical thrust is constant) and thus the amount of power required to operate the front rotors.

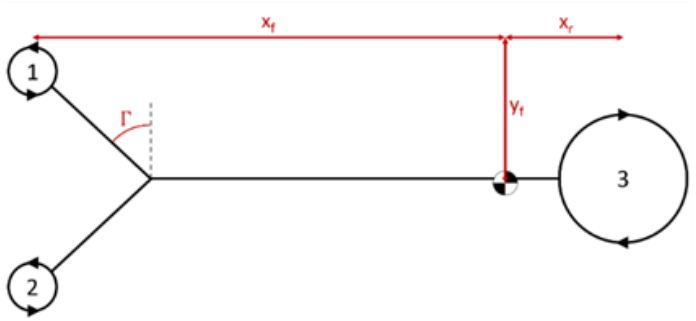

Fig. 2. Schematic representation of the proposed tri-rotor configuration (not to scale).

Γ :Arms' opening angle

x_f :longitudinal distance between front rotors and aircraft center of gravity

x_r :longitudinal distance between rear rotor and aircraft center of gravity

y_f :lateral distance between each front rotor and aircraft center of gravity

Given that the objective of the present study was to explore a new multi-rotor configuration for application to a VTOL, fixed-wing aircraft, it was deemed necessary to start the process by deducting the equations which would later support the development of a preliminary flight dynamics model (FDM) for vertical flight stages. Once these equations were obtained, equilibrium condition studies were performed as to establish the conditions under which this multi-rotor aircraft configuration could perform stable, hovering flight. Once an initial understanding of the configurations' capabilities was gained, the development of the test vehicle commenced with particular focus on the development of the mechanisms required to perform thrust vectoring with all three rotors. These mechanisms, when built, were, in their term, tested to map their actuation and to explore their performance. In parallel, a personalized PX4 autopilot firmware was devised to control this novel configuration aircraft in the subsequent test flights. Once the vehicle was concluded, it was subjected to a battery of test flights to assert the airworthiness of both the vehicle itself and of the configuration as a concept. Finally, with the collected data, a frequency-response system identification method was applied to obtain a suitable dynamics model from experimental data.

In the following subsections, this sequence of steps is to be explored in more detail.

2. Configuration Study

2.1 Flight Dynamics Model

With the goal of better comprehending the expected vertical flight dynamics of the future FW vehicle which encompasses the proposed multi-rotor configuration, it was first necessary to derive the appropriate flight dynamics model (FDM).

The dynamic equations, which describe the motion of the aircraft, were derived from the typical Newton-Euler equations (Roskam, 1998; Phillips, 2009; Beard & McLain, 2012). Given that the current iteration of the vehicle is electric (despite the final one having a hybrid electric propulsion system), it is possible to manipulate the equations in such a way that a constant mass and inertia tensor are considered. The main distinction between the derived FDM and a common multi-rotor FDM will reside in the formulation of the propulsive forces and moments which act on the aircraft (alongside the contributions of gravity and aerodynamics). For the presented multi-rotor configuration, the formulation of the propulsive forces and moments will take the form shown in Equation 1. In these expressions, "T_n" and "τ_n" represent the thrust and drag torque magnitudes generated by rotor n, according to the numbering provided in figure Fig. 2 while "x_f", "x_r" and "y_f" represent the distances portrayed in the same figure. Furthermore, "δ_{arms}" stands for the tilting angle of the front rotors (0° for vertical) and "μ" for the rear rotor tilting angle (90° at vertical). Furthermore, the contributions of aerodynamics (Pedro et al., 2021), gravity, and gyroscopic effects (Phillips, 2009) towards the aircraft's vertical flight dynamics were also considered.

$$\begin{cases} F_{x_{prop}} = (-T_1 + T_2)\sin\delta_{arms}\cos\Gamma + \\ \quad +T_3\cos\mu \\ F_{y_{prop}} = (T_1 + T_2)\sin\delta_{arms}\sin\Gamma \\ F_{z_{prop}} = -(T_1 + T_2)\cos\delta_{arms} - T_3\sin\mu \\ M_{x_{prop}} = (-T_1 + T_2)y_f\cos\delta_{arms} + \\ \quad +(\tau_1 - \tau_2)\sin\delta_{arms}\cos\Gamma + \\ \quad +\tau_3\cos\mu \\ M_{y_{prop}} = (T_1 + T_2)x_f\cos\delta_{arms} - \\ \quad -T_3\,x_r\sin\mu - \\ \quad -(\tau_1 + \tau_2)\sin\delta_{arms}\sin\Gamma \\ M_{z_{prop}} = (T_1 + T_2)x_f\sin\delta_{arms}\sin\Gamma + \\ \quad +(T_1 + T_2)y_f\sin\delta_{arms}\cos\Gamma + \\ \quad +(\tau_1 + \tau_2)\cos\delta_{arms} - \tau_3\sin\mu \end{cases} \quad (1)$$

2.2 Equilibrium Condition Analysis

Once the dynamics equations were derived, an equilibrium condition analysis was carried out through the use of a non-linear solver algorithm with the purpose of determining the attitude and actuator outputs

required for the conceptualized test vehicle to hover steadily under various constant wind conditions.

This algorithm, being based on an optimization approach, required the definition of a cost function. The methodology which was considered consisted of minimizing the sum of the mechanical power developed by the three rotors (P_i). As so, the program was to find values for a set of pre-defined variables, regarding the vehicle's attitude (roll angle – ϕ; pitch angle – θ) and actuation (rotational speed of the i rotor – Ω_i; tilt angle of front rotors – δ_{arms}) which would enable for said minimization to happen. The optimization problem was thus defined as shown in Equation 2.

$$min \sum_{i=1}^{3} P_i \quad (2)$$

$$w.r.t. \ [\phi, \theta, \Omega_1, \Omega_2, \Omega_3, \delta_{arms}]$$

$$\begin{cases} F_{x_a} + F_{x_{prop}} + F_{x_g} = 0 \\ F_{y_a} + F_{y_{prop}} + F_{y_g} = 0 \\ F_{z_a} + F_{z_{prop}} + F_{z_g} = 0 \\ M_{x_a} + M_{x_{prop}} = 0 \\ M_{y_a} + M_{y_{prop}} = 0 \\ M_{z_a} + M_{z_{prop}} = 0 \end{cases}$$

Here, F stands for forces, M for moments and subscripts a, prop and g stand for the contributions of aerodynamics, propulsive system and gravity towards the system, respectively.

As for the values in between which the optimization variables could vary, these are provided in Table 1.

Table 1. Study variables' boundaries.

Variable	Lower Bound	Upper Bound
ϕ	-30°	30°
θ	-30°	30°
Ω_1	0 rpm	8200 rpm
Ω_2	0 rpm	8200 rpm
Ω_3	0 rpm	6374 rpm

Once the algorithm had been established, several simulations were performed where the magnitudes and directions of (constant) incoming wind gusts were varied and the attitude of the aircraft and expected actuation registered. This allowed to conclude on the expected tendencies of this novel configuration under different hovering flight scenarios as well as to obtain an initial vertical flight envelope. This flight envelope contains the maximum allowable gust magnitudes for each direction based on the actuation and attitude limits that were established, namely the allowable roll and pitch angles, maximum tilt angle that the frontal rotors can achieve and maximum allowable rotational speed of all three rotors, as provided on Table 1.

The first study which was carried out using the developed optimization tool had the objective of determining the attitude and actuation assumed in vertical flight by the future fixed-wing vehicle (FW VTOL) for which the explored multi-rotor configuration was conceptualized under zero-wind conditions. The results obtained from such simulations are available in Table 2.

Table 2. Attitude and actuation during steady hovering flight under zero-wind conditions.

Variable	FW VTOL
ϕ	-0.338°
θ	0°
Ω_1	6047 rpm
Ω_2	6047 rpm
Ω_3	4909 rpm

From the analysis of these results, it is possible to reach some conclusions regarding the behaviour of the configuration in hover. Even though this may not prove truthful for all vehicles which assume this multi-rotor configuration, for the present study case it was concluded that the drag torque developed by the rear rotor of the vehicle surpassed the accumulated drag torques developed by the front rotors in hovering flight conditions. This is translated, considering the sense of rotation defined for the various propellers in Figure 2, into an accumulated drag torque which is different from zero in magnitude and that assumes negative values along the vertical (yaw) axis of the aircraft's local referential. As so, from the need to counterbalance this phenomenon through the tilting action of the frontal rotors, to obtain a thrust vectoring such that this torque imbalance is neutralized, the frontal rotors will have to tilt to the right. This allows for the development of a lateral (Y-positive) thrust component and an associated, positive, torque along the yaw axis which will thus balance the accumulated drag torques. This tilting action is then translated by a positive value of the δ_arms variable. Such a thrust vectoring action, however, despite allowing to achieve a balance of torques in yaw, creates an imbalance of forces along the local Y axis in levelled flight. As so, and in order for the aircraft not to drift to the right as a consequence of this imbalance, the vehicle will also reveal a tendency to roll to the left, which allows for this lateral thrust to be balanced by a local component of the aircraft's weight. The pitch angle will expectedly remain null while the rotational speeds of the different rotors are dependent on the specific powertrain characteristics for each vehicle. In the hypothetical case of the balance of torques along the yaw axis revealing a greater equilibrium of drag torques or even a reversal of the verified situation (accumulated drag torques of the frontal rotors surpassing in magnitude the one of the rear one), the stationary hovering flight attitude and actuation will change. Nevertheless, the underlying logic as to why the aircraft

assumes such attitude/actuation will remain unchanged.

The devised optimization tool was also used to obtain a preliminary vertical flight envelope regarding the gust magnitudes (and directions) under which the conceptualized vehicle would be able to operate, in hovering flight, while respecting the operational boundaries defined in Table 1 and maintaining a fixed position. Such results are provided in Table 3.

Finally, an additional study on the relation between the angle assumed by the rear rotor and the forward speed achieved by the future FW VTOL vehicle during a hypothetical transition manoeuvre was also carried out using a modified version of the tool which allowed to obtain the results previously presented.

Table 3: Maximum allowable gust magnitudes by direction and study case.

Variable	FW VTOL
Front	>10
Rear	>10
Left	4
Right	4
Up	7
Down	4

The optimization process for this study case was identical to the one presented earlier, with the distinction of considering an additional optimization variable regarding the tilting angle of the rear rotor. The results relative to the optimal transition scenario (where the total mechanical power required to maintain levelled flight at a constant altitude is minimized and wind gusts are null across all directions) are thus presented in Figure 3. The aerodynamic model which was used assumed that the transition was performed with a null pitch angle and with the canard incidence set at the same value as in trimmed flight at cruise speed.

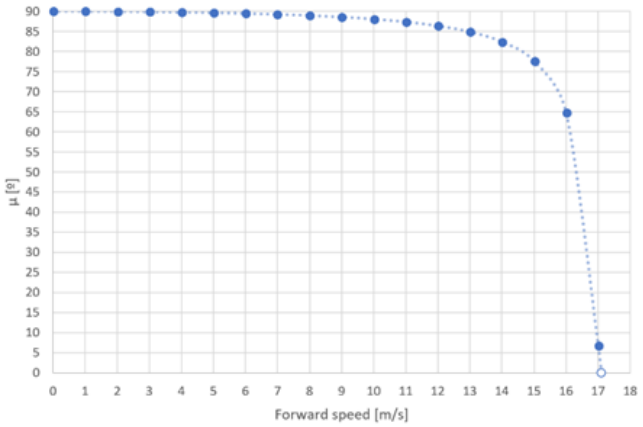

Fig. 3. Relation between rear rotor tilting angle and forward speed achieved by the aircraft for optimal transition scenario.

μ : Rear rotor's tilting angle.

Considering that the theoretical stall speed for the conceptualized FW VTOL aircraft has been established at 13 m/s (Pedro et al., 2021), it was deemed possible that such forward flight condition could be achieved with a rear rotor tilting angle as low as 5º (considering that the required time is provided for the vehicle to acquire such forward velocity). From the analysis of the provided graph, it is also noticeable that once the theoretical stall speed is achieved, a ramp-up in the progression of the rear rotor's tilting angle with the forward speed is also verified. This result was expected, given, firstly, the increase in the contribution of the aerodynamic surfaces (wing and canard) in the generation of lift, which reduces the need for the rotors to generate vertical thrust (in fact, throughout the transition process, a gradual decrease in rotational velocity is also verified for all rotors) and secondly, since the increasing forward speed also brings an increase in horizontal drag, the demand for horizontal thrust is simultaneously enlarged, hence the reduction of the tilting angle of the rear rotor in the later stages of this transition process.

3. Vehicle Design

3.1 Flight Controller Development

In order to perform the proof-of-concept flights which could attest to the airworthiness of the proposed configuration, a test vehicle was built, and a custom flight control firmware was developed. This later step was done in the PX4 environment, through the development of a custom airframe configuration. Even though there were two pre-existent Y-shaped tri-rotor flight controllers available in the PX4 repository, neither of them was applicable to the proposed configuration. There were three reasons for this: 1) Both of these models assumed that all three rotors were equidistant from the aircraft's centre of gravity (CG), which does not apply to the presented case that presents a 20/80 thrust distribution between the front and rear rotors; 2) The sense of rotation of the rotors was different from the ones envisioned for the proposed configuration; 3) The pre-existent controllers presumed that yaw control was dependent on the laterally tilting action of the rear rotor while for our configuration this task is assigned to the frontal rotors tilting mechanism instead.

Once the characteristics of the proposed configuration were translated into the required files and the compilation of the firmware took place, the obtained autopilot was flashed into a PixHawk 4 board. Communication with the hardware was done through QGroundControl.

One of the main aspects of concern during said development was the neutralization of possible coupled dynamics. This is of particular interest given the fact that the sense of rotation of the frontal rotors is opposite to the sense of the rear one. Although this design aspect

was intended, for minimization of the natural drag torque imbalance along the yaw axis and thus of the lateral thrust vector required to achieve said balance (minimizing overall power to achieve stable, stationary, hovering flight), it brought up a possible undesirable effect. This effect was associated to the typical approach of multi-rotor flight controllers towards yaw attitude management. The common approach consists of changing the rotational speed of specific rotors, depending on the defined sense of rotation, to perform yaw attitude changes. However, given the proposed configuration, the application of a similar yaw control methodology would derive in a coupled action along the pitch axis. The solution which was found, and that took advantage of the fact that the proposed configuration grants thrust vectoring capabilities to the frontal rotors, was to assign full control over the yaw attitude to the front tilt mechanism while preventing the flight controller from changing the rotational velocities of the rotors when yaw attitude changes were required. As so, one can say that control over the pitch and roll axis, as well as of heave actions, were deemed dependent on the manipulation of the rotational velocities of the different rotors, as is usual, while authority over the yaw attitude was attributed solely to the front tilt mechanism action.

3.2. Tilt Mechanisms Development

Regarding the design of the test vehicle, the two subsystems which present particular interest due to their novelty and fundamentality to the functioning of the proposed multi-rotor concept are the front and rear rotors' tilt mechanisms. These were developed from an initial conceptual drawing until the final prototyping stage during the course of this investigation.

Fig. 4. CAD models for both the rear (top) and front (bottom) rotors' tilting mechanisms.

The rear rotor design was developed with the ever-present intention of simulating the introduction of an internal combustion engine to power the rear rotor, as will be required in the future larger-scale version of the fixed-wing VTOL aircraft. It was also determined that such power unit should be fixed relative to the airframe, in a way that a 90º gearbox is required to transfer the mechanical power between the fixed power source and the tilting output shaft of the system, where the propeller is mounted on. As in any mechanical system, however, this gearbox will present losses, which will influence the overall efficiency of the rear rotor system. This phenomenon shall be studied in a later stage of this work.

Regarding the frontal rotors' tilting mechanism, one of the main considerations that were taken into account was that the chosen design should allow for the future modification of the system, as to allow for the retracting action of the frontal arms of the tri-rotor during the horizontal flight stages of the future FW-VTOL vehicle. As so, it was deemed necessary that each arm was fitted with a dedicated actuator (servo). This choice would not only provide redundancy to the yaw attitude management system, in the case of a failure occurring, but also allow for the separation of the designed tilt mechanism support (in orange, at the bottom of Fig. 4) into two symmetrical parts, capable of rotating independently and thus allowing for the future development of an adequate retraction mechanism based on this design. This additional mechanism was, however, not developed for the current test multi-rotor due to not having any real influence on the dynamics of the vehicle apart from the additional weight contribution.

3.3 Ground Testing

Once the different mechanisms were built, their actuation was mapped before their fitment onto the airframe. This allowed to update the previously devised FDM and to gather valuable data for future interpretation of the flight logs. Static thrust testing was also conducted for both the front and rear rotors' systems with the same objective. The aforementioned study on the loss of performance caused by the introduction of a 90° gearbox between the rear electric motor and propeller shaft was also conducted, allowing to compare the power required to obtain similar thrust values both in direct drive and with the complete rear tilt mechanism system. To collect said results, firstly, static thrust tests where the rear rotor's propeller was mounted, as is usual, on the rear motor's shaft were performed. Then, after the assembly of the rear rotor tilting mechanism had been completed, the gearbox was fixed using two wedges, as to align the output propeller shaft with the static thrust test bench and additional thrust tests were carried out, with the obtained results being displayed graphically on Figure 5.

These results show that there is a clear increase in the electrical power required by the motor for the case of the complete rotor tilt system, as expected. From the obtained values it was possible to estimate, for example, that to generate the amount of thrust required from the rear rotor under hovering flight conditions, the increase

in power that would be required to drive the complete rear rotor system when compared with the direct drive case would be of around 19%. This loss in efficiency is mainly due to the energy losses associated with the introduction of the 90° gearbox in the system. In fact, the efficiency (loss) curve which was obtained also proved consistent with the typical gearbox efficiency.

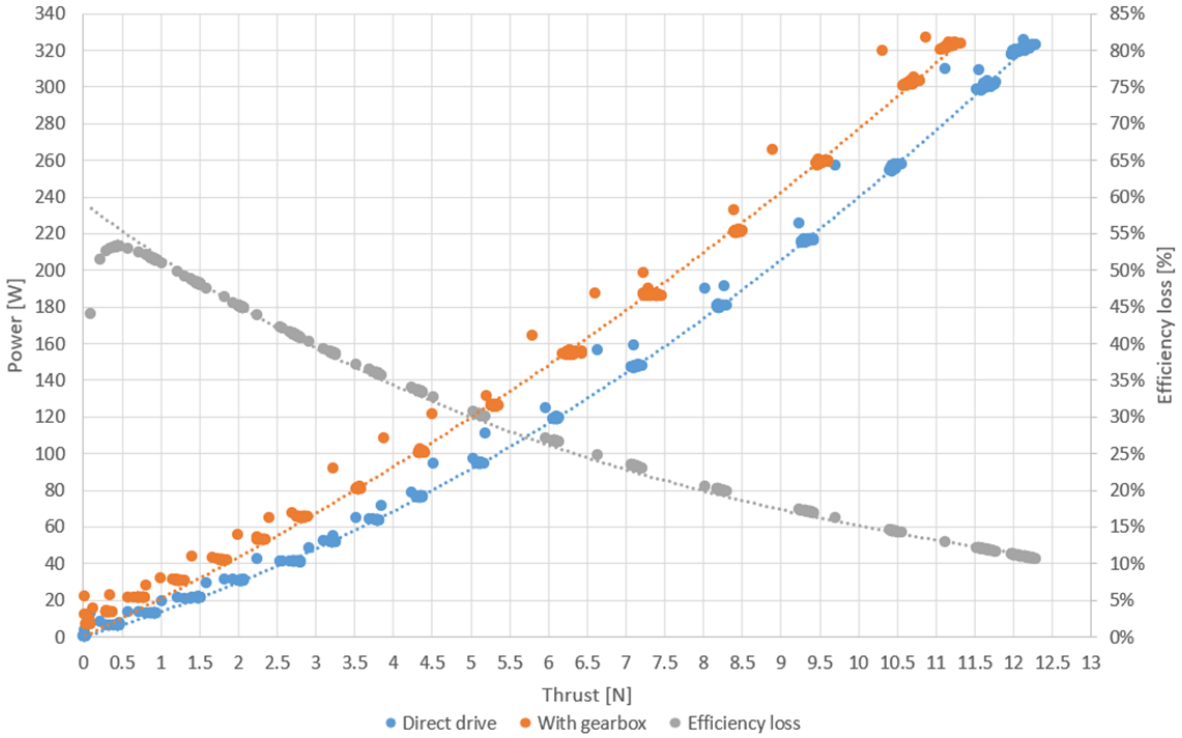

Fig. 5. Static thrust test results for the rear ESC/motor/ propeller system in direct drive and when fitted to the rear tilting mechanism.

Behaviour registered by several authors (Bogdan & Zoltan, 2017; Sekar, 2019), who have previously verified marked tendencies of such mechanical systems to minimize their losses when an increase in the loading conditions is verified.

Other ground tests which were performed involved continuous operation static thrust testing of the rear rotor system. These were done for temperature survey of the gearbox's gears and particularly of the electric motor's temperature when exposed to such continuous operating conditions. The main driver for this test was the concern that the motor, not being directly in the wake of the propeller as it was designed to be during its operation, would overheat and experience a loss in performance due to magnet demagnetization (Zhou et al., 2012; Ruoho et al., 2010). However, it was found that the temperatures achieved were considerably lower than the maximum allowable ones stated by the manufacturer, in a way that the subsystem could then be considered safe and thus mounted on the vehicle's airframe.

4. Flight Testing

After all the subsystems were tested individually and the multi-rotor prototype completed, flight testing could then commence. The first flights were performed indoors, with the prototype tethered, as to ensure the safety of the intervenient and of the vehicle itself in these early stages of testing. These tests allowed to tune the different aircraft systems, from the controller to the airframe and power distribution system, which were objects of continuous upgrades during this preliminary testing stage. Once the vehicle's performance and controllability were deemed satisfactory, the tethers were removed, and the team proceeded to perform the first untethered flight (Fig. 6). During this test, the aircraft proved capable of performing stable hovering flight while maintaining position, as required during a vertical take-off or landing manoeuvre, and also to perform manoeuvres across all three attitude axis, with the pilot reporting that the vehicle was easily controllable and that its dynamics were fairly predictable despite being a novel aircraft configuration.

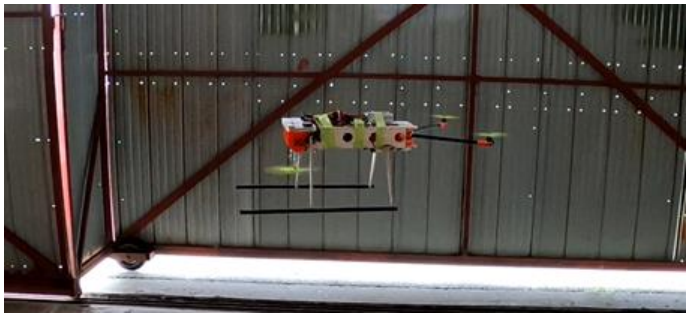

Fig. 6. Test vehicle during indoor, untethered flight testing.

Based on these results, the team felt confident in proceeding with the following flight tests outdoors (Fig. 7).

The first set of exterior tests consisted of five flights encompassing manoeuvres such as chirps, doublets, and periods of static hovering flight, which were done with the purpose of collecting data for later system identification. As so, an initial practice flight was carried out for the pilot to be familiarized with the different manoeuvres and associated tendencies of the aircraft. This was followed by three other flights, one dedicated to each of the local attitude axis (roll, pitch and yaw). In each of these flights, the pilot commanded the vehicle to perform various sets of chirps and doublets, always on the same axis during each test, intercalating these manoeuvres with periods of hovering flight. After this, another flight was performed (the validation flight), where sets of chirps and doublets were performed once again but this time across alternating axes, in a way that there was at least one example of each manoeuvre across each of the three axes for later validation of the flight dynamics models obtained from system identification. Having data from this final validation flight allows to assess the robustness of the model when replicating a different flight from the ones used to generate the dynamics model.

Finally, the only capability of the configuration that had not been tested until this moment was the ability to initiate and maintain stable forward flight by tilting the rear rotor system. Considering that the developed experimental vehicle lacked the traditional lifting surfaces of a fixed-wing aircraft, it was obvious that a complete transition between vertical and horizontal flight could not take place. However, the objective which was defined for this test was solely the evaluation of the capability of this multi-rotor configuration and of the flight controller to initiate a simulated transition manoeuvre. As so, a final test flight where the aft rotor was tilted by 5° was performed. Previous parametric studies yielded that the thrust vectorization that would derive from this actuation would allow for the aircraft to maintain a levelled attitude and a constant altitude while also gaining forward momentum as would be required during a transition flight manoeuvre.

Fig. 7. Test tri-rotor during outdoor flight testing.

The results obtained were very satisfactory, with the aircraft revealing itself as capable of initiating and maintaining stable forward flight with minimal to no pilot intervention for attitude correction being required.

5. System Identification

Upon collection of the required flight data from the previously mentioned flight tests, the following objective was to obtain a dynamics model from said experimental data.

The chosen system identification approach used in this work was based on a frequency-response model (Tischler & Remple, 2012). This approach, translated into a custom transfer-function estimation tool, took as inputs the rate setpoints of the flight controller during the test flights performed for each of the different attitude axes and the angular rate response registered by the gyroscope for that same axis. At the same time, and for each file of flight test data, the user was required to provide the program with the time intervals where the different manoeuvres took place during the respective test. Then, with this information, the flight data of the three SID flights (one relative to each attitude axis) was partitioned in a way that each sample was composed of one manoeuvre on one axis. Next, all possible combinations of these manoeuvres for a given axis were obtained, yielding a certain number of simulated flight examples. Each of these simulated flights would then be used to estimate one transfer function, which related the inputs and outputs for the set of manoeuvres encompassed by that flight. After this point, each of the obtained transfer functions would be tested against the additional validation flight data (which had not been used in the estimation of said transfer functions) for the respective axis. Then, the transfer functions which provided the highest fitting, or in other words that best replicated the validation flight outputs when provided with the same inputs, were said to represent the aircraft's dynamic behaviour for that axis.

It should be noted that the provided model is linear, which means that the coupled dynamics are neglected. This can be reflected in an undesirable reduction of the fitting of the replicated dynamics to the original ones, considering that the proposed concept presents some marked couplings. Even though, as explained in subsection 3.1., some of these coupling tendencies were dealt with when defining the flight controller, others could not be neutralized. One of the most prominent couplings occurred between the variation of the pitch attitude and a subsequent reflection on the yaw attitude. This effect showed itself particularly during high-frequency pitching manoeuvres, where the rapid variation of the thrust developed by the front rotors, required to achieve the desired chirp manoeuvre along this axis, would cause an unrequested chirp along the

yaw axis of equal frequency and smaller amplitude (Fig. 9 and Fig. 10). This was caused by the thrust vectoring of the thrust developed by the front rotors, which while allowing to manage the yaw attitude of the vehicle during the vertical flight stages, also exposes it to such coupled dynamics.

Nevertheless, the dynamics model retrieved from such an approach presents itself as a capable tool when it comes to the replication of the relation between inputs and outputs for the same axis and can be used in, for example, autopilot optimization tasks. Furthermore, when applied to vehicles with configurations less prone to dynamic couplings, the obtained models prove even more accurate in the replication of the overall behaviour of the vehicle, yielding superior fittings between simulated and real flight dynamics to the ones verified for the current application. The goodness of fitment values obtained for the presented case study are provided in the figures below ("G").

6. Conclusions

The work presented in this paper characterizes the airworthiness of the proposed multi-rotor configuration for future application on the VTOL system of a fixed-wing aircraft.

During the course of the reported work, an initial study on the expected behaviour of a future fixed- wing VTOL aircraft fitted with the proposed tilt tri-rotor propulsive system configuration in vertical flight was carried out.

Such study culminated in the comprehension of the attitude and actuation that would be expected of said aircraft during hovering, stationary flight under several wind conditions; in the obtention of a preliminary vertical flight envelope regarding the maximum acceptable gust magnitudes for various directions that would still allow for the vehicle to maintain hovering, stationary flight; and on the expected attitude and actuation of the conceptualized vehicle when transitioning from vertical to horizontal flight by means of the tilting action of the rear rotor.

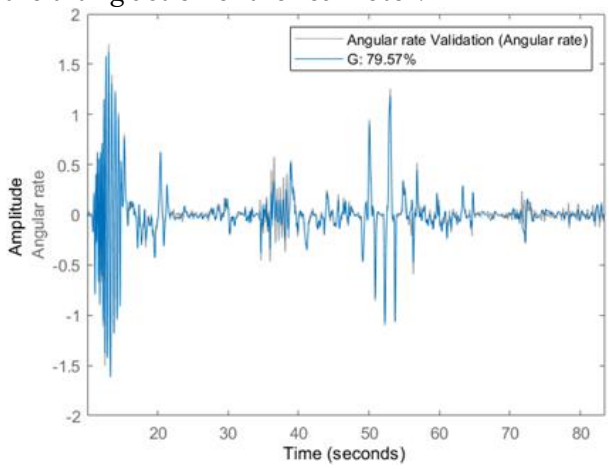

Fig. 8. Comparison between replicated and recorded roll dynamics during the validation flight.

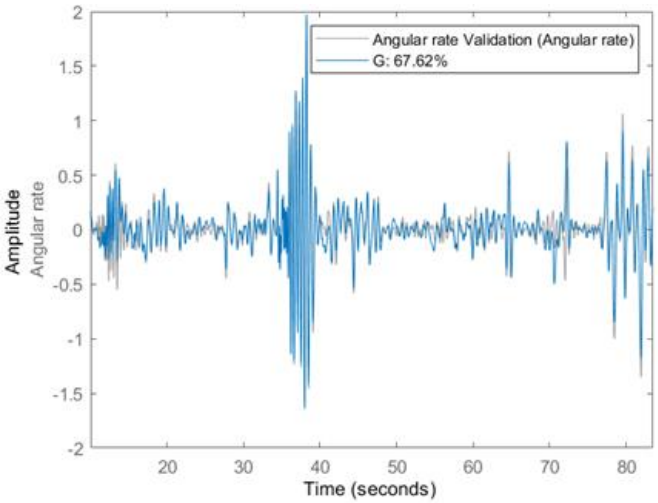

Fig. 9. Comparison between replicated and recorded pitch dynamics during the validation flight.

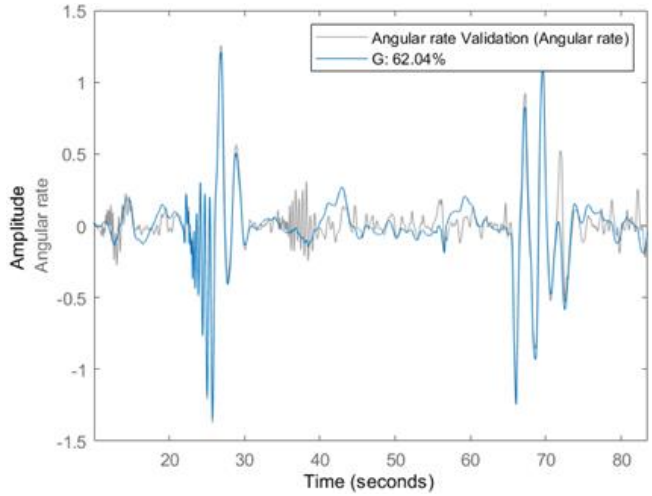

Fig. 10. Comparison between replicated and recorded yaw dynamics during the validation flight.

Furthermore, the solutions proposed for both the front and rear rotor tilting mechanisms were successfully developed and tested.

Next, the multi-rotor prototype that was developed during the course of this investigation was flight tested successfully, both indoors and outdoors, proving not only the ability of the aircraft and thus of the configuration to sustain continuous and stable hovering flight when exposed to external disturbances but also the ability to manoeuvre adequately along all attitude axis with various frequencies. Moreover, the important milestone of initiating and performing stable forward flight through the action of the rear tilting mechanism was also achieved, paving the way for future transition condition studies of the fixed-wing aircraft that is being developed to be made.

Finally, a newly developed, frequency-response based, SID tool was applied to the collected data, providing a model which yielded satisfactory results when it came to the replication of the real flight test dynamics, despite neglecting some of the coupled dynamics associated with the proposed configuration.

Nomenclature

VTOL	: Vertical Take-Off and Landing
UAV	: Unmanned Aerial Vehicle
FDM	: Flight Dynamics Model
SID	: System Identification

CRediT Author Statement

António Arco: Conceptualization, Methodology, Software, Validation, Formal Analysis, Investigation, Data Curation, Writing – Original Draft, Visualization. **José Lobo do Vale**: Conceptualization, Methodology, Validation, Formal Analysis, Investigation, Writing – Review & Editing, Supervision. **Sean Bazzocchi:** Conceptualization, Software, Writing – Original Draft. **Afzal Suleman:** Conceptualization, Resources, Writing – Review & Editing, Supervision, Project Administration, Funding Acquisition.

References

Beard, R. W. And Mclain, T. W. (2012). Small Unmanned Aircraft: Theory And Practice (1st Ed.). Princeton, New Jersey: Princeton University Press.

Bogdan, C. And Zoltan, K., (2017). Efficiency Investigation on A Helical Gear Transmission. Analele Universităţii "Eftimie Murgu" Reşiţa, Fascicola Inginerie, 24, 55-66.

Goetzendorf-Grabowski, T., Tarnowski, A., Figat, M., Mieloszyk, J. & Hernik, B. (2020). Lightweight Unmanned Aerial Vehicle for Emergency Medical Service – Synthesis of The Layout. Proceedings Of the Institution of Mechanical Engineers Part G Journal of Aerospace Engineering, 1-17. DOI: 10.1177/0954410020910584.

Gu, X., Xian, B. And Li, J. (2021). Model Free Adaptive Control Design for A Tilt Trirotor Unmanned Aerial Vehicle with Quaternion Feedback: Theory and Implementation. International Journal of Adaptative Control and Signal Processing, 36, 122-137. DOI: 10.1002/Acs.3344

Mohamed, M. K. And Lanzon, A. (2012). Design and Control of Novel Tri-Rotor UAV. 2012 UKACC International Conference on Control, 304-309. DOI: 10.1109/CONTROL.2012.6334647

Pedro, S., Tomás, D., Lobo Do Vale, J. & Suleman, A. (2021). Design And Performance Quantification of VTOL Systems for A Canard Aircraft. The Aeronautical Journal, 98, 91-105. DOI: 10.1017/Aer.2021.63.

Phillips, W.F. (2009) Mechanics of Flight (2nd Ed.). Hoboken, New Jersey: John Wiley & Sons, Inc.

Papachristos, C. And Tzes, A. (2012). Modeling And Control Simulation of An Unmanned Tilt Tri-Rotor Aerial Vehicle. 2012 IEEE International Conference on Industrial Technology, 840-845. DOI: 10.1109/ICIT.2012.6210043

Ruoho, S., Kolehmainen, J., Ikaheimo, J. & Arkkio, A. (2010). Interdependence Of Demagnetization, Loading, And Temperature Rise in A Permanent-Magnet Synchronous Motor. IEEE Transactions on Magnetics, 46(3), 949–953. DOI: 10.1109/TMAG.2009.2033592.

Roskam, J. (1998). Airplane Flight Dynamics and Automatic Flight Controls (2nd Ed.). Lawrence, Kansas: Design, Analysis and Research Corporation.

Saeed, A. S., Younes, A. B., Cai, C. & Cai, G. (2018). A Survey of Hybrid Unmanned Aerial Vehicles. Progress In Aerospace Sciences, 1-24. DOI: 10.1016/J.Paerosci.2018.03.007.

Salazar-Cruz S., Lozano R. & Escareño, J. (2009). Stabilization And Nonlinear Control for A Novel Trirotor Mini-Aircraft. Control Engineering Practice, 17, 886–894. DOI: 10.1016/J.Conengprac.2009.02.013

Sekar, R. P., (2019). Determination Of Load Dependent Gear Loss Factor on Asymmetric Spur Gear. Mechanism And Machine Theory, 135, 322–335. DOI: 10.1016/J.Mechmachtheory.2019.02.011

Tischler, M. B. & Remple, R. K. (2012). Aircraft And Rotorcraft System Identification (2nd Ed.). Reston, Virginia: American Institute of Aeronautics and Astronautics.

Zhou, P., Lin, D., Xiao, Y., Lambert, N. & Rahman., M.A. (2012). Temperature-Dependent Demagnetization Model of Permanent Magnets for Finite Element Analysis. IEEE Transactions on Magnetics, 48(2), 1031–1034. DOI: 10.1109/TMAG.2011.2172395.

International Journal of Aviation Science and Technology

Research Article

An Approach to Preliminary Design of a Quadrotor Cargo UAV

Fikret Kamil Corbaci *[1], Yunus Emre Dogan[2]

[1]Ankara Yıldırım Beyazıt University, Aeronautics and Astronautics Engineering Department, Ankara/ Turkey
fikretkamil.corbaci@gmail.com - 0000-0002-0499-8694
[2]Ankara Yıldırım Beyazıt University, Mechanical Engineering Department Ankara/ Turkey
ynsemrd@gmail.com- 0009-0005-6250-0523

Abstract

Unmanned aerial vehicles (UAV) are widely used in many different application areas today. UAVs are very cheaper than the other aerial platform and also their give opportunity to users in operating flexibility. It can be mentioned that the cargo transportation of UAV application area has high potential to grow. Compared to traditional highway delivery methods, cargo drones can offer cost savings by eliminating the need for human drivers, reducing fuel consumption, and optimizing delivery routes. Cargo drones can revolutionize the e-commerce industry by offering same-day or even same-hour delivery options. This can improve customer satisfaction, reduce shipping costs, and enable businesses to expand their operations. The main purpose of the study is to develop a preliminary design method for a quadrotor Cargo UAV to be used for cargo transportation. Within the scope of preliminary design activities, the initial sizing, optimizations and performance analyzes of the components were made. By using these results of the design, it was observed that the number of design iterations and the design time were significantly reduced.

Keywords

Unmanned Aerial Vehicle (UAV)
Product Design
Optimization
Cargo Transportation
Quadrotor

Time Scale of Article

Received 15 July 2023
Revised to 6 September 2023
Accepted 22 September 2023
Online date 30 December 2023

1. Introduction

Unmanned aerial systems are devices that can effectively carry out numerous missions in both military and civilian domains due to their diverse payload capacities, various performance features, and cost-effective operation. These tools are increasingly preferred across various fields such as agriculture and photography as a replacement for human labor. With their robust autonomous flight capabilities, high mobility, low cost, and fuel efficiency, drones are increasingly utilized in active and complex offensive applications. These applications include meteorological studies, photography, air cargo transport, forest fire detection, search-rescue operations, and it is anticipated that new areas for drone utilization will emerge in the coming years.

In recent years, the advancement of unmanned aerial vehicles (UAVs) has led to the emergence of cargo drones as an innovative solution for logistics and transportation (Pugliese et al, 2020). These unmanned vehicles have the potential to change the way goods are transported, offering faster, more efficient, and environment friendly delivery options. Cargo drones, also known as delivery drones, are autonomous or remotely piloted vehicles specifically designed to transport goods (Jeongeun et al, 2019). These aerial vehicles use advanced navigation systems, sensors, and artificial intelligence algorithms to ensure safe and precise delivery operations. They can carry payloads ranging from small packages such as

*: Corresponding Author Fikret Kamil Corbaci, fikretkamil.corbaci@gmail.com
DOI: 10.23890/IJAST.vm04is02.0202

official document to heavier loads, depending on their design and capabilities.

Cargo drones have a huge potential to significantly reduce delivery times, especially in urban areas with congested road networks (Elouarouar and Medromi, 2022). By bypassing traffic and taking direct aerial routes, drones can swiftly transport goods, enabling rapid delivery and enhanced customer satisfaction. Compared to traditional highway delivery methods, cargo drones can offer cost savings by eliminating the need for human drivers, reducing fuel consumption, and optimizing delivery routes. These savings can potentially translate into more affordable and accessible goods for consumers. Furthermore, with the growing concerns over carbon emissions and environmental impact of it, cargo drones present a green alternative to traditional transportation. By relying on electric, drones produce fewer greenhouse gas emissions, contributing to more sustainable future.

Cargo drones also have an opportunity to reach remote and inaccessible areas that do not have adequate infrastructure, such as islands, rural areas, or disaster regions. This accessibility can ensure fast delivery of necessary supplies, medical aid, and humanitarian assistance.

When it comes to practice, cargo drones have some difficulties and limitations in terms of regulation, range, and cargo capacity. The adoption of cargo drones faces regulatory challenges related to airspace management, safety, and privacy concerns (Ahirwar et al, 2019). Governments and aviation authorities need to develop comprehensive frameworks to address these issues, ensuring the safe integration of drones into existing airspace management systems.

While cargo drone technology continues to advance, limitations still exist regarding payload capacity and range. Larger and heavier deliveries require more robust drones with longer flight endurance. Overcoming these technical constraints is crucial for the integration of cargo drones into logistics operations.

In addition, delivery operations can be affected by adverse weather conditions, such as strong winds, rain, fog, which may impact flight safety and efficiency. Developing drones with improved weather resistance and navigation capabilities is essential for their reliability and scalability.

Cargo drones, which continue to evolve despite limitations and challenges, have the potential to make a significant impact in many different areas. Cargo drones can revolutionize the e-commerce industry by offering same-day or even same-hour delivery options. This can improve customer satisfaction, reduce shipping costs, and enable businesses to expand their operations. Cargo drones also have the potential to revolutionize healthcare logistics by delivering medical supplies, vaccines, and even organs for transplantation in a timely and efficient manner. They can also support emergency services by rapidly transporting critical equipment or providing situational awareness in disaster areas.

2. Method

To have an optimal Cargo UAV preliminary design, mission profile-based requirements should be guided during the design process. In order to achieve optimized design solutions, flight time inefficiency, losses in payload capacity, time and cost losses, etc. should also be taken into account and the design process should be carried out step by step.

It can be mentioned that quadcopter design and performance analyses related activities are divided into four subtitles as conceptual design for quadcopter frame geometry selection and frame sizing, gross take off weight (GTOW) optimization (Winslow et al, 2018), electronic component selection, and flight performance analyses at the last step.

After determination of frame geometry and frame sizing, focus was increased onto optimization of GTOW development of a by using a parametric approach which was proposed at our previous research (Corbaci and Dogan, 2023). The parameters related to the weight of Quadrotor were already determined as thrust and maximum continuous current, battery capacity, propeller diameter and frame size at previous study. These are used as the basic parameters on which the system features of the Cargo UAV depend throughout the study.

As given Flowchart at Fig.1, first of all, we obtained the main design inputs and checked them if they were consistent. After getting them, we determined the initial frame size and material type to optimize the strength of the quadrotor structure. Next, in order to get maximum thrust, we start to iteration and estimate the initial GTOW using the parametric approach with the help of the parameters selected above. We perform the selection of motor by using maximum thrust parameter, the selection of propeller by using propeller diameter parameter and battery selection by using cell number and capacity parameters.

Thus, so in the final step of iteration, the total weight, including cargo and avionics, is revealed. We need to decide whether to continue the iteration by carrying out a performance CFD analysis of the UAV, whose carrier body, subsystems used and weights have been revealed.

If it turns out that we don't need to drive the iteration, we can assume that the preliminary design of the drone is obtained. Although our work was in the preliminary design phase, we also checked whether we were

progressing on a competitive concept by estimating the cost. In this way, we gained the opportunity to make changes on the selected components.

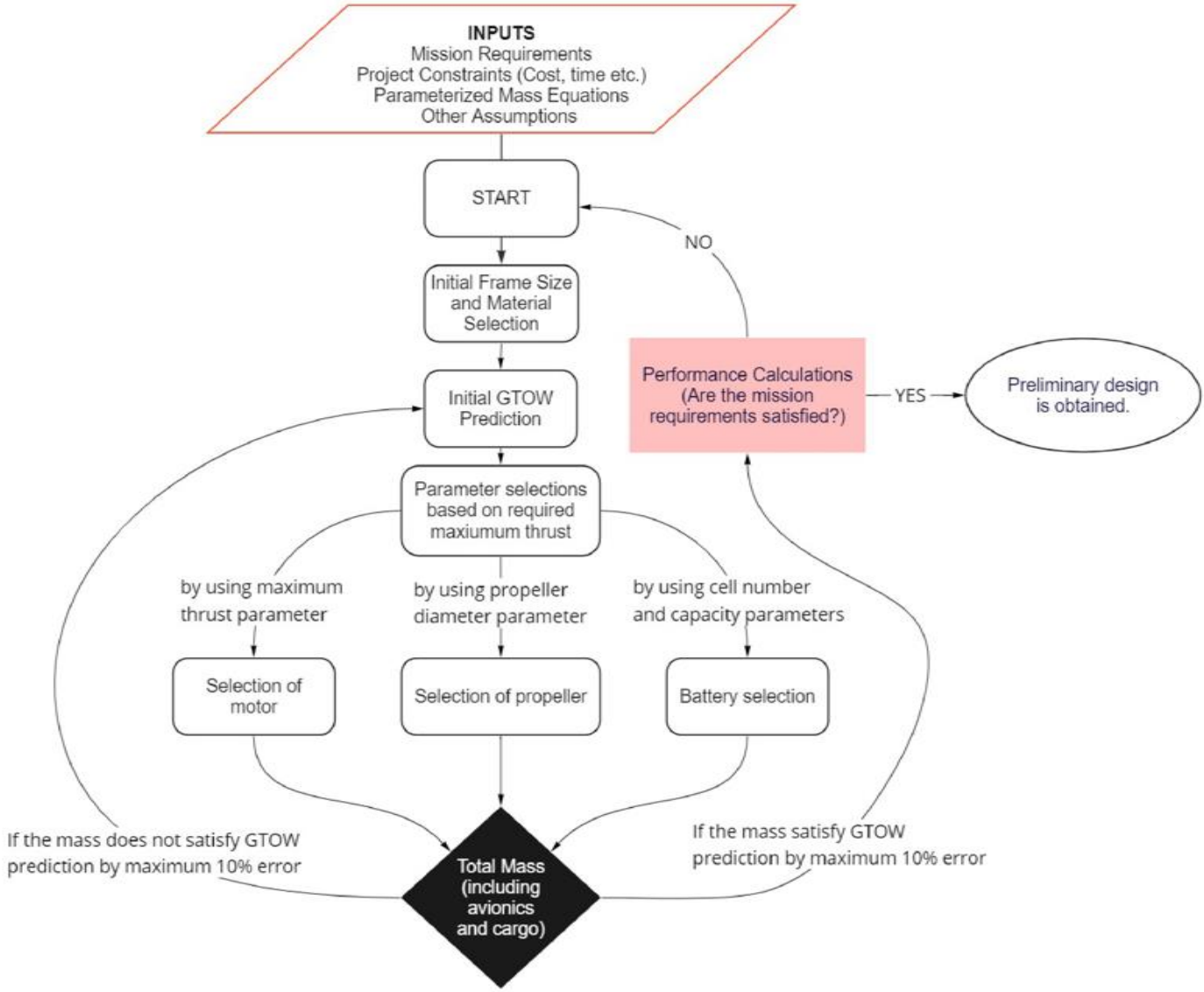

Figure 1. Flowchart of the iterative activities to obtain preliminary design of UAV

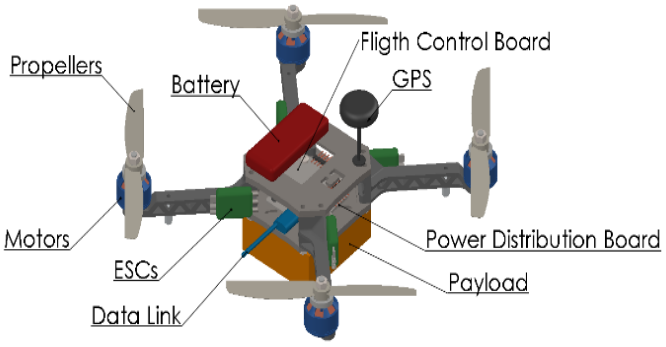

Figure 2. Fundamental subsystems of a quadrotor UAV

After the parameters of the final product are determined in the Preliminary Design Phase, the relevant systems, subsystems and components are maturely selected as represented in Figure 2.

Related component requirements were obtained from mission requirements and design features that meet these requirements were created compatibly. By using this component allocation, Cargo UAV System Chart was established for determined design features and presented at Fig.3.

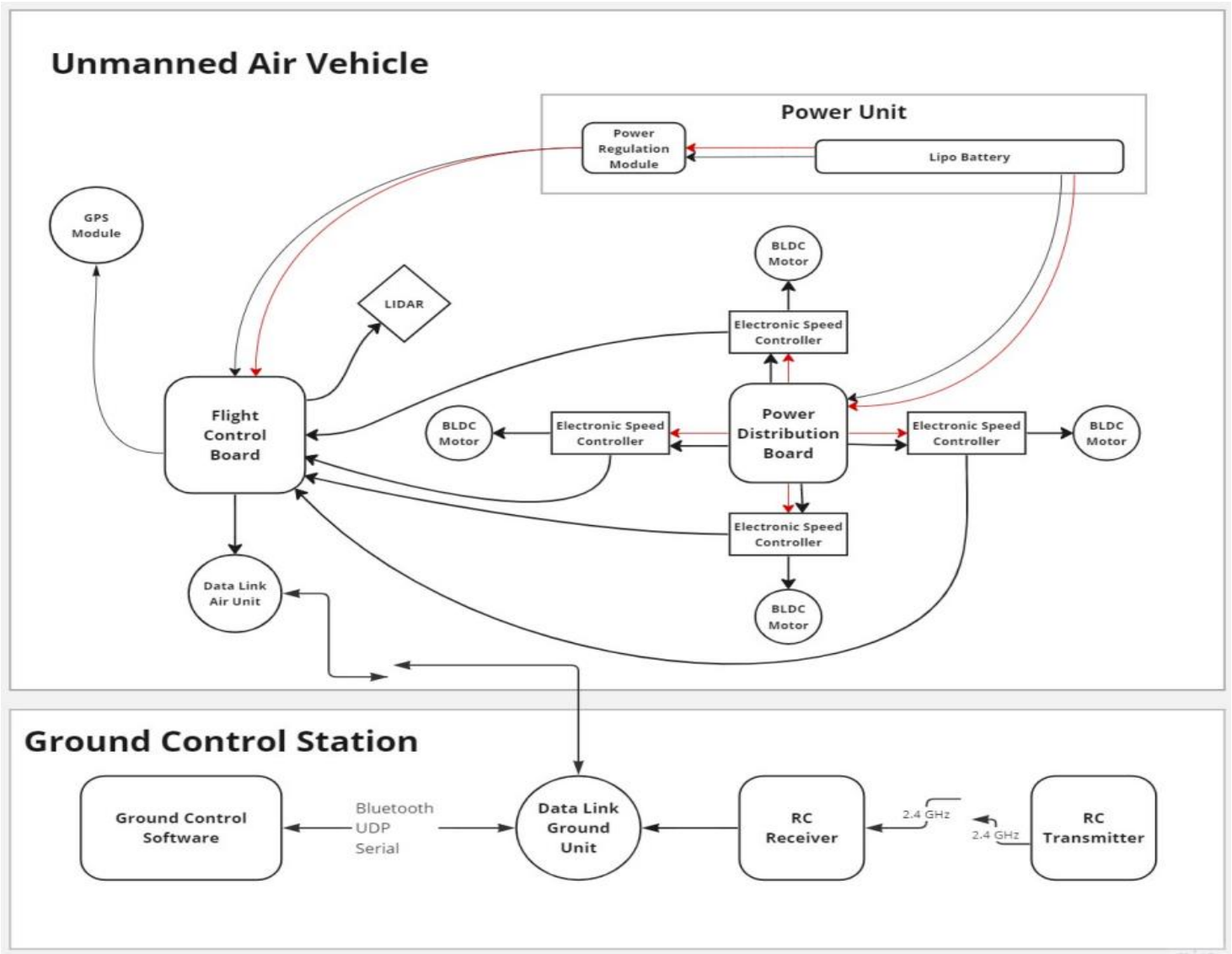

Figure 3. System Chart of the quadrotor UAV

2.1. Mission Profile

It is aimed to design a quadcopter which is used for local air cargo transportation in small urban areas and on-campus deliveries. The distance in between two delivery points are foreseen as approx. 1,500 m. The load to be carried by the vehicle consists of authentic documents that have maximum 200 g weight. In a single delivery, the drone takes off, climbs to the lowest altitude of 40 m and moves at cruising speed towards the delivery point. When it reaches the delivery point, it lands and stops the engines for safety. With the completion of the delivery, the drone rises to an altitude of 40 m again and returns to the starting point for the next delivery to be loaded. It is assumed that the quadrotor has 3.44 m/s^2. acceleration at starting point and -1.67 m/s^2 deceleration at target point. And all other information for flight plan of the UAV are given at Fig.4 in detail.

2.2. Mission Requirements

After the preliminary evaluation for the determined mission profile, the basic mission requirements of the unmanned aerial vehicle were determined as in the Table.1. These mission requirements are considered as benchmarking values during design evaluation.

Table 1. Minimum performance requirements

No	Requirement	Value
1	Average Cruise Velocity	5 m/s
2	GTOW	12.5 N
3	Minimum Flight Time	10 min
4	Payload Capacity	0.200 kg
5	Communication Range	1,500 m
6	Mass of Avionics	0.200 kg

Other important assumptions related to quadrotor UAV design could be mentioned as ABS material will be used; it will consist of 2 plates, upper and lower and have true-X geometry.

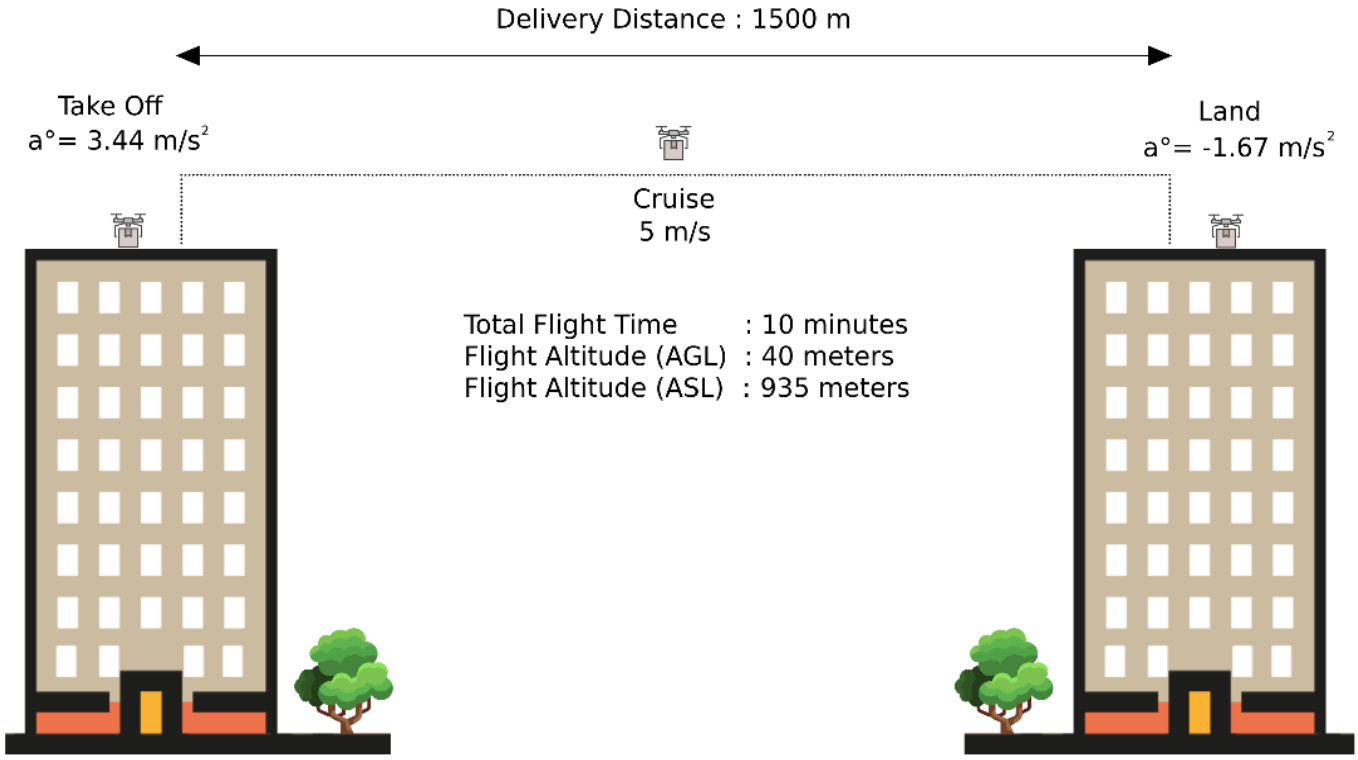

Figure 4. Flight Plan of the Quadrotor UAV

3. Preliminary Design of Quadrotor UAV

3.1. Determination of Initial GTOW

To start the design iteration, first of all, we have to determine an initial GTOW. In our previous study a regression analysis based approach was proposed successfully (Corbaci and Dogan, 2023). According to this approach, the masses of the components should be calculated primarily in order to see that it can perform the expected performance in the targeted mission specifications. One of the most important design inputs to determine the masses of the components at this stage is the Cargo UAV Gross Take Off Weight (GTOW). It is assumed that GTOW consists of the masses [g] of the engine (m_m), ESC (m_E), battery (m_B), propeller (m_p), frame (m_f), avionics (m_A) and payload (m_{PL}), which are the main components in the UAV.

$$GTOW = (m_m + m_E + m_B + m_p + m_f + m_A + m_{PL}).g \ [N] \quad (1)$$

In the preliminary design, it is necessary to determine the initial GTOW which will be created by the preliminary estimate of the mass to be revealed for each of the components. All relevant component masses were separately determined with respect to predetermined parameters for each component by using regression analyses. While doing this, the tables prepared for the product alternatives that are sold commercially for each component and containing catalog data about both mass and the relevant parameter were used. When the payload changes, this initial value is re-estimated and iteration continues accordingly.

The equations that emerged after the regression analyzes were formed as follows:

A. Mass of Motor (m_m) with respect to Maximum Thrust of Motor (T):

The weight of a BLDC motor can be parameterized by Maximum Thrust of Motor (T) since the more thrust requires more power, then bigger size and higher mass. It may be established a linear correlation between Mass of Motor (m_m) and Maximum Thrust of Motor (T) available in the market, as shown in Fig.5 and Eq.2

$$m_m = 1E-07(T)\text{^}3 - 0.0003(T)\text{^}2 + 0.2783(T) - 56.133\ [g] \quad (2)$$

B. Mass of ESC (m_E) with respect to Maximum Continuous Current of ESC ((I_{max}):

According to the study with 55 different ESCs produced by various manufacturers, Mass of ESC (m_E) is linearly parameterized by using their Maximum Continuous Current of ESC ((I_{max}) as shown in the Fig. 6 and Eq. 3

C. C. Mass of the Battery (m_B) with respect to Capacity of the Battery (C) and number of cells:

Mass of the Battery (m_B) can be parameterized by cell numbers of 3, 4, and 8 and Capacity of the Battery (C) as shown in the Fig. 7 and relevant equations for 3, 4, and 6 cell numbers are given in equations 4, 5 and 6 respectively.

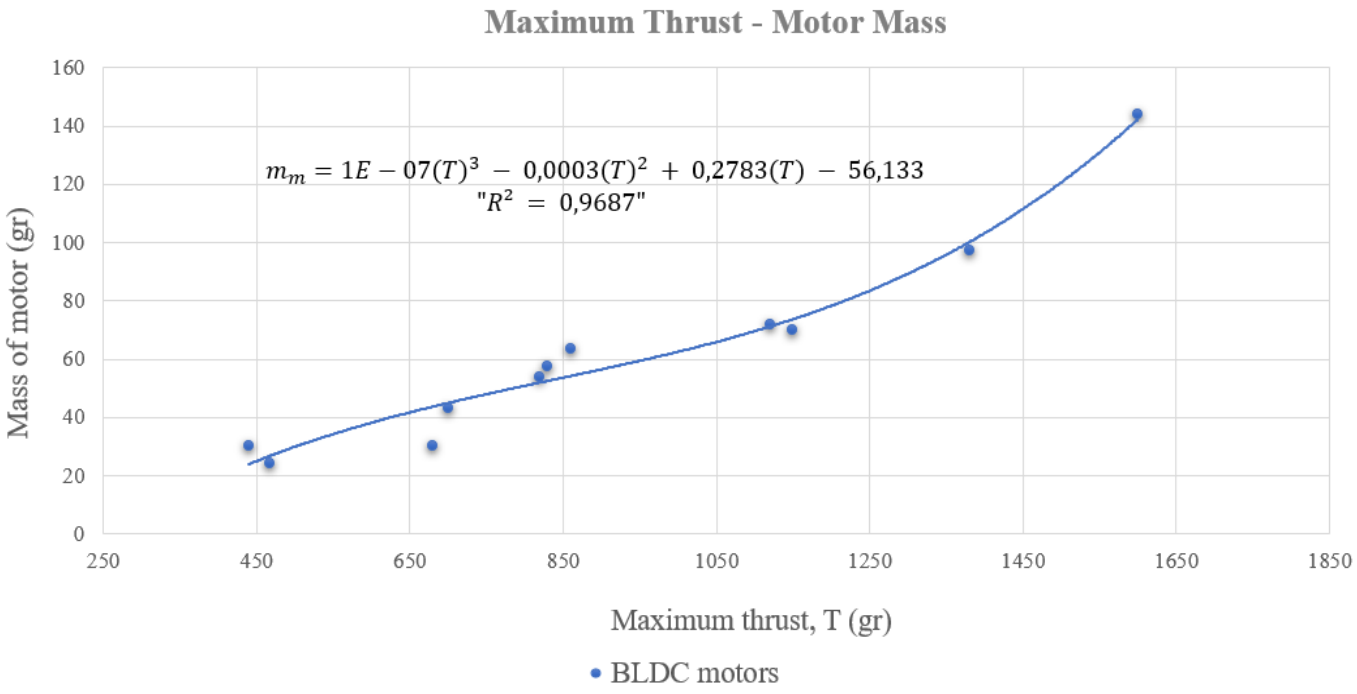

Figure. 5. Mass of Motor (m_m) with respect to Maximum Thrust of Motor (T)

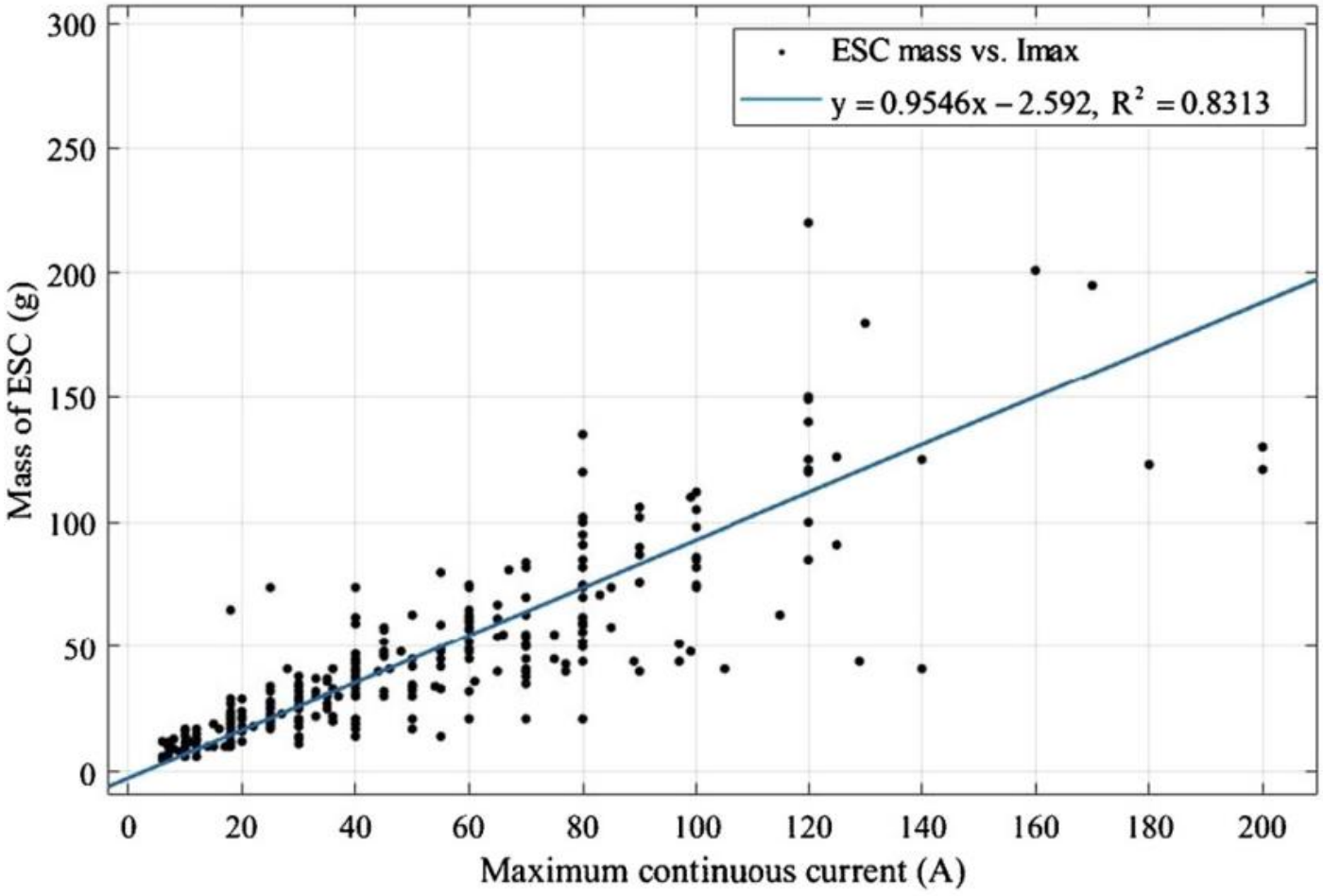

Figure 6. Mass of ESC (m_E) with respect to Maximum Continuous Current of ESC ((I_{max}), (Vu NA et al, 2019)

$$m_E = 0.9546(I_{max}) - 2.592\ [g] \quad (3)$$

$$For\ n=3,\ \ m_B = 0.0625(C) + 35.526\ [g] \quad (4)$$

$$For\ n=4,\ \ m_B = 0.761(C) + 69.522\ [g] \quad (5)$$

$$For\ n=6,\ \ m_B = 0.1169(C) + 132.0\ [g] \quad (6)$$

D. C. Mass of the Battery (m_B) with respect to Capacity of the Battery (C) and number of cells:

Mass of the Battery (m_B) can be parameterized by cell numbers of 3, 4, and 8 and Capacity of the Battery (C) as shown in the Fig. 7 and relevant equations for 3, 4, and 6 cell numbers are given in equations 4, 5 and 6 respectively.

E. Mass of the Propeller (m_p) with respect to Diameter of the Propeller (d_p):

Mass of the Propeller (m_p) for more than 50 carbon fiber propellers in UIUC database can be parameterized in terms of Diameter of the Propeller (d_p)as shown in Fig.8 and Eq.7.

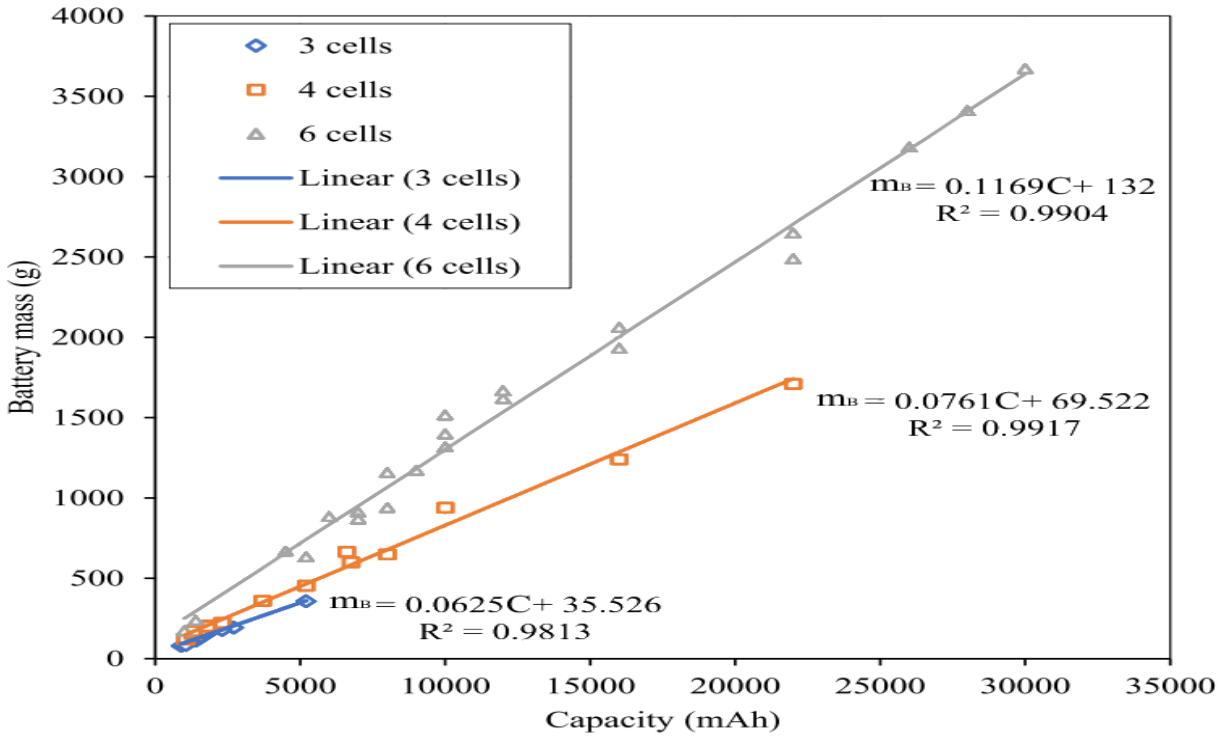

Figure 7. Mass of the Battery (m_B) with respect to Capacity of the Battery (C) , (Vu NA et al, 2019)

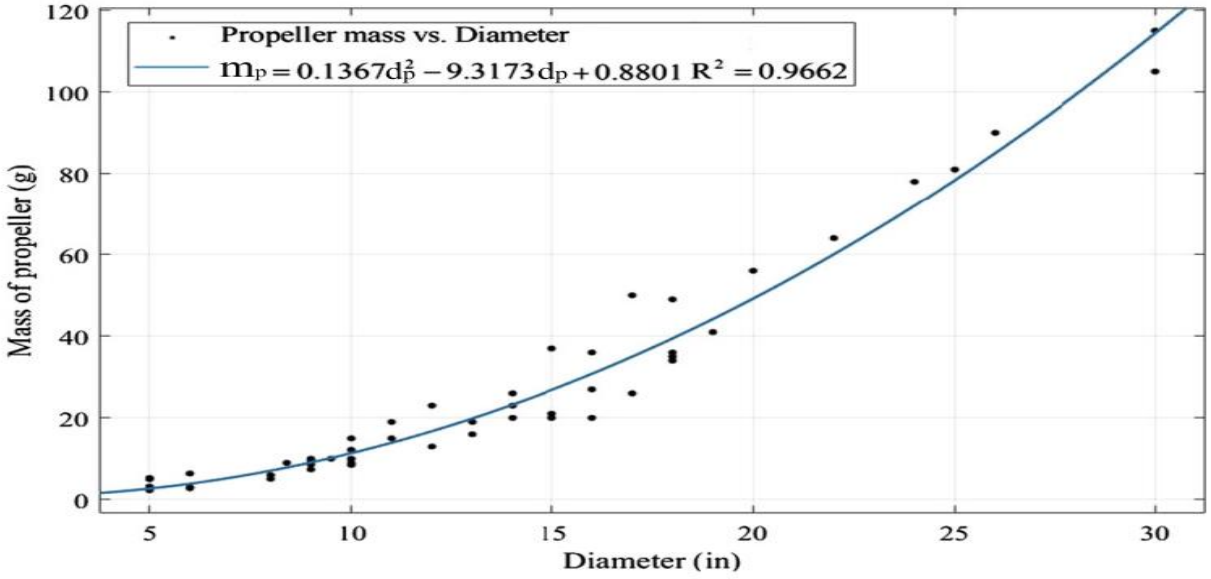

Figure 8. Mass of the Propeller (m_p) with respect to Diameter of the Propeller (d_p), (Vu NA et al, 2019)

$$m_p = 0.1367(d_p)\text{^}2 - 9.317(d_p) + 0.881\ [g] \quad (7)$$

F. Mass of the Frame (m_f) with respect to Diagonal Size of the Frame (l) and Thickness (t):

Mass of the Frame (m_f) is correlated linearly with respect to Diagonal Size of the Frame (l) and with 3 mm and 4 mm Thickness (t) and selected ABS material with density of averagely 1.04 kg/m^3. The results are given in Fig.9 and Eq.8 and Eq.9 respectively.

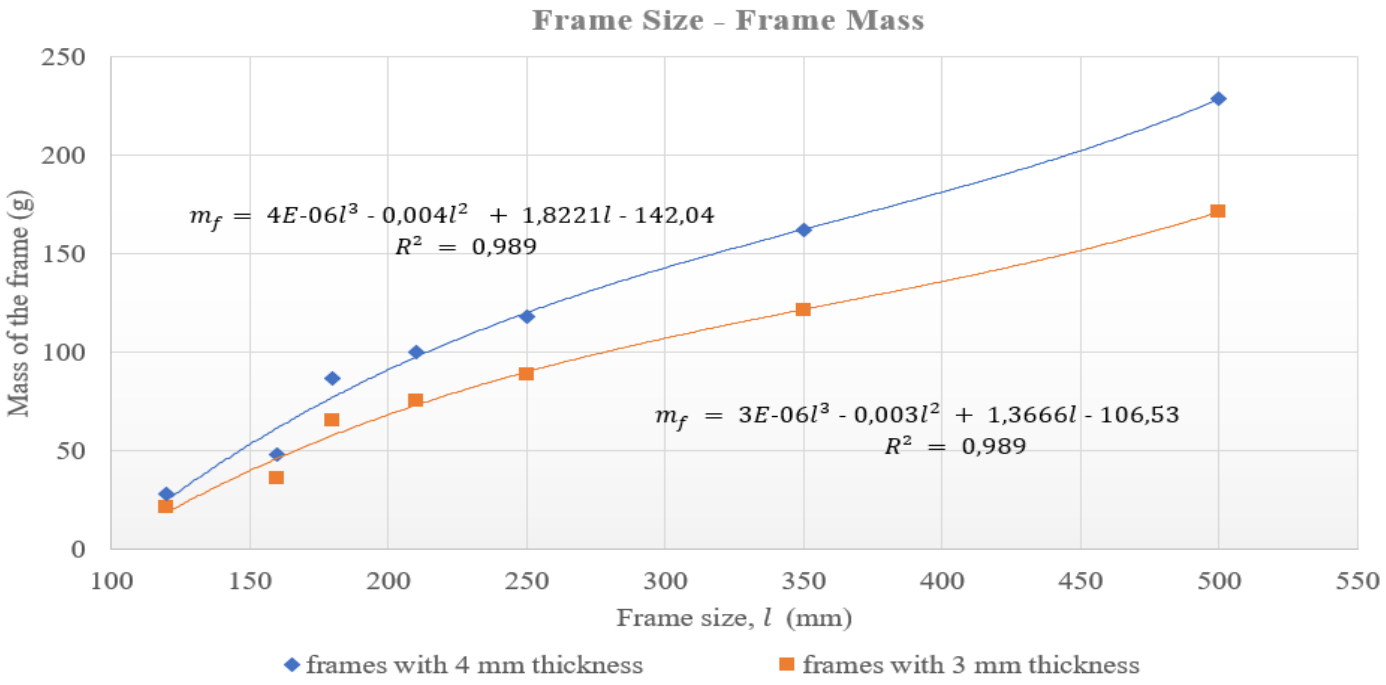

Figure 9. Mass of the Frame (m_f) with respect to Diagonal Size of the Frame (l) and Thickness (t)

For $t=3mm, m_f = 3E-06(l)^3 - 0.003(l)^2 + 1.3666(l) - 06.53$ *[g]* (8)

For $t=4mm, m_f = 4E-06(l)^3 - 0.004(l)^2 + 1.8221(l) - 142.04$ *[g]* (9)

Thus, inital GTOW was determined as a function of all selected parameters.

$$GTOW = f(T, I_{max}, C, n, d_p, l, t) \quad [N] \tag{10}$$

This initial GTOW (Eq.10) found will be used in the preliminary design of all components, and the necessary selections are easily completed as follows. As a result of the regression analysis and initial GTOW determination, the overall mass profile of the quadcopter is obtained. Based on the GTOW, required thrust values and propulsion system components are selected. Then, based on the propulsion system and frame weights, expected air cargo and payload capacities are corrected. GTOW including payloads were assumed as 12.50 N to calculate initial required thrust for each motor.

In the following sections, based on the initial GTOW (12.50 N) determined up to this point, performance analyses of the quadcopter are made in order to determine whether a second iteration of sizing is needed.

4. CFD Analyses and Performance Evaluations

Aerodynamic performance of the propellers of a quadcopter has considerable impact on quadcopter overall performance. Aerodynamic performance of a propeller can be defined in terms of some unitless parameters that are thrust coefficient (C_T), power coefficient (C_P), advance ratio (J), and propeller efficiency (η). (McCormic, 1994). The parameters are defined as follows:

$$C_T = \frac{T}{\rho \times n^2 \times D^2} \tag{11}$$

$$C_P = \frac{P}{\rho \times n^3 \times D^5} \tag{12}$$

$$J = \frac{V}{n \times D} \tag{13}$$

$$\eta = J \times \frac{C_T}{C_P} \tag{14}$$

where n is the rotational speed in revolutions per second and D is the propeller diameter (McCormic, 1994). Thus, thrust and power coefficients are functions of advance ratio, accordingly, Reynolds number and geometry of the propeller (Brandt and Selig, 2011). Reynolds number of the propeller is calculated based on the propeller chord at the 75% propeller blade-station (Brandt and Selig, 2011).

$$C_T = f(J, Re, propeller\ geometry) \tag{15}$$

$$C_P = f(J, Re, propeller\ geometry) \tag{16}$$

Computational fluid dynamics (CFD) analysis is performed to examine thrust performance of the propeller according to various airspeed and rotational speed values (Kutty and Rajendran, 2017). As a steady-state approximation, the Multiple Reference Frame (MRF) approach is applied to simulate rotation of the propeller without rotating mesh.

In the pre-processing step, the propeller geometry that is created in the Solidworks CAD software is imported the ANSYS Workbench Software. The computational domain is created as a static cylindrical zone and a rotating cylindrical subzone in it. The boundaries of the

zones are adjusted in sufficient dimensions based on the thickness studies (Stajuda et al, 2016) not to adversely affect the flow. Also, very large sizes are avoided to not to prolong the analysis time. The dimension of the computational domain is given in Fig.10.

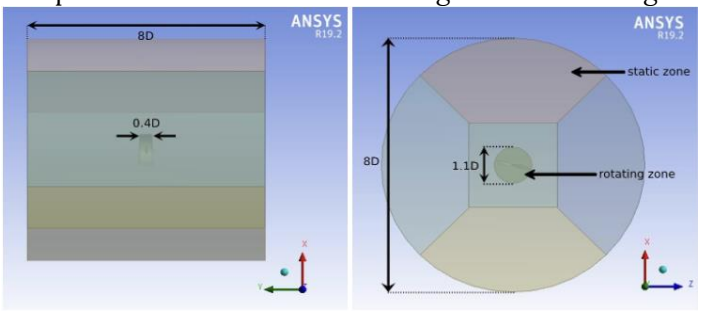

Figure.10 Computational domain dimensions from side and front views.

Table 2. Boundary Conditions

Boundary Name	Condition	Turbulence Intensity
Inlet	1 Atm static pressure and V∞= 0 m/s	1%
Outlet	1 Atm static pressure	1%

The computational domain is discretized by using ANSYS Fluent with the maximum skewness of 0.8 and minimum orthogonal quality of 0.2.

Two boundary conditions are set in solver step as shown in the Table 2. The inlet boundary condition describes the entrance of flow, and the outlet boundary condition describes exit of the flow. Cell zone condition setup is adjusted to the rotational speed values of the propeller for frame rotation.

The turbulence model is selected as k-ω SST model. In computational fluid dynamics, the k–omega (k–ω) turbulence model is a common two-equation turbulence model that is used as an approximation for the Reynolds averaged Navier–Stokes equations (RANS).

In the post-processing step, the thrust forces, pressure on the propeller, velocity streamlines, and volumetric renders of rotating computational domain with respect to several rpm values are compiled and visualized. Thrust and power coefficient results obtained by CFD analysis and experimental results are given in the Table 3.

Table 3. Propeller performance results (Propeller Thrust and Power Coefficients)

rpm	Re	C_T*	C_P*	C_T**	C_P**	C_T***	C_P***
4008	21e03	0.1161	0.0481	0.0817	0.0337	37.7%	35.2%
4500	23e03	0.1171	0.0481	0.0819	0.0336	35.3%	35.5%
5013	26e03	0.1176	0.0482	0.0821	0.0336	35.5%	35.7%
6500	33e03	0.1194	0.0482	0.0825	0.0333	36.5%	36.5%

*Experimental Results, **CFD Results

When the difference between numerical results and experimental results are examined, it is obviously seen that a significant difference is occurred. Increases in the rpm values cause consistent increases in the thrust coefficient and hence the thrust force increases. Also, it should not be neglected that the flow over a propeller is highly complex, it may require to run a transient analysis by expecting more accurate values with contrast to a steady-state analysis. By using transient analysis, dynamic mesh approach is can be used to simulate rotation of the propeller more accurately.

Further, when it is checked the pressure contour given in the Fig.11 and Fig.12, the thrust generation by the pressure gradient between propeller surfaces (upstream and downstream of disc) can be seen. Also, an increase in the pressure gradient with respect to increasing rotational velocity is expected.

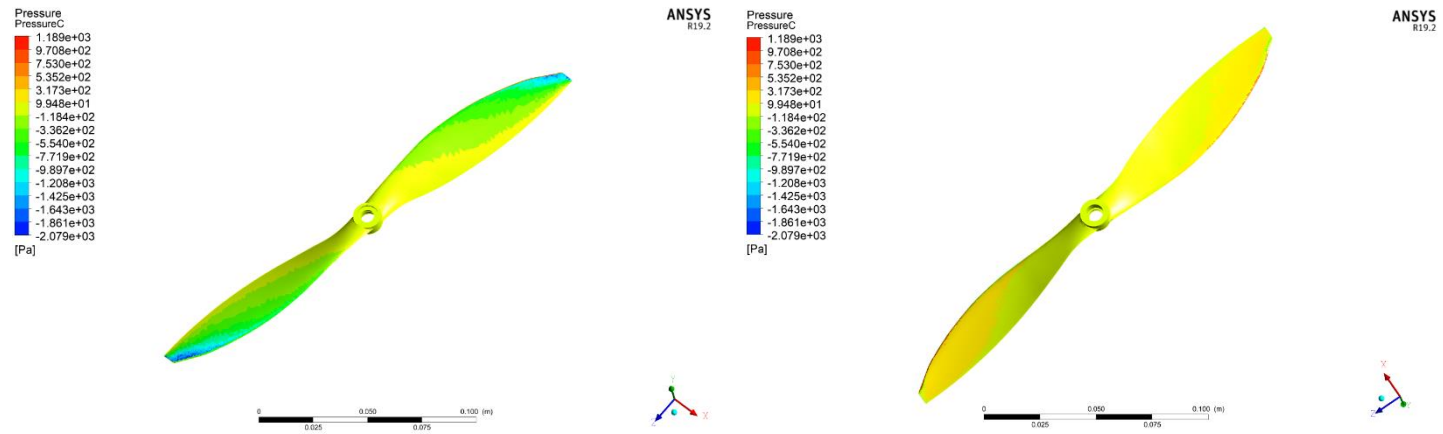

Figure 11. Pressure contour of the propeller a) front surface b) and back surface at 4008 rpm.

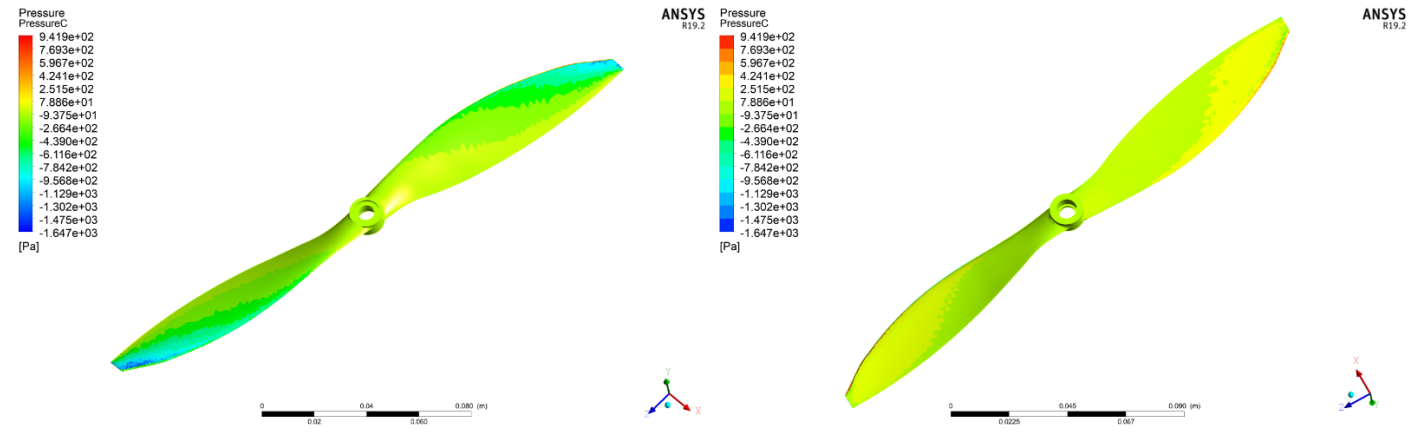

Figure 12. Pressure contour of the propeller a) front surface and b) back surface 4500 rpm.

Fig.13 and Fig.14 represent the forward velocity streamlines of the propeller in view of XY plane for 4008 and 6500 rpm values. It is clear from the figures that the velocity of the air in the rotating zone increases as the rotational velocity increases. The propeller induces a rotational velocity and accelerates air. As the rotational velocity of the propeller increases, the speed of air passes the propeller increases.

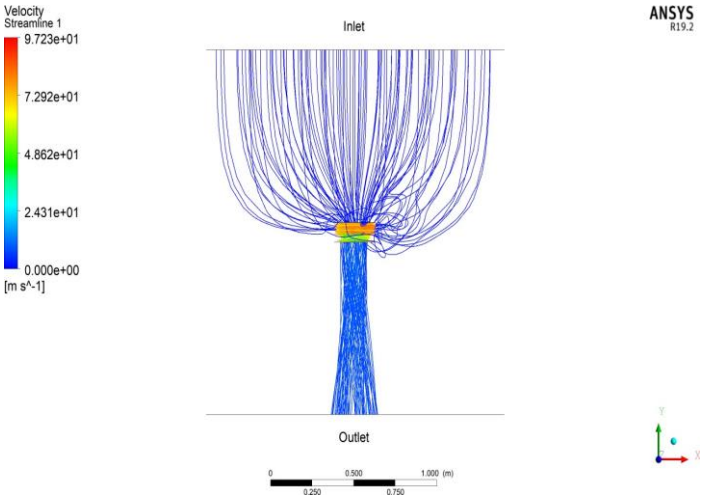

Figure 13. Forward velocity profile of computational domain at 4008 rpm.

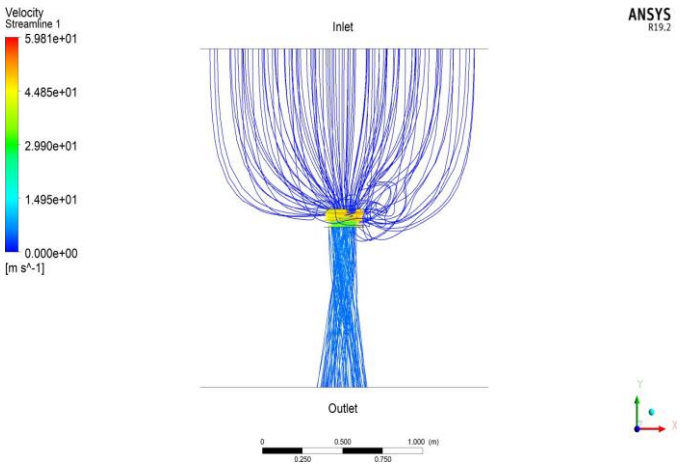

Figure 14. Forward velocity profile of computational domain at 6500 rpm

5. Results and Discussion

Preliminary design activities were carried out in order to provide the mission requirements selected based on the mission profile of the Cargo quadrotor UAV. Reducing the design iteration times within the scope of these activities will make a significant contribution to the designers. In the study, the focus is on pre-determining the components in the UAV at the Preliminary design stage and specified in Fig.3 with the current selection parameters and checking the required performance qualifications according to the weight of the UAV that will emerge after this selection. For this, the values that will ensure its performance in the take-off phase, and especially the Gross Take Off Weight (GTOW) should be taken into account, as the usage phase expected to show the highest capability from the UAV. However, in doing so, we need a systematic approach to find an accurate value and take it into account. We take this approach in the form of regression with the parameters that we will choose in all components to reach the initial GTOW. In this study, regression analyzes put forward in this way are detailed. For each component type, different existing products were examined, and a regression was created between the important basic parameters and component weight values. For some components, the values found in the literature have been taken into account. Thus, the initial GTOW calculation has been completed with the approaches created for all relevant component groups.

Thanks to the initial GTOW found, it is possible to make the first iteration of the design. After this stage, the preliminary design iteration continues by examining the effect of the resulting GTOW value on the selected components until the specified acceptable levels are reached. A comparison was made between the GTOW obtained as a result of the final component selections within the scope of the preliminary design, which emerged after these processes, and the initial GTOW obtained from the estimation regression approach as given at Table 4.

Table 4. Calculated mass compared to solution design mass based on selections

No	Component	Calculated Mass [g]	Solution Design Mass [g]	%Difference	Share-Calc %	Share-Act %
1	Motor (x4)	100.52	234.00	132.8%	8%	17%
2	Frame	162.25	252.80	55.8%	13%	19%
3	Battery	248.00	255.00	2.8%	20%	19%
4	Propeller (x4)	64.00	36.00	-43.8%	5%	3%
5	ESC (x4)	104.20	148.00	42.0%	8%	11%
6	Avionics	371.00	234.10	-42.3%	30%	16%
7	Air Cargo	200.00	200.00	-	-	-
8	TOTAL	1,250.00	1,359.90	8.8%		

6. Conclusions

After the comparison, it was observed that the success rate of the GTOW estimation regression approach presented in the study was at a reasonable level. With this method, it has been observed that the design iterations, which yielded results in a high level of compliance with the mission requirements, were carried out in shorter time periods.

It may be useful to mention the issues that can be addressed in the future as additional studies. In this context, after the approach used in this study, a structure can be created in which the resolution of the analyzes and calculations taken into account for the design iteration can be controlled. In addition, it would be beneficial to conduct additional trials with more effective alternatives such as Coupled analysis, with emphasis on diversification of performance analysis.

Nomenclature

UAV	: Unmanned Aerial Vehicle
GTOW	: Gross Take of Weight
ESC	: Electronic Speed Controller
GPS	: Global Positioning System
LIDAR	: Laser Imaging Detection and Ranging
g	: Gravitational Constant
CFD	: Computational Fluid Dynamics
BLDC	: Brushless Direct Current

CRediT Author Statement

Both authors committed that this statement page reflects an accurate and detailed description of their diverse contributions to the proposed Article as follows; **Fikret Kamil Corbaci**: Conceptualization, Methodology, Writing – Original Draft, Supervision, Writing – Review & Editing, Validation. **Yunus Emre Dogan:** Writing – Original Draft, Visualization, Investigation, Formal Analysis

References

Ahirwar, S., Swarnkar, R., Bhukya, S. and Namwade, G. (2019). Application of drone in agriculture. International Journal of Current Microbiology and Applied Sciences, 8(01), pp.2500-2505. https://doi.org/10.20546/ijcmas.2019.801.264

Brandt, J. and Selig, M., (2011). January. Propeller Performance Data at Low Reynolds Numbers. In 49th AIAA Aerospace Sciences Meeting including the New Horizons Forum and Aerospace Exposition (p. 1255). https://doi.org/10.2514/6.2011-1255

Corbaci, F.K. and Dogan, Y.E., (2023), Parametric Approach To Initial Weight Determination At Preliminary Design Of A Quadrotor Cargo UAV, ISUDEF '23 International Symposium on Unmanned Systems: AI, Design and Efficiency 2023, Sustainable Aviation.

Elouarouar, S. and Medromi, H. (2022). Multi-Rotors Unmanned Aerial Vehicles Power Supply and Energy Management. E3S Web of Conferences, 336, p.00068. https://doi.org/10.1051/e3sconf/202233600068

Jeongeun, K., Seungwon, K., Chanyoung, J. and Hyoungil, S. (2019). Unmanned Aerial Vehicles in Agriculture: A Review of Perspective of Platform, Control, and Applications. IEEE Transactions and Journals, Volume 4, 2016, pp.1-17. https://doi.org/10.1109/ACCESS.2019.2932119

Kutty, H.A. and Rajendran, P., (2017). 3D CFD Simulation and Experimental Validation of Small APC Slow Flyer Propeller Blade. Aerospace, 4(1), p.10. https://doi.org/10.3390/aerospace4010010

McCormick, B.W., (1994). Aerodynamics, Aeronautics, and Flight Mechanics. John Wiley & Sons. p.300.

Pugliese, L.D.P., Guerriero, F. and Macrina, G. (2020). Using drones for parcels delivery process. Procedia Manufacturing, 42, pp.488-497. https://doi.org/10.1016/j.promfg.2020.02.043

Stajuda, M., Karczewski, M., Obidowski, D. and Jóźwik, K., (2016). Development of A CFD Model for Propeller Simulation. Mechanics & Mechanical Engineering, 20(4):579-593.

Vu NA, Dang DK, Dinh TL (2019). Electric propulsion system sizing methodology for an agriculture multicopter. Aerospace science and technology, 90:314-326. https://doi.org/10.1016/j.ast.2019.04.044

Winslow J, Hrishikeshavan V, and Chopra I, (2018). Design methodology for small-scale unmanned quadrotors. Journal of Aircraft, 55(3):1062-1070. https://doi.org/10.2514/1.C034483

International Journal of Aviation Science and Technology

Research Article

Investigating Dynamic Behavior and Control Systems of the F-16 Aircraft: Mathematical Modelling and Autopilot Design

Masoud Norouzi[1*], Elbrus Caferov[2],

[1] *Istanbul Technical University, Aerospace Engineering Department, Istanbul, Turkiye*
norouzi20@itu.edu.tr- 0000-0002-7326-5021
[2] *Istanbul Technical University, Aerospace Engineering Department, Istanbul, Turkiye*
cafer@itu.edu.tr- 0000-0002-7742-2514

Abstract

The development of control systems for aerial vehicles necessitates a meticulous examination of their dynamic behavior. This research delves into an in-depth investigation of the dynamic behavior of the F-16 aircraft, employing refined mathematical models to analyze both its longitudinal and lateral motions, as well as their corresponding modes. These mathematical models are formulated in two conventional representations: state space equations and transfer functions. By utilizing these mathematical representations, two displacement autopilots have been developed, consisting of a pitch attitude autopilot based on the longitudinal equations and a roll attitude autopilot designed using the lateral equations. Proportional Integral Derivative (PID) controllers, encompassing inner loops, as well as Linear Quadratic Controllers (LQR), have been recruited as control system units. The control structures have undergone analysis utilizing Simulink models. The analyses have yielded favorable damping characteristics and faster responses in both longitudinal and lateral movements and modes.

Keywords

Flight Dynamics
Longitudinal Motion
Lateral Motion
Displacement Autopilots
LQR
PID
F-16 Aircraft

Time Scale of Article

Received 24 July 2023
Revised to 15 November 2023
Accepted 15 November 2023
Online date 30 December 2023

1. Introduction

The F-16 aircraft represents a multi-role fighter renowned for its exceptional maneuverability. Its prowess has been demonstrated in both air-to-air and air-to-surface missions. This high level of agility is attained by intentionally shifting the center of gravity(CG) from the stable region to the unstable region, resulting in a state of relaxed static stability (Reichert, 1993). Whenever the CG position falls within the unstable region, the F-16 aircraft can only sustain flight by relying on a flight control system known as the Control Augmentation System (CAS). This sophisticated flight control system alters the dynamic characteristics of the F-16, ensuring its stability even when the CG position is situated within the unstable CG region. Moreover, this control system offers the pilot the advantage of choosing task-specific control laws. For instance, a specialized control augmentation system is indispensable for high-performance fighter aircraft like the F-16, as it allows the pilot to execute intricate maneuvers, pushing the aircraft to its performance limits while performing tasks such as precision target tracking (Stevens and Lewis, 1992).

The issue of aircraft control has engendered a novel conundrum for control engineers within the scientific domain. It is widely acknowledged that aircraft dynamics exhibit a profoundly nonlinear nature, manifesting a robust interplay between longitudinal and lateral dynamics. This coupling intensifies markedly as the aircraft undertakes maneuvers at escalated angular rates and heightened angles of attack. Consequently, the development of a dependable controller becomes imperative to counteract such effects, all the while preserving noteworthy resilience against unaccounted-

*: Corresponding Author Masoud Norouzi, norouzi20@itu.edu.tr
DOI: 10.23890/IJAST.vm04is02.0203

for dynamics and parameter variations. Within the realm of flight control systems, the requisites for optimal performance fluctuate at varying attack angles. Notably, when the angle of attack is low, the primary performance objective lies in attaining impeccable maneuverability. Conversely, at high angles of attack, where the aircraft approaches or enters the stall regime, utmost emphasis must be placed upon preserving flight stability, albeit at the expense of some flight quality compromise. Moreover, in the context of fighter aircraft, the performance requisites may also undergo metamorphosis contingent upon the specifics of flight operations, encompassing factors like speed, attitude, pilot commands, and others (Ijaz et al., 2021). Stability analysis emerges as a momentous phenomenon necessitating comprehensive consideration to achieve the envisaged mission in consonance with the specific aircraft archetype. Noteworthy determinants encompass passenger comfort, the pilot's command over aircraft manipulation, the meticulous calculation of flight performance, sensor precision, and a myriad of other criteria divulged through an intricate evaluation of the aircraft's inherent stability. The ever-evolving technological landscape, characterized by amplified technical capacities, heightened maneuverability in temporal domains, and the proliferation of time-varying data such as ammunition and fuel specifics, impels the urgency of performance and efficiency computations alongside rigorous precision assessments. These verifications entail the meticulous utilization of aerodynamic efficiency data stemming from the aircraft's architectural blueprint, coupled with motion equations predicated upon aerodynamic coefficients, control surface efficacy evaluations, flight performance computations, and a host of other multifaceted considerations (Özcan and Caferov, 2022). Traditionally, flight control systems have been meticulously fashioned through the utilization of mathematical aircraft models, which undergo linearization at multiple operation points, leading to the programming of controller parameters contingent upon prevailing flight conditions (Andrade et al., 2017).

Autopilot systems have demonstrated a significant function in advancing aviation, as they actively enhance navigation protocols, aviation management, and the overall stability and control of the aerial vehicles (Nelson 1998). The inclusion of nonlinear terms in control algorithms introduces intricacy and heightened computational expenses. As a result, PID control algorithms have proven to be effective, owing to their straightforward nature, ease of implementation, and commendable performance across various instances (Kada and Ghazzawi 2011). Due to this nonlinearity, the conventional approach to designing flight control systems involves the utilization of mathematical models of the aircraft that are linearized at different flight conditions. Consequently, the controller parameters or gains are "scheduled" or adjusted based on the flight operating conditions (Vo and Seshagiri, 2008). The F-16 Air Combat Fighter leverages the concept of relaxed static stability (RSS) in the pitch axis, imparting amplified aerodynamic lift and mitigated trim drag. This technological breakthrough constitutes a paramount achievement for the F-16, entailing a state where the aircraft attains equilibrium along the pitch axis during subsonic flight conditions, such that the wing's center of lift aligns with or precedes the center of gravity. Consequently, the inclusion of a lifting tail becomes imperative. The RSS system exhibits a tendency to swiftly deviate if continuous activation of pitch stability augmentation is not sustained (Ammons, 1978).

In the present work, the progression towards the goals will be methodically executed through a gradual step-by-step approach, ensuring a meticulous achievement of each milestone. Consequently, the study is divided into two distinct sections, with each section comprising two groups. The initial section requires substantial effort and serves as the foundation for subsequent advancements, wherein the tools and knowledge gained from the first section are utilized. In the second section, control systems are designed for the constructed model. Both longitudinal and lateral aspects are individually addressed within each section, resulting in the subdivision of each section into two distinct groups. The dynamics model of system will be constructed by considering its geometrical, mechanical and aerodynamic characteristics of the aircraft. Wherever possible, extracted parameters from literature were listed in tables as much as possible and other needed parameters were calculated employing presented formulations from referred sources. Mathematical model of aircraft was developed in convenient representations to study its dynamic behavior. Then appropriate control systems for both longitudinal and lateral dynamics of modeled system were designed. The PID control method is widely utilized in the aviation industry due to its combination of simplicity and performance. In addition to the classical PID approach, the LQR method, recognized as a modern control technique, has been implemented as an alternative approach within the control systems structure.

2. Flight Dynamics and Modes of Motion; State Space Equations

The study commenced by deriving the flight dynamic equations and identifying the associated parameters. The resulting model will be presented in both state-space and transfer function formats, encompassing both longitudinal and lateral behaviors. The characteristics of these motions and their modes will be elucidated through the examination of the eigenvalues of the state

matrix. The state space representation of an aircraft is a mathematical presentation that describes the dynamic behavior of that aircraft using a set of state variables and input-output equations. This representation is commonly used in control engineering and flight dynamics analysis.

The state space model can be articulated in the subsequent manner (Eq 1):

$$\dot{x} = Ax + Bu\ , y = Cx \tag{1}$$

A :State Matrix

B :Input Matrix

C :Output Matrix

x :State Vector, Longitudinal; 〖x=[u,w,q, θ]〗 ^T

x :State Vector, Lateral; 〖x=[u,w,q, θ]〗 ^T

u :Input Vector

Developing a specific state space representation for an aircraft requires detailed knowledge of the aircraft's dynamics, aerodynamics, and control systems. The three matrices A to C are typically determined through system identification techniques, simulations, or flight test data analysis. Once the state space model is established, it can be used for various analyses, including stability analysis, control design, and performance evaluation.

The initial aim of this investigatin is to determine the matrices A and B, which are constructed using stability derivatives. The system matrix (state matrix) and input matrix (control matrix) for the longitudinal motion of the aircraft are provided as follows:

$$A = \begin{bmatrix} X_u & X_w & 0 & -g \\ Z_u & Z_w & u_0 & 0 \\ M_u + M_{\dot{w}}Z_u & M_w + M_{\dot{w}}Z_w & M_q + M_{\dot{w}}u_0 & 0 \\ 0 & 0 & 1 & 0 \end{bmatrix} \tag{2}$$

$$B = \begin{bmatrix} X_{\delta_e} & X_{\delta_T} \\ Z_{\delta_e} & Z_{\delta_T} \\ M_\delta + M_{\dot{w}}Z_\delta & M_{\delta_T} + M_{\dot{w}}Z_{\delta_T} \\ 0 & 0 \end{bmatrix} \tag{3}$$

Parameters inside matrices are combination of the stability derivatives. All these elements will be calculated separately.

$$X_u = \frac{1}{m}\frac{\partial X}{\partial u} = \frac{-QS(C_{D_u} + 2C_{D_0})}{mu_0} \tag{4}$$

$$X_W = \frac{QS(C_{L_0} - C_{D_\alpha})}{mu_0} \tag{5}$$

$$Z_u = \frac{-QS(C_{L_u} + 2C_{L_0})}{mu_0} \tag{6}$$

$$Z_w = \frac{-QS(C_{D_0} + C_{L_\alpha})}{mu_0} \tag{7}$$

$$M_u = \frac{QSc}{u_0 I_y} C_{m_u} \tag{8}$$

$$M_{\dot{w}} = \frac{-QSc^2}{2u_0^2 I_y} C_{m_{\dot{\alpha}}} \tag{9}$$

$$M_w = \frac{QSc}{u_0 I_y} C_{m_\alpha} \tag{10}$$

$$M_q = \frac{QSc^2}{2u_0 I_y} C_{m_q} \tag{11}$$

$$Z_{\delta_e} = \frac{-QS}{m} C_{Z_{\delta_e}} \tag{12}$$

$$M_{\delta_e} = \frac{QSc}{I_y} C_{m_{\delta_e}} \tag{13}$$

$$X_{\delta_e} = \frac{1}{m}\frac{\partial X}{\partial \delta_e} \tag{14}$$

$$X_{\delta_T} = \frac{1}{m}\frac{\partial X}{\partial \delta_T} \tag{15}$$

Which the including constants are as follow:

$$C_{L_u} = \frac{M^2}{1 - M^2} C_{L_0} \tag{16}$$

$$C_{m_{\dot{\alpha}}} = -2\eta C_{L_{\alpha_t}} V_H \frac{l_t}{c}\frac{d\varepsilon}{d\alpha} \tag{17}$$

$$V_H = \frac{S_t l_t}{S_w c_w} \tag{18}$$

$$\frac{d\varepsilon}{d\alpha} = \frac{2C_{L_{\alpha_w}}}{\pi A R_w} \tag{19}$$

$$C_{m_u} = \frac{\partial C_m}{\partial M} M \tag{20}$$

$$C_{Z_{\delta_e}} = -C_{L_{\alpha_t}} \tau . \eta \frac{S_t}{S} \tag{21}$$

$$C_{m_{\delta_e}} = C_{Z_{\delta_e}} \frac{l_t}{c} \tag{22}$$

Initial flight condition is supposed to be an altitude of 30,000 ft and flying angle of attack to be five degrees. Starting from atmospheric calculation using given altitude and Mach number. Temperature at an altitude is calculated using equation $T_{ISA} = T_0 - Bh$ and B is 2°C drop in temperature for each 1000 ft ascent. Under ISA conditions, at sea level T_0=15°C so $T_{ISA} = -45°C = 228.15\ K$ at desired altitude. Speed of sound calculated using (Eq 23):

$$a = \sqrt{\gamma RT} = 303\ m/s \tag{23}$$

γ :specific heat ratio (~1.4 for normal air at S.T.P)

R :gas constant (287.26 for air)

T :absolute temperature (k)

Then the initial speed of the aircraft can be reached using (Eq 24):

$$u_0 = M \times a = 0.6 \times 303 = 182\ \frac{m}{s} \tag{24}$$

For calculating air density, following equation (Eq 25) is used:

$$\frac{\rho}{\rho_0} = \left(1 - \frac{Bh}{T_0}\right)^{\frac{g}{RB}} \left(\frac{T_0}{T_0 - Bh}\right) = 0.374 \tag{25}$$

Air density at sea level (ρ_0) is 1.225 kg/m^3 so at the given altitude ρ=0.46 kg/m^3 then dynamic pressure can be obtained using (Eq 26):

$$Q = \frac{\rho u_0^2}{2} = 7618.52 \tag{26}$$

The Table 1 contains the mass and geometric attributes of the aircraft. The mathematical model is based on streamlined high-fidelity data sourced from NASA Langley wind-tunnel experiments performed on a scaled model of the studying airplane (Nguyen et al., 1979). "l_t" and "S_t "will be calculated using model geometry, further explanation is shown in Fig. 1 (Wikimedia drawing). " $C_{L_{\alpha_t}}$ " for biconvex airfoil of tail at M=0.6 achieved **2.86** from literature (Nguyen et al., 1979). It's assumed that $\eta = 1$. Calculated data are listed in Table 2. Before starting to calculate stability derivatives, the required nondimensional coefficients can be found in Table 3 from literature (Nguyen et al., 1979) or obtained using given above relations (Eq 16-22).

Table 1. Geometric Characteristics of the Aircraft

Parameter	**Weight [N]**	I_X **[kg.m2]**	I_Y **[kg.m2]**	I_Z **[kg.m2]**	I_{XZ} **[kg.m2]**	**b [m]**	**S [m2]**	**c [m]**	**CG location**	**AR**	**HT rc [m]**	**HT tc [m]**	b_t **[m]**
Value	91188	12875	75674	85552	1331	9.144	27.87	3.45	0.35 c	3.0	3.03	0.64	5.48

Table 2. Geometric Characteristics of the Horizontal Tail

Parameter	l_t**[m]**	S_t**[m2]**	**VH**	**dε/dα**	$C_{L_{\alpha_t}}$
Value	4.4	10.05	0.46	1.35	2.86

Table 3. Non-Dimensional Derivatives of Longitudinal Stability

Parameter	C_{D_0}	C_{L_0}	C_{m_q}	C_{L_α}	C_{X_q}	C_{Z_q}	C_{m_α}	$C_{L_{\alpha_w}}$	C_{D_α}	C_{L_u}	$C_{m_{\dot{\alpha}}}$	C_{m_u}	$C_{Z_{\delta_e}}$	$C_{m_{\delta_e}}$
Value	0.006	0.367	-5.45	3.11	2.46	-30.5	0.092	6.36	0.285	0.206	-4.530	0.159	-1.031	-1.315

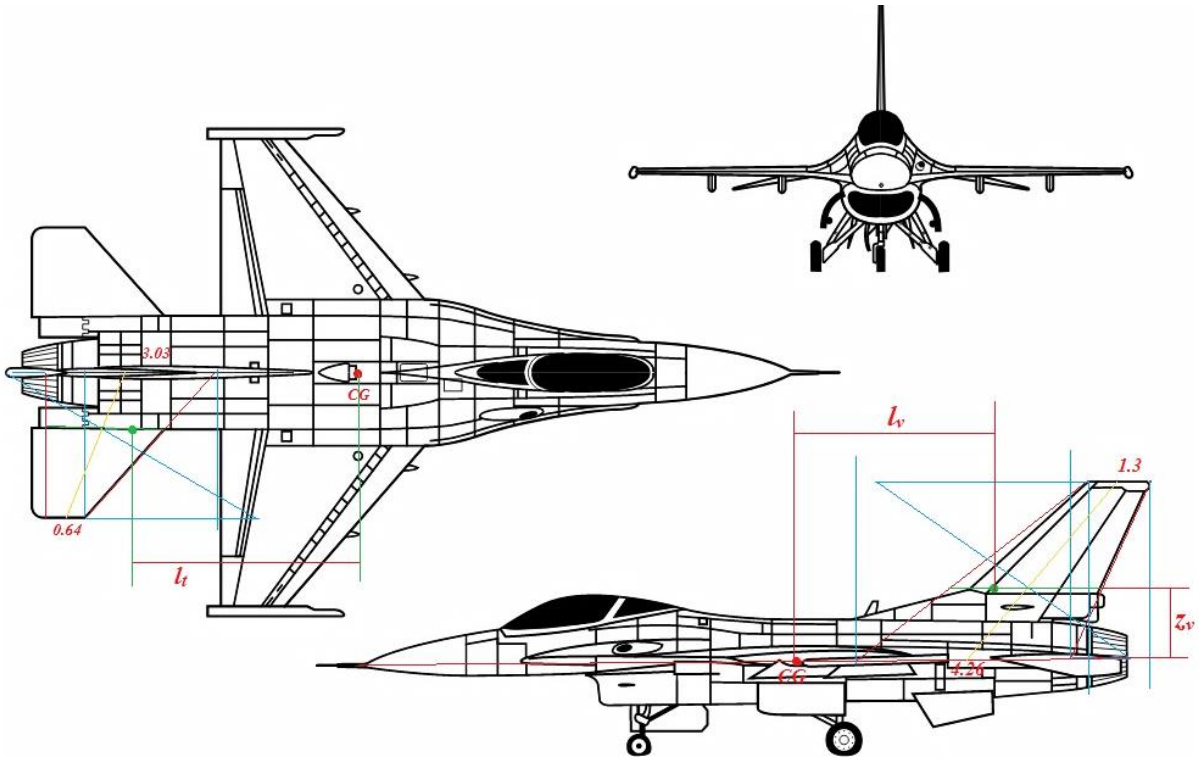

Fig. 1. Three view drawing of the F-16 aircraft (Wikimedia drawing), Linear dimensions are in meters

Table 4. Engine Characteristics

Parameter	**Idle Thrust** [N]	**Maximum Thrust** [N]	**Military Thrust [N]**
Value	1557	41300	20728

Table 5. Longitudinal Stability Derivatives

Parameter	X_u	X_W	Z_u	Z_w	$M_{\dot{w}}$	M_u	M_w	M_q	Z_{δ_e}	M_{δ_e}	X_{δ_e}	X_{δ_T}
Value	−0.0016	0.0103	-0.1179	-0.3907	0.0023	0.0085	0.0049	-0.5	23.5329	-12.7322	3.651	4.2711

Now the main parameters, i.e., stability derivatives can be achieved using mentioned relations (Eq 4-15). They are listed in Table 5 and thus forming of state and input matrices is feasible anymore. Two intended matrices (Eq 2&3) are introduced in the following:

$$A = \begin{bmatrix} -0.0016 & 0.0103 & 0 & -9.8 \\ -0.1179 & -0.3907 & 182 & 0 \\ 0.0082 & 0.0040 & -0.0814 & 0 \\ 0 & 0 & 1 & 0 \end{bmatrix} \quad (27)$$

$$B = \begin{bmatrix} 3.6510 & 4.2711 \\ 23.5329 & 0 \\ -12.6781 & 0 \\ 0 & 0 \end{bmatrix} \quad (28)$$

Previous matrices indicate longitudinal motion of the aircraft. The lateral motion is studied in the succeeding. State matrix "A" and Input matrix "B" are introduced below:

$$A = \begin{bmatrix} \frac{Y_\beta}{u_0} & \frac{Y_p}{u_0} & 0 & \frac{g\cos\theta_0}{u_0} \\ L_\beta & L_p & L_r & 0 \\ N_\beta & N_p & N_r & 0 \\ 0 & 1 & 0 & 0 \end{bmatrix} \quad B = \begin{bmatrix} 0 & \frac{Y_{\delta_r}}{u_0} \\ L_{\delta_a} & L_{\delta_r} \\ N_{\delta_a} & N_{\delta_r} \\ 0 & 0 \end{bmatrix} \quad (29)$$

Parameters inside matrices are a combination of the stability derivatives. All these elements will be calculated separately as previously it's done for longitudinal section.

$$Y_\beta = \frac{QS}{m} C_{Y_\beta} \quad (30)$$

$$L_\beta = \frac{QSb}{I_x} C_{l_\beta} \quad (31)$$

$$N_\beta = \frac{QSb}{I_z} C_{n_\beta} \quad (32)$$

$$Y_p = \frac{QSb}{2mu_0} C_{Y_p} \quad (33)$$

$$Y_r = \frac{QSb}{2mu_0} C_{Y_r} \quad (34)$$

$$L_p = \frac{QSb^2}{2I_x u_0} C_{l_p} \quad (35)$$

$$L_r = \frac{QSb^2}{2I_x u_0} C_{l_r} \quad (36)$$

$$N_p = \frac{QSb^2}{2I_x u_0} C_{n_p} \quad (37)$$

$$N_r = \frac{QSb^2}{2I_x u_0} C_{n_r} \quad (38)$$

$$Y_{\delta_r} = \frac{QS}{m} C_{Y_{\delta_r}} \quad (39)$$

$$L_{\delta_r} = \frac{QSb}{I_x} C_{l_{\delta_r}} \quad (40)$$

$$L_{\delta_a} = \frac{QSb}{I_x} C_{l_{\delta_a}} \quad (41)$$

$$N_{\delta_r} = \frac{QSb}{I_z} C_{n_{\delta_r}} \quad (42)$$

$$N_{\delta_a} = \frac{QSb}{I_z} C_{n_{\delta_a}} \quad (43)$$

Due to accessibility of all needed non dimensional coefficients from direct data or guessing using available plots in literature (Nguyen et al., 1979). There is no need to recalculate them, these data are listed in Table 6. The vertical tail characteristics are listed in Table 7 to be used for determining some coefficients that have to be calculated.

$$C_{l_{\delta_a}} = \frac{2C_{L_{\alpha_w}} \tau}{Sb} \int_{y_1}^{y_2} cy\, dy \quad (44)$$

$$C_{n_{\delta_a}} = 2KC_{L_0} C_{l_{\delta_a}} \quad (45)$$

For simplification of presented relation in (Eq 44) an illustration of the model is shown in Fig.2, an equation can be developed to determine (Eq 44). Using Thales's theorem for blue triangle in the Fig.2, it's been resulted:

$$\frac{(c-c_t)}{(c_r-c_t)} = \frac{\frac{b}{2}-y}{b/2} \quad \rightarrow \quad c = c_r - \frac{(c_r-c_t)}{(\frac{b}{2})} y \quad (46)$$

By substituting of this term instead of "c" integral term in (Eq 44) will be solved easily:

$$\int_{y_1}^{y_2} cy\, dy = \int_{y_1}^{y_2} \left(c_r y - \frac{(c_r-c_t)}{\frac{b}{2}} y^2 \right) dy$$

$$= \frac{c_r}{2} y^2 |_{y_1}^{y_2} - \frac{(c_r-c_t)}{\frac{3b}{2}} y^3 |_{y_1}^{y_2} \quad (47)$$

Two recently calculated derivatives have been included in Table 6. The elements of the studying matrices have been obtained using (Eq 30-43), and the resulting parameters are listed in Table 8. The state and input matrices for lateral motion can be formed using relations of (Eq 29). Controllability and observability matrices of "A" are full rank, i.e., state matrix "A" is controllable and observable.

$$A = \begin{bmatrix} -0.1504 & 0.0021 & -0.9970 & 0.0538 \\ -28.0786 & -1.6441 & 0.3334 & 0 \\ 5.4806 & -0.0810 & -1.5039 & 0 \\ 0 & 1 & 0 & 0 \end{bmatrix} \quad (48)$$

$$B = \begin{bmatrix} 0 & 0.0252 \\ 47.9237 & 9.5907 \\ -1.4297 & -1.9086 \\ 0 & 0 \end{bmatrix} \quad (49)$$

Table 6. Non-Dimensional Derivatives of Lateral Stability

Parameter	C_{Y_r}	C_{n_r}	C_{l_r}	C_{l_β}	C_{Y_β}	C_{Y_p}	C_{n_p}	C_{l_p}	C_{n_β}	$C_{Y_{\delta_r}}$	$C_{l_{\delta_r}}$	$C_{n_{\delta_r}}$	$C_{l_{\delta_a}}$	$C_{n_{\delta_a}}$
Value	0.939	-0.397	0.088	-0.186	-1.199	0.679	-0.021	-0.434	0.241	0.201	0.064	-0.084	0.318	-0.063

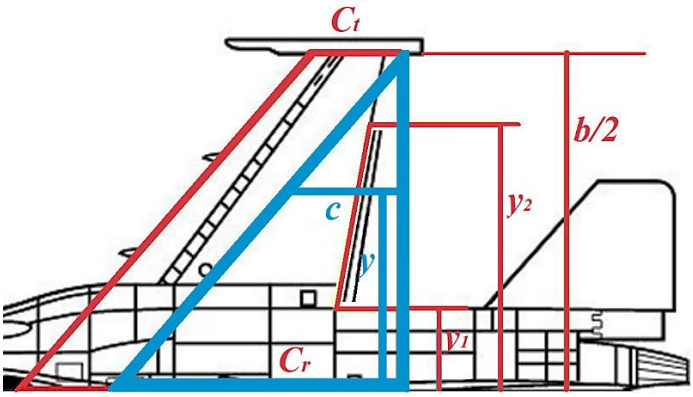

Fig. 2. Top View of the F-16, to Determine Some Geometric Dimensions (Wikimedia drawing).

Table 7. Geometric Characteristics of the Vertical Tail

Parameter	S_v [m2]	S_R [m2]	τr	τa	S_f [m2]	K	lv [m]	zv [m]	Vv	$C_{L_{\alpha_v}}$
Value	4.0	1.08	0.49	0.40	2.78	-0.27	3.8	1.3	0.06	2.86

Table 8. Lateral Stability Derivatives

Parameter	Y_β	L_β	N_β	Y_p	Y_r	L_p	L_r	N_p	N_r	Y_{δ_r}	L_{δ_r}	L_{δ_a}	N_{δ_r}	N_{δ_a}
Value	-27.38	-28.08	5.481	0.389	0.538	-1.644	0.333	-0.081	-1.504	4.588	9.591	47.92	-1.908	-1.429

3. Flight Dynamics and Modes of Motion; Transfer Functions

A very useful concept in the analysis and design of control systems is the transfer function. The transfer function gives the relationship between the output of and input to a system. In the case of aircraft dynamics, it specifies the relationship between the motion variables and the control input. To avoid undue mathematical complexity, simpler mathematical models are developed using longitudinal and lateral approximation so that the idea behind various autopilots can be examined (Nelson, 1998). For longitudinal modes, short-period (Eq 50) and phugoid mode (Eq 51) are introduced.

$$\frac{\Delta\alpha}{\Delta\delta_e}=\frac{As+B}{As^2+Bs+C} \quad , \quad \frac{\Delta q}{\Delta\delta_e}=\frac{As+B}{As^2+Bs+C} \tag{50}$$

$$\frac{\Delta u}{\Delta\delta_e}=\frac{As+B}{As^2+Bs+C} \quad , \quad \frac{\Delta\theta}{\Delta\delta_e}=\frac{As+B}{As^2+Bs+C} \tag{51}$$

Table 9. Constants A, B and C in the (Eq 50) and (Eq 51).

Fraction part	A	B	C
		Short-Period	
$\Delta\delta$	1	$-(M_q+M_{\dot\alpha}+Z_\alpha/u_0)$	$Z_\alpha M_q/u_0-M_\alpha$
$\Delta\alpha$	Z_δ/u_0	$M_\delta-M_qZ_\delta/u_0$	-
Δq	$M_\delta+M_{\dot\alpha}Z_\delta/u_0$	$M_\alpha Z_\delta/u_0-M_\delta Z_\alpha/u_0$	-
		Phugoid	
$\Delta\delta$	1	$-X_u$	$-Z_u g/u_0$
Δu	X_δ	gZ_δ/u_0	-
$\Delta\theta$	$-Z_\delta/u_0$	$X_uZ_\delta/u_0-X_\delta Z_u/u_0$	-

The values of present constants in above equations are listed in Table 9.

Table 10. Transfer Functions of Longitudinal Modes

	Modes
	Short-Period
$\frac{\Delta\alpha}{\Delta\delta_e}$	$\frac{(0.1293)s+(-12.7968)}{s^2+(0.4721)s+(-0.6964)}$
$\frac{\Delta q}{\Delta\delta_e}$	$\frac{(-12.7863)s+(5.0898)}{s^2+(0.4721)s+(-0.6964)}$
	Phugoid
$\frac{\Delta u}{\Delta\delta_e}$	$\frac{(3.6510)s+(1.2684)}{s^2+(0.0016)s+(0.0063)}$
$\frac{\Delta\theta}{\Delta\delta_e}$	$\frac{(-0.1293)s+(0.0021)}{s^2+(0.0016)s+(0.0063)}$

Substituting model characteristics in contents of Table 9 and using (Eq 50-51), resulted transfer functions are listed in Table 10.

The below relations (Eq 52) also used in (Eq 50) determination.

$$M_\alpha=u_0M_w \ , \ M_{\dot\alpha}=u_0M_{\dot w} \ , \ Z_\alpha=u_0Z_w \tag{52}$$

The same process is applying for lateral modes; Roll dynamics (Eq 53) and Dutch roll mode (Eq 54).

$$\frac{\Delta p}{\Delta\delta_a}=\frac{L_{\delta_a}}{s-L_p} \quad , \quad \frac{\Delta\emptyset}{\Delta\delta_a}=\frac{L_{\delta_a}}{s(s-L_p)} \tag{53}$$

$$\frac{\Delta\beta}{\Delta\delta_r}=\frac{As+B}{As^2+Bs+C} \quad , \quad \frac{\Delta r}{\Delta\delta_r}=\frac{As+B}{As^2+Bs+C} \tag{54}$$

$$\frac{\Delta\beta}{\Delta\delta_a}=\frac{As+B}{As^2+Bs+C} \quad , \quad \frac{\Delta r}{\Delta\delta_a}=\frac{As+B}{As^2+Bs+C}$$

Table 11. Constants A, B and C in the (Eq 54) For Dutch Roll Mode

Fraction part		A	B	C
$\Delta\boldsymbol{\delta}$		1	$-(Y_\beta + u_0 N_r)/u_0$	$(Y_\beta N_r - Y_r N_\beta + u_0 N_\beta)/u_0$
$\boldsymbol{\delta_r}$	$\Delta\boldsymbol{\beta}$	Y_r/u_0	$(Y_r N_{\delta_r} - Y_{\delta_r} N_r - u_0 N_{\delta_r})/u_0$	-
	$\Delta\boldsymbol{r}$	N_{δ_r}	$(N_\beta Y_{\delta_r} - Y_\beta N_{\delta_r})/u_0$	-
$\boldsymbol{\delta_a}$	$\Delta\boldsymbol{\beta}$	0	$(Y_r N_{\delta_a} - u_0 N_{\delta_a})/u_0$	-
	$\Delta\boldsymbol{r}$	N_{δ_a}	$-Y_\beta N_{\delta_a}/u_0$	-

Presented constants in (Eq 54) detailed in Table 11. Using model characteristics in (Eq 53-54), resulted transfer functions for lateral modes are listed in Table 12.

Table 12. Transfer Functions of Lateral Modes

Modes	
Roll Dynamics	
$\frac{\Delta p}{\Delta \delta_a}$	$\frac{47.9237}{s + 1.6441}$
$\frac{\Delta \emptyset}{\Delta \delta_a}$	$\frac{47.9237}{s(s + 1.6441)}$
Dutch Roll	
$\frac{\Delta \beta}{\Delta \delta_r}$	$\frac{(0.0029)s + (1.9408)}{s^2 + (1.6543)s + (5.6906)}$
$\frac{\Delta r}{\Delta \delta_r}$	$\frac{(-1.9086)s + (-0.1489)}{s^2 + (1.6543)s + (5.6906)}$
$\frac{\Delta \beta}{\Delta \delta_a}$	$\frac{(1.4254)}{s^2 + (1.6543)s + (5.6906)}$
$\frac{\Delta r}{\Delta \delta_a}$	$\frac{(-1.4297)s + (-0.2150)}{s^2 + (1.6543)s + (5.6906)}$

Eigenvalues of matrix A are roots of the characteristic equation of system and are obtained by solving this equation: $|\lambda I - A| = 0$. Matrix A for short-period mode is shown in (Eq 55).

$$A = \begin{bmatrix} Z_\alpha/u_0 & 1 \\ M_\alpha + M_{\dot\alpha} Z_\alpha/u_0 & M_q + M_{\dot\alpha} \end{bmatrix} \rightarrow A_{sh} = \begin{bmatrix} -0.3907 & 1 \\ 0.7282 & -0.0814 \end{bmatrix} \quad (55)$$

Eigenvalues for short period mode are resulted "λ_1= **-1.1033", "λ_2= 0.6312".** This mode is including an unstable pole in the right side of the origin. Eigenvalues for phugoid mode are "$\boldsymbol{\lambda_{1,2}}$**= -0.0008 ± 0.0767i"** which shows almost a stable situation. Matrix A for phugoid mode is shown in (Eq 56).

$$A = \begin{bmatrix} X_u & -g \\ -\frac{Z_u}{u_0} & 0 \end{bmatrix} \rightarrow A_{ph} = \begin{bmatrix} -0.0016 & -9.81 \\ 0.0006 & 0 \end{bmatrix} \quad (56)$$

Determined eigenvalue for roll mode can be acquired using (Eq 57) that is resulted"$\boldsymbol{\lambda_{roll} = -1.6441}$" which is a stable and reasonable root in the left side of the origin.

$$\lambda_{roll} = L_p \quad (57)$$

For Dutch roll mode we neglected rolling moment equation and stated that depend on sideslip and yawing rate as is shown in (Eq 58). Eigenvalues for Dutch roll mode are "$\boldsymbol{\lambda_{1,2}}$**= -0.8272 ± 2.2374i".** These values indicate a stable situation for this mode.

$$\begin{bmatrix} \Delta\dot\beta \\ \Delta\dot r \end{bmatrix} = \begin{bmatrix} Y_\beta/u_0 & (Y_r/u_0) - 1 \\ N_\beta & N_r \end{bmatrix} \begin{bmatrix} \Delta\beta \\ \Delta r \end{bmatrix} \rightarrow A = \begin{bmatrix} -0.1504 & -0.9970 \\ 5.4806 & -1.5039 \end{bmatrix} \quad (58)$$

Furthermore, it is important to mention that the spiral mode, which is considered one of the lateral modes, has not been considered in this study. The corresponding eigenvalue for the spiral mode has been determined to be "$\boldsymbol{\lambda_{spiral} = -1.4388}$". Typically, this value is in close proximity to the origin.

This pole arrangement on s-plane is usual for an aircraft with aft CG (Denieul et al., 2017). As manufacturer says and pilots confirm; this aircraft is very unstable. Moreover, flap effectiveness of this kind of elevator (Stabilator) is one. All these are preconditions for having an agile vehicle. For simulation, engine is supposed to work in half of its maximum thrust ($\delta_T = 0.5$) that is about in military thrust range (Nguyen et al., 1979). For lateral states behavior, roll angle is the most affected to aileron input, after that roll rate is sensitive to this control surface. Rudder deflection causes sideslip and yaw moment, since yaw and roll motions inevitably related to each other, as a lateral motion we study, both yaw and roll rates and also sideslip and roll angles are affected enormously

4. Control Modelling; Autopilot Design

In previous section it was discussed about two types of aircraft stability and achieved related mathematical model in both state space and transfer function representations. In this section the objective is embedding an appropriate controller in these models and reaching desired and reasonable states. A simple pitch control autopilot has been developed to maintain longitudinal stability of the model; using conventional PID and LQR, trying to hold pitch angle close to desired input as much as possible without any noise in final signal. By using inner rate feedback loop we are able to stabilize system. The model's block diagram is shown in Fig. 3.

In the event that the PID controller parameters (namely, the gains of the proportional, integral, and derivative terms) are inappropriately selected, the controlled process input may become unstable, exhibiting a diverging output, either with or without oscillations, and limited solely by saturation or mechanical failure. The underlying cause of instability lies in an excessive gain, especially in the presence of significant lag. Generally, response stabilization is imperative, ensuring the absence of oscillations under all combinations of process conditions and set points, although, on certain occasions, marginal stability (bounded oscillation) may be deemed acceptable or desirable. Introducing a PID

controller to an F-16 aircraft will lead to an enhanced steady-state solution, reduced rise time, and an improved transient response, thus yielding greater accuracy in its performance (Sayegh, 2014).

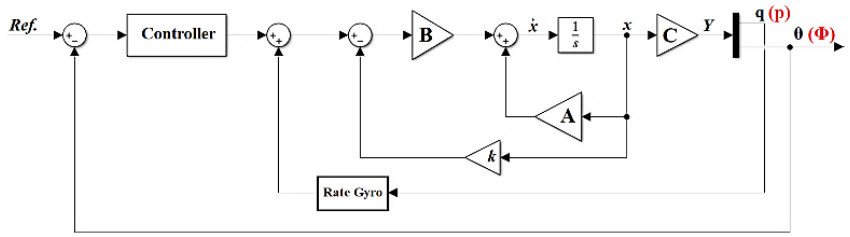

Fig. 3. Pitch/Roll autopilot block diagram in state space form using PID controller

It can be demonstrated that if the system is state-controllable, it becomes feasible to devise a linear control law that can achieve any desired closed-loop eigenvalue structure. For a single-input system, the control law is represented by (Eq 59), where "η" denotes the control input, and "k" is a column matrix or vector of unknown gains. The Bass-Gura method offers a straightforward approach to determine the gains required for a specific eigenvalue structure. The plant matrix, in general, may not be in the companion form. If the system is not in the companion form, we can employ a transformation using (Eq 60), wherein "V" denotes the controllability test matrix, "W" forms a triangular matrix based on the coefficients of the open-loop characteristic equation, and "$\bar{a}$" and "a" represent the coefficients of the desired closed-loop characteristic equation and the coefficients of the open-loop plant matrix characteristic equation, respectively (Nelson, 1998). This parameters for studying model are listed in Table 13. By incorporating the "$\boldsymbol{k}$" parameter into the block diagram illustrated in Fig. 3, and leveraging the inner loop(s) and PID controller, a robust methodology can be established to address instability and achieve desirable outcomes within the control systems architecture.

$$\eta = -k^T x \tag{59}$$

$$k = [(VW)^T]^{-1}[\bar{a} - a] \tag{60}$$

Table 13. Performance values of PID

a	$\bar{a}$	V	W
		longitudinal	
0.4737 - 0.6942 0.0640 0.0268	0.8 0.8 0.1 0.1	$\begin{bmatrix} 3.7 & 0.2 & 100.4 & 0 \\ 23.5 & -2317 & 1115 & -2151 \\ -12.7 & 1.2 & -9.4 & 6 \\ 0 & -12.7 & 1.2 & -9.4 \end{bmatrix}$	$\begin{bmatrix} 1 & 0.47 & -0.69 & 0.64 \\ 0 & 1 & 0.47 & -0.69 \\ 0 & 0 & 1 & 0.47 \\ 0 & 0 & 0 & 1 \end{bmatrix}$
		Lateral	
3.2984 8.4961 13.2236 2.1735	3.3 8.5 13.2 2	$\begin{bmatrix} 0 & 1.5 & 3.9 & -22 \\ 48 & -79 & 87 & -247 \\ -1.4 & -1.7 & 17.4 & -11.8 \\ 0 & 48 & -79 & 87 \end{bmatrix}$	$\begin{bmatrix} 1 & 3.29 & 8.49 & 13.22 \\ 0 & 1 & 3.29 & 8.49 \\ 0 & 0 & 1 & 3.29 \\ 0 & 0 & 0 & 1 \end{bmatrix}$

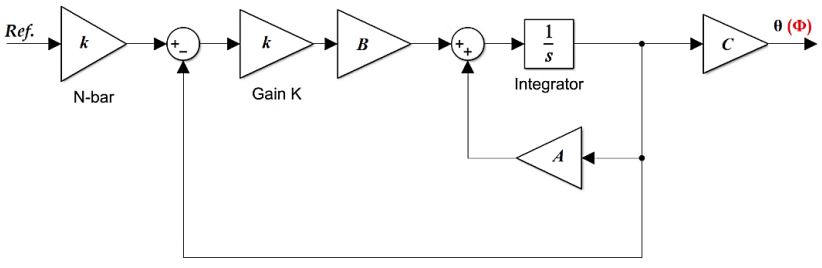

Fig. 4. Pitch/Roll autopilot block diagram using LQR controller

LQR controller as a modern control approach is another strategy which is used here to build the pitch autopilot. This autopilot's block diagram including state-space matrices and controller gains is shown in Fig. 4.

Results from two approaches are shown in Fig. 5. For longitudinal pitch control. Investigating the results for Pitch revealed that rise time from PID method is about 0.1 second, settling time for two percent of final value is around 1 second, with 14 percent overshoot. Without

accounting on inner loop, the system at most could be marginally stable with lots of disturbing oscillations and here the importance of the inner loop in increasing damping of the system is obvious. From LQR results rise time was around 2.3 seconds and settling time around 4 seconds with no overshoot, which is too slow.

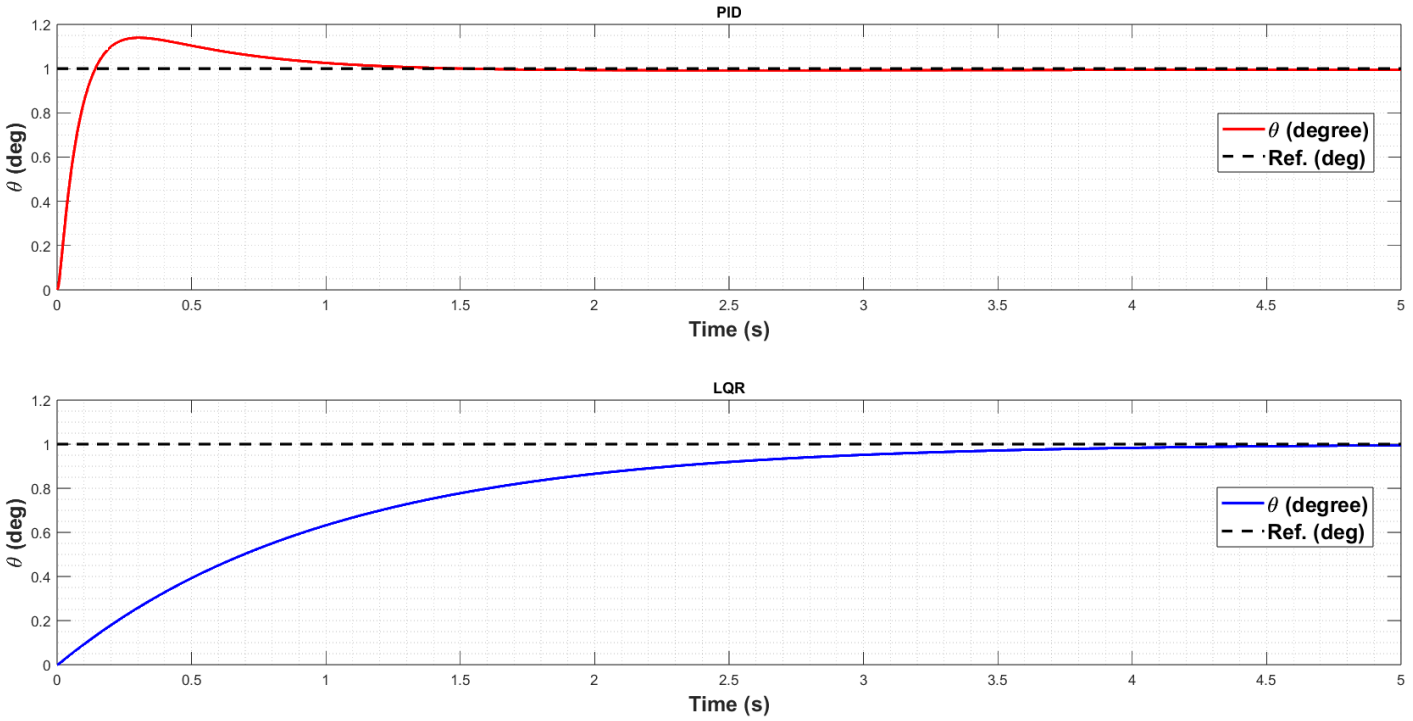

Fig. 5. Pitch control using **top**) PID **down**) LQR controller

In the F16 aircraft, both the aileron and the stabilator, which functions as a differential tail, contribute to roll and lateral motion to enhance maneuverability. When the aileron is deflected by 4 degrees, the differential tail deflects approximately 1 degree. However, the involvement of the differential tail in the system has not been considered in this study. The roll attitude autopilot design is presented in Fig. 3, while the control block diagram for the roll autopilot, utilizing the LQR approach, is depicted in Fig. 4. The system's response to these configurations is illustrated in Fig. 6.

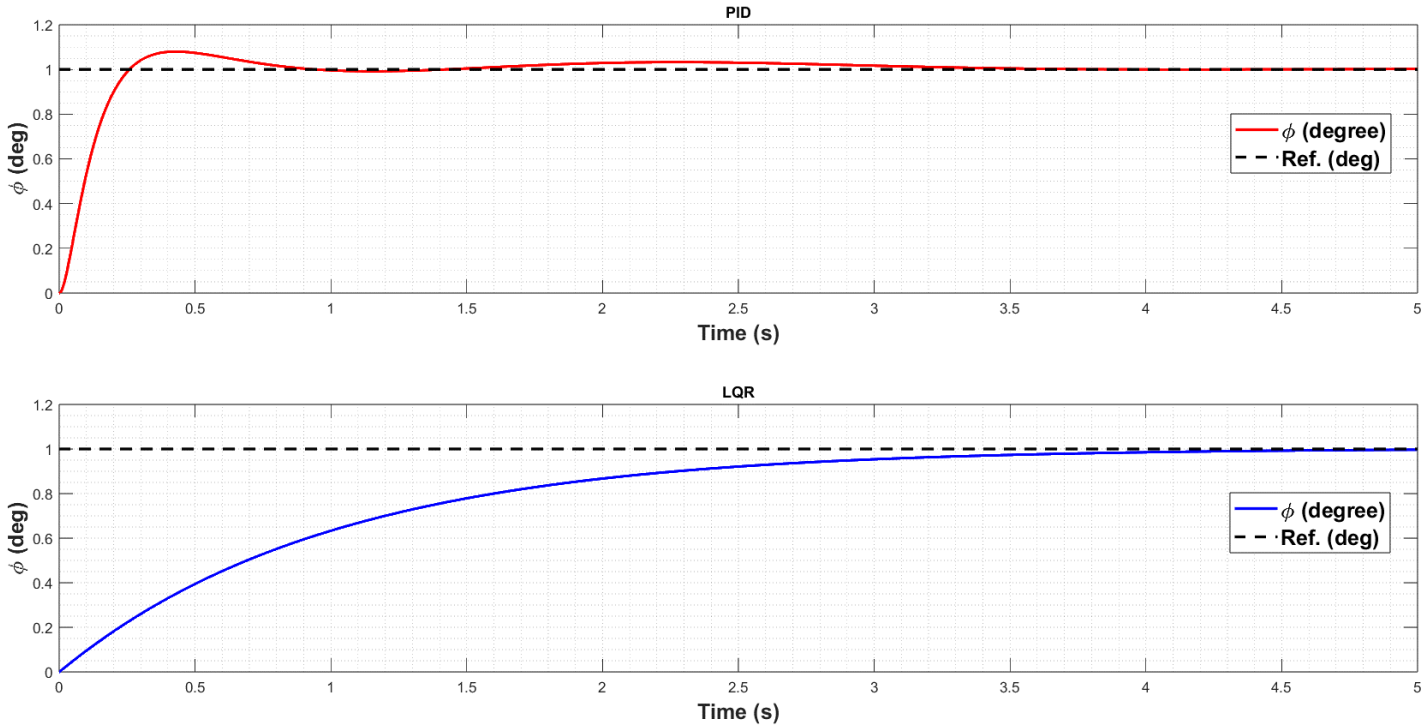

Fig. 6. Roll control using **top**) PID **down**) LQR controller

5. Results and Discussion

PID control is a classical control method widely used in various engineering applications, including aircraft control systems. It operates based on error feedback, continuously adjusting the control inputs (control surfaces) in proportion to the contrast between the desired and current states. On the other hand LQR is a modern control technique based on optimal control theory. It considers a cost function that quantifies the system's performance and aims to minimize it. LQR is capable of providing an optimal control law that balances the trade-off between control effort and performance. The choice between PID and LQR control for the F-16 pitch and roll autopilot design depends on several factors, including performance requirements, implementation complexity, and available resources. LQR generally provides superior performance compared to PID control in terms of precision, stability, and ability to handle disturbances. LQR's optimal control formulation allows for fine-tuning control efforts to achieve desired performance. PID control is relatively straightforward to implement and tune. It has been used successfully in many control systems, including older aircraft models. However, it may require more tuning effort to achieve desired performance. LQR is more adaptable to various operating conditions and can handle a broader range of aircraft dynamics. As aircraft become more advanced and incorporate additional complexities, LQR's flexibility becomes advantageous. PID control is computationally lighter and may be preferred for systems with limited processing power. LQR, being an optimal control approach, might require more computational resources. Finally, the implementation complexity and available resources should also be taken into consideration when making the final design decision.

Whitin this study, the PID controller yields a rise time of approximately 0.2 seconds and a settling time of about 3 seconds for two percent of the final value, accompanied by an overshoot of 8 percent. On the other hand, employing the LQR approach results in a rise time of around 2 seconds and a settling time of approximately 4 seconds, with no overshoot. The second approach demonstrates the absence of overshoot; however, it is slower in comparison. In contrast, the first approach exhibits a slight overshoot, which is inevitable, but offers significantly faster performance. The detailed results obtained from the simulations are presented in Table 14. The outcomes for both the pitch and roll autopilots are deemed satisfactory and reasonable when compared to the existing literature (Ahmed et al., 2019), (Stachowiak and Bosworth, 2004) and (Lu and Wu, 2005). Here, considerably superior outcomes are achieved in comparison to those presented in the initial literature. Moreover, it is important to acknowledge that a variety of results may be observed within an acceptable range, attributable to the collection of information from diverse sources under distinct operating conditions. Furthermore, by altering the Q and R matrices in the LQR strategy, superior results can be attained. Nevertheless, it is preferable to adhere to the main approach to avoid the complexities of model instability and ensure the validity of the simulation data.

6. Conclusions

Within this study, state-space representations were constructed for both longitudinal and lateral dynamics of the system. Additionally, transfer functions were derived to describe the dynamic modes. Subsequently, two autopilots were designed for pitch and roll control, employing both PID and LQR methods. The PID technique has demonstrated its remarkable effectiveness in the design of autopilots, surpassing the performance achieved by the LQR control system. This superiority is evident in Table 14, where the results of the PID approach outperform those of the LQR control system across various performance criteria under this typical simulation conditions.

Table 14. Performance values of PID and LQR

Method	Rise time	Settling time	Overshoot
Pitch Autopilot			
PID	0.10 s	1.07 s	13.9 %
LQR	2.28 s	3.85 s	0
Roll Autopilot			
PID	0.17 s	2.88 s	7.9 %
LQR	2.18 s	3.75 s	0

In future research endeavors, it is recommended to enhance the realism of the study by incorporating the dynamics of actuators through the utilization of appropriate transfer functions. Additionally, the dynamic representations obtained can be employed to design additional autopilot systems using both the PID and LQR approaches. While it can be acknowledged that modern control theories, such as "Adaptive Control", "Model Predictive Control (MPC)", "Sliding Mode Control (SMC)", "H-infinity Control", "Fuzzy Logic Control" and "Neural Networks" are known to exhibit robust performance in autopilot design and contribute to the overall effectiveness and safety of aircraft operations, The primary aim of this study was to establish a comprehensive understanding of the principles underlying analytical modelling of aircraft dynamics and the analysis of its control systems. The main focus was to take the initial step in this field of study with precision, thereby establishing a solid groundwork for future research and exploration.

Nomenclature

S.T.P	: Standard Temperature and Pressure
b	: Wing Span
S	: Wing Area
c	: Mean Aerodynamic Chord
CG	: Centre of Gravity
AR	: Wing Aspect Ratio
HT	: Horizontal Tail
rc	: Root Chord
tc	: Tip Chord
b_t	: Tail Span
l_t	: Distance Between CG and Aerodynamic Centre of HT
S_t	: Horizontal Tail Area
V_H	: Tail Volume Ratio
$d\varepsilon/d\alpha$	: Downwash Change
η	: Flap Effectiveness
S_v	: Vertical Tail Area
S_R	: Rudder Area
τ_r	: Rudder Effectiveness
τ_a	: Flaperon Effectiveness
S_f	: Flaperon Area
K	: Empirical Factor
VT	: Vertical Tail
l_v	: Horizontal Range Between Aerodynamic Centre of VT and CG
Z_v	:Vertical Range Between Aerodynamic Centre of VT and CG

CRediT Author Statement

Masoud Norouzi: Methodology, Software, Data Curation, Validation, Formal Analysis, Writing-Original Draft, Visualization, Writing-Review & Editing. **Elbrus M. Caferov**: Conceptualization, Project Administration, Supervision, Resources.

References

Ahmed, W., Li, Z., Maqsood, H. and Anwar, B., (2019). System Modelling and Controller Design for Lateral and Longitudinal Motion of F-16. Automation, Control and Intelligent Systems. Vol. 7, No. 1, 2019, pp. 39-45. doi: 10.11648/j.acis.20190701.15

Ammons, E.E., (1978). F-16 Flight Control System Redundancy Concepts, General Dynamics, Fort Worth Division, Fort Worth, Texas, USA

Andrade, J.P.P, Campos, V.A.F., Potts, A.S. and Garcia, C., (2017). Damping Improvement of a F-16 Aircraft through Linear Matrix Inequalities. International Federation of Automatic Control (IFAC) Hosting by Elsevier Ltd., IFAC PapersOnLine 50-1 (2017) 3947–3952

Denieul, Y., Guibé, J.B., Alazard, D., Toussaint, C., Taquin, G., (2017), Multicontrol Surface Optimization for Blended Wing-Body Under Handling Quality Constraints. Journal of Aircraft, American Institute of Aeronautics and Astronautics ,pp.1-14. DOI: 10.2514/1.C034268

Ijaz, S., Fuyang, C., Hamayun, M.T. and Anwaar, H. (2021). Adaptive integral-sliding-mode control strategy for maneuvering control of F16 aircraft subject to aerodynamic uncertainty. Applied Mathematics and Computation 402 (2021) 126053, www.elsevier.com/locate/amc

Kada, B. and Ghazzawi, Y., (2011), Robust PID Controller Design for an UAV Flight Control System. World Congress on Engineering and Computer Science (WCECS), San Francisco, USA, ISBN: 978-988-19251-7-6

Li, B. and Wu, F., (2005). Probabilistic Robust Control Design for An F-16 Aircraft. AIAA Guidance, Navigation, and Control Conference and Exhibit, San Francisco, California

Nelson, R.C., (1998). Flight Stability and Automatic Control, WCB/McGraw-Hill, ISBN 0-07-046273-9

Nguyen, L.T., Ogburn, M.E, Gilbert, W.P., Kibler, K.S., Brown, P.W. and Deal, P.L., (1979). Simulator Study of Stall/Post-Stall Characteristics of a Fighter Airplane With Relaxed Longitudinal Static Stability, NASA Technical Paper 1538, Langley Research Center, Hampton, Virginia, available at: https://www.cs.odu.edu/~mln/ltrs-pdfs/NASA-79-tp1538.pdf (accessed 20 April 2022)

Özcan, A.B. and Caferov, E., (2022). Frequency Domain Analysis of F-16 Aircraft in a Variety of Flight Conditions. International Journal of Aviation Science and Technology, Volume 3, Issue 1, (2022), 21-34, DOI: 10.23890/IJAST.vm03is01.0103

Reichert, G., (1992/1993). Flugmechanik III: Flugeigenschaftskriterien, Elastisches Flugzeug und Aktive Steuerung, Vorlesungsmanuskript, Institut fuer Flugmechanik des TU Braunschweig, Germany

Sayegh, Z.E. and Deghidy, A., (2014). Auto Pilot Design for F-16. Technical Report, A Project Submitted to the Graduate Faculty of The University of Concordia, Montreal, Quebec, Canada, DOI:10.13140/RG.2.2.36709.91362, https://www.researchgate.net/publication/325450374

Stachowiak, S.J. and Bosworth, J.T, (2004). Flight Test Results for the F-16XL With a Digital Flight Control System. NASA/TP-2004-212046, NASA Dryden Flight Research Center Edwards, California, USA

Stevens, B.L. and Lewis, F.L., (1992). Aircraft Control and Simulation, A Wiley-Interscience Publication, John Wiley & Sons, Inc.

Vo, H. and Seshagiri, S., (2008). Robust Control of F-16

Lateral Dynamics. International Journal of Mechanical, Industrial and Aerospace Engineering, DOI: 10.1109/IECON.2008.4757977, Source: IEEE Xplore

Wikimedia drawing, A 3-view line drawing of the General Dynamics F-16 Fighting Falcon, Page URL: https://commons.wikimedia.org/wiki/File:General_Dynamics_F-16_Fighting_Falcon_3-view_line_drawing.svg

International Journal of Aviation Science and Technology

Research Article

VPSA-Based Transfer Function Identification of Single DoF Copter System

Kübra Çiftçi[1], Muhammed Arif Şen[2], Hasan Huseyin Bilgic[3*]

[1] *Sivas University of Science and Technology, Sivas, Turkey*
kubraciftci@sivas.edu.tr- 0000-0002-4899-7650

[2] *Konya Technical University, Konya, Turkey*
masen@ktun.edu.tr- 0000-0002-6081-2102

[3] *Necmettin Erbakan University, Konya, Turkey*
hhbilgic@erbakan.edu.tr- 0000-0001-6006-8056

Abstract

In this study, an experimental set of a Single-DoF Copter system is created and transfer functions that could model the dynamics of the physical system with high accuracy were investigated. In order to model the dynamics of the physical system with the highest accuracy, the five different transfer functions have been proposed, in which the zero and pole values are determined by optimizing with the Vibrating Particle System Algorithm. Integral Square Error (ISE), Integral Time Square Error (ITSE), Integral Absolute Error (IAE), Integral Time Absolute Error (ITAE) functions, which are widely used in the literature in determining transfer functions, are determined as fitness functions. In order to verify the transfer functions, the responses of the transfer functions and the experimental system response are presented comparatively, and their suitability was evaluated. It has been observed that the proposed method is successful in defining the transfer function of the experimental system, and the compatibility of the obtained transfer functions with the system response is between 75.407% and 98.612% accuracy.

Keywords

VPSA
System Identification
Transfer Function
Single-dof Copter

Time Scale of Article

Received 28 September 2023
Revised until 2 December 2023
Accepted 5 December 2023
Online date 30 December 2023

1. Introduction

Helicopters are systems that attract the attention of researchers working in the field of control due to their relatively complex structure, the multitude of parameters that need to be controlled, and their exposure to external environmental noise. These systems are frequently preferred systems because they do not need a runway for landing and take-off. Creating mathematical models of helicopters and similar systems with minimum error is directly related to the precise control of these systems. Models created by assuming linear system elements often do not converge accurately with experimental results. The reasons for this can be listed as non-linear system elements being considered linear at certain intervals, noises and disturbances in the system and the environment. The methods used to obtain the correct model that describes the system behaviour are examined in two parts. The first of these is modelling using the system's equations of motion (Pehlivan and Akuner 2020). Another is system identification methods based on experimental data (Saengphet et al. 2017).

Creating mathematical models of systems using equations of motion can often be complex and challenging. At the same time, the model obtained as a result of the mathematical modelling process may not be similar to the real system behaviour. In such cases,

*: Corresponding Author Hasan Huseyin Bilgic, hhbilgic@erbakan.edu.tr
DOI: 10.23890/IJAST.vm04is02.0204

various system identification methods are used (Hoffer et al. 2014; Geluardi et al. 2018; Somov et al. 2021; Özcan and Caferov 2022). System identification methods, which are important sub-fields of control engineering, provide convenience in obtaining linear models such as transfer function and state space model of systems. Some of the advantages of this method are that it can be applied to linear or non-linear systems, saves time and often shows successful results. This method is based on the data set obtained from the system to be modelled. The data set to be used is created by applying appropriate input values and collecting system outputs. According to the existence of the data set and the system model, system identification studies are examined in three basic categories: black box, gray box and white box. Among these, the black box system identification method is frequently encountered in the literature (Bogdanski and Best 2017). With this method, only the data set of the system to be modelled is available during the modelling process.

Fidan and Erkan used the black box system identification method in the system identification of the boost converter. First, input and output data were obtained through experimental studies and then three different transfer functions were obtained with Matlab/System Identification toolbox. Among these transfer functions, a transfer function with one zero and four poles with a performance value of 87.26% was selected. In order to verify this model, the system was simulated on Simulink environment and similar results were obtained. After the system identification, PI (proportional integral) controller based on Particle Swarm Optimization algorithm was designed (Fidan and Erkan 2023). Similarly, in the study conducted by Özden et al., linear black box modelling methods were used to model an air heating system. In the study where ARX (auto regressive with exogeneous inputs), ARMAX (auto regressive moving average with exogenous variable models) and OE (output error) modelling methods were used, models with various structures were obtained using analysis methods. As a result of examining models under various performance criteria, it was observed that the best result was the ARMAX model (Tugal et al. 2010).

In the study by Altan and Hacıoğlu, a linear Output Error identification method was used to create the transfer function of the three-axis gimbal system on the UAV (Unmanned Aerial Vehicles). After creating the required data set for the process, the data was divided into two parts to be used in modelling and validation processes. For the transfer function obtained with an accuracy rate of 91.46%, validations were made under disturbance effects and it was predicted that it would make a great contribution to the control of the system (Altan and Hacioglu 2017).

Okçu and Leblebicioğlu were approached a new model with the closed loop system identification method in order to verify the existing mathematical model for a helicopter. In their study, a flight simulation was made using the nonlinear equations of motion of the system and the obtained data was used as input data for the system identification process. The frequency responses of the system were examined. Since it was observed that linear and non-linear models show similar results, it was predicted that these responses would be similar to the frequency responses of the linear model. Simulations were carried out in SAS (Stability Augmentation System) model, which is the simplest autopilot mode. As a result of the simulations performed in the study in which CIO (combined input-output) and direct approach were used, it was observed that the frequency responses of the model obtained using the CIO approach and the current model were similar (Doğa Okcu and Leblebicioğlu 2022).

In the study conducted by Salameh et al., system identification was carried out by collecting data on the hovering situation of a quadcopter. SISO (single-input single-output) and MIMO (multiple-input multiple-output) models were determined through the system identification process using the ARX model. The results obtained showed that the system identification method can be used in modelling quadcopters in the hovering (Salameh et al. 2015).

Machine learning-based system identification methods are increasingly used. Artificial Neural Network-based system identification methods can be given as examples of these methods (Fahmi Pairan et al. 2020). System identification method based on metaheuristic optimization algorithms is also another method used. A system identification process for a quadrotor was carried out using metaheuristic methods by Oliveira et al. In the study where Particle Swarm Optimization algorithm, Adaptive Particle Swarm Optimization algorithm and Cuckoo Optimization algorithm were used, a NARX (non-linear autoregressive exogenous) model was used for each state variable. The found models were compared using various performance criteria. The results obtained showed that metaheuristic optimization algorithms gave successful results for this process (de Oliveira et al. 2019). Similarly in the study by Zaloğlu et al., the system identification process was carried out using the existing data set for an experimental setup based on measuring air temperature. Five different metaheuristic optimization algorithms were used to determine the transfer functions for the system identification. These algorithms were evaluated for various performance criteria and it was observed that the Artificial Ecosystem-Based optimization algorithm gave better results. When the results obtained were examined, it was determined that metaheuristic optimization algorithms were successful in system

identification applications (Zaloğlu et al. 2023).

In this study, an experimental setup of a Single DoF Copter system was designed and prototyped. Then transfer functions that would ideally meet the system dynamics were investigated. A metaheuristic optimization algorithm was used to determine appropriate transfer functions. Fitness functions with different structures were used and the results were presented comparatively. In the introduction section, recent relevant literature studies are given. In the second section, the experimental setup and the methodology of the study are explained. In the results and discussion section, research results showing the performance of the proposed transfer function are presented. In the conclusion, the findings were evaluated and suggestions for further studies were stated.

2. Method

2.1. Experimental Setup

Interest in research on UAVs, which have many uses in our lives such as exploration, surveillance, agricultural spraying, transportation, photography and video shooting, is increasing day by day. At the same time, interest in helicopters and drones, which are vertical take-off and landing systems that eliminate the need for runways, is increasing due to their superior features compared to aircraft. The Single DoF helicopter system, which is an example of these systems, is frequently encountered in the literature (Ťapák and Huba 2018).

The system used in this study consists of a rotor that is jointed so that it can move circularly on a planar platform and a brushless motor connected to the end of the rotor. In the system shown in Figure 1; Arduino Uno is used as a microcontroller, and the necessary thrust is provided by a brushless DC (direct current) motor. The power supply of the system is provided by a 12V DC power supply, and the angular position of the rotor is measured with a 10K Potentiometer. Additionally, a 30A ESC (electronic speed controller) connected to the microcontroller is used to produce constant impulse. The system works in real-time with Matlab/Simulink via Arduino Uno.

Figure 2 presents the connection diagram of the system elements. The shaft jointed with the rotor is supported on the chassis with the help of bearings. The shaft and potentiometer are linked. The microcontroller communicates with the PC and all inputs and outputs of the system are read in real time through the block diagrams of the system created in the Simulink environment. Analog signals generated on the potentiometer by the movement of the shaft are converted into angle values and recorded. The step input applied to the system is transmitted to the ESC as PWM (pulse width modulation) signals and a constant impulse value is applied to the system. The experimental data obtained was used to define the transfer functions. Step input of 8.75 V was applied to the motor. Data on the time-dependent angular position of the beam was collected with sample time of 0.02.

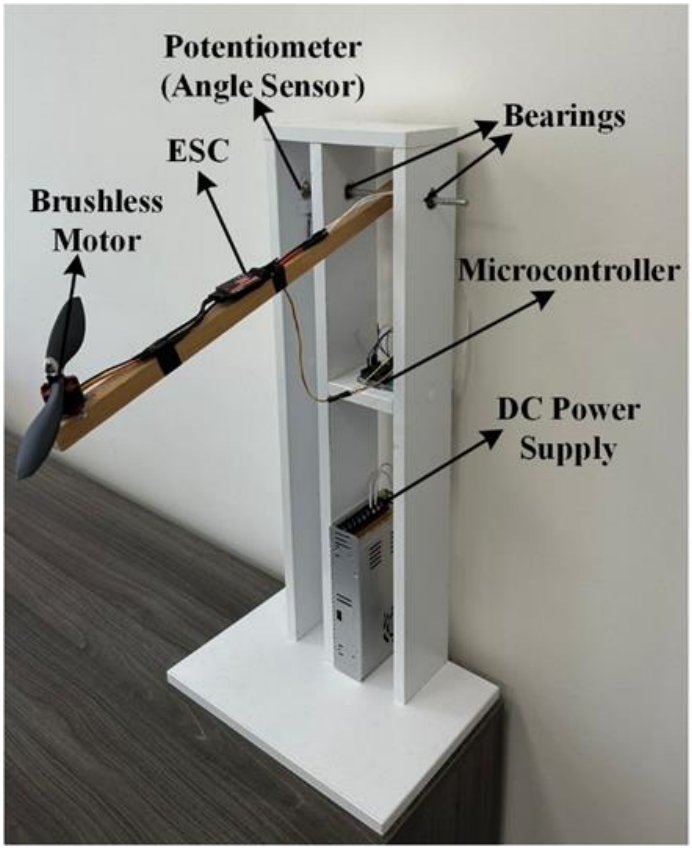

Fig. 1. The experimental setup of single DoF copter

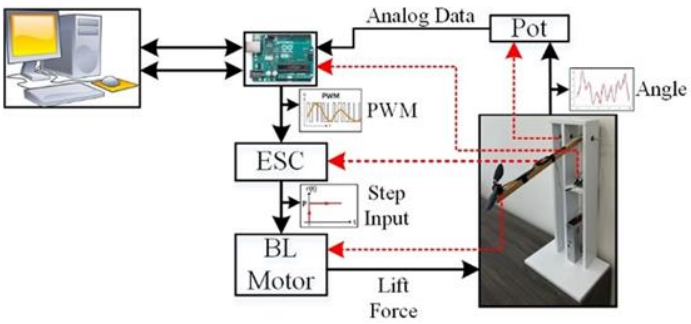

Fig. 2. The system elements and connection diagram

2.2. System Identification

The models designed as a result of modelling studies for systems must be similar to the experimental system behaviour. Otherwise, development studies with the system are unlikely to be successful. Therefore, the modelling process should be done accurately and completely. It is often not possible to obtain exact models of systems with equations of motion. Moreover, the model response may not match the experimental response. In such cases, the system identification method, which is an experimental method, is often

preferred (Wei et al. 2017; Ivler et al. 2021; Simmons 2021). There are many examples in the literature of the use of the system identification method in creating models of difficult and complex systems such as aircrafts, helicopters and quadcopters (Geluardi et al. 2018; Yu et al. 2020; Ebrahimi and Barzamini 2021).

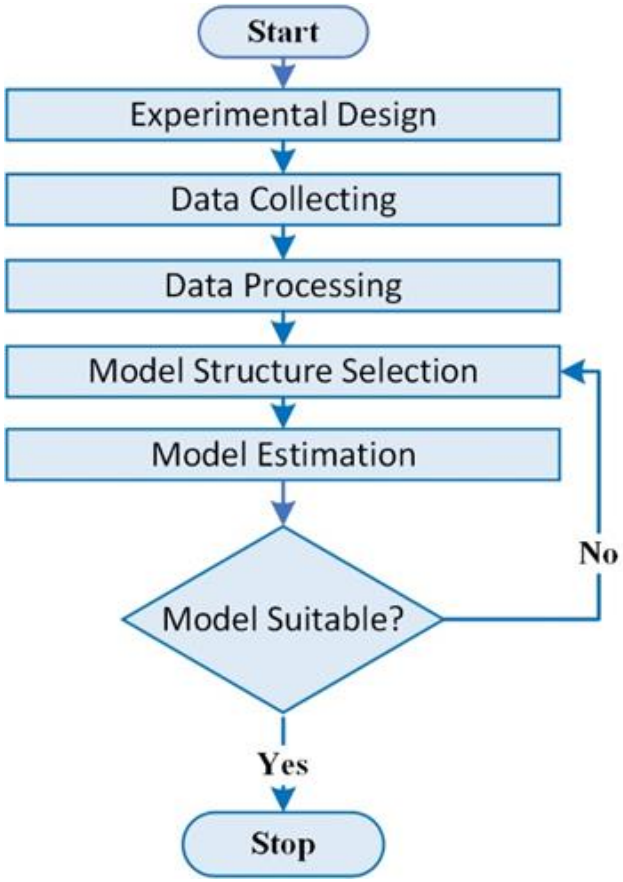

Fig. 3. The stages of system identification

In system identification methods, the process is performed with the experimental data set obtained for the system to be modelled. Obtaining the data set completely and appropriately affects the success of the system identification process significantly. In this part, the input signal to be applied to the system must be selected correctly. In input signal selection, which is one of the most important steps in the system identification process, step functions, PRBS (pseudo random binary sequence) and sinusoidal signals are frequently preferred (Sanatel 2020), (Sayll et al. 2023).

System identification methods are examined under three sections according to the known states of the system model. The first of these sections is white box definition, where the system model is fully known (Nugroho and Akmeliawati 2018). Another is the grey box system identification method, in which the model is determined with the data set in cases where the equations expressing the system are known but the parameters are unknown (Yuan and Katupitiya 2011). The last one is the black box system identification method, which is a modelling process performed using only the data set without any information about the system (Fidan et al. 2022). By using the system identification method, models such as the transfer unction of the system and the state-space model can be obtained more easily and accurately.

2.3. Vibrating Particle System Algorithm

Vibrating Particle System algorithm, one of the metaheuristic search algorithms, is based on the single degree of freedom vibration motion of damped systems. VPSA is a Physics-Based algorithm that is among meta-heuristics algorithms. Thanks to its inspired by the free vibration of under-damping systems, it can be used for solve complex problems including real-world different types of data (Almufti 2022).The flow chart of the algorithm is given in Figure 4.

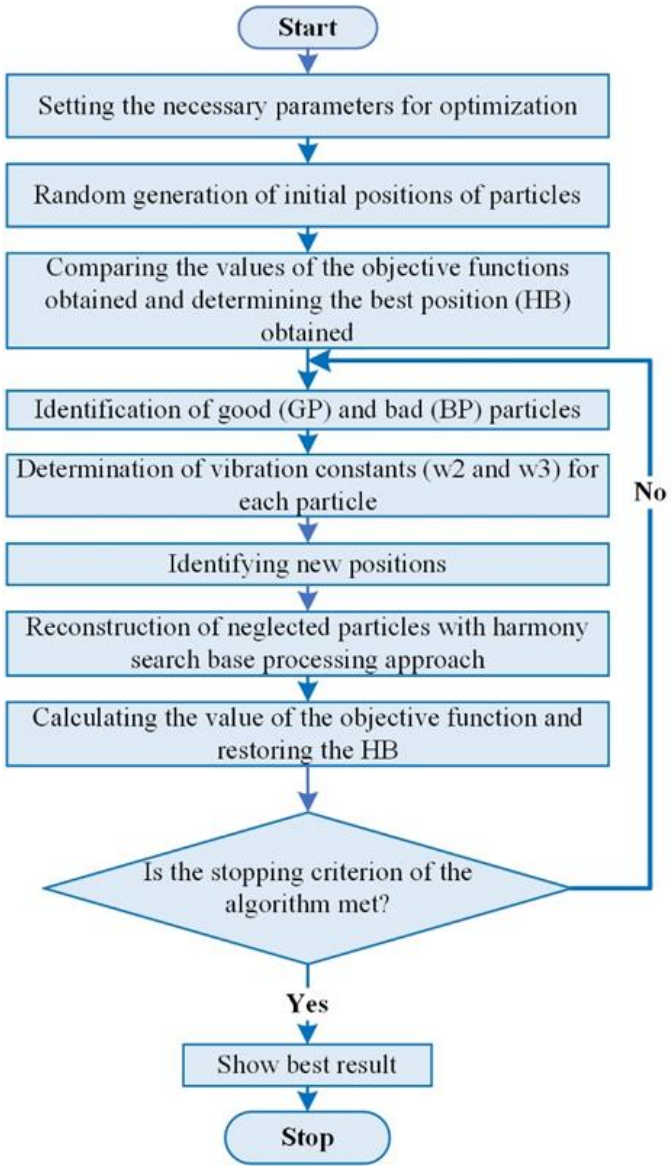

Fig. 4. VPSA flowchart(Kaveh et al. 2017)

For this population-based algorithm, which is based on the motion of vibrating particles, initially the number of iterations, the number of vibrating particles, α, w_1, w_2, w_3, p parameters are determined. Then the initial positions

of the particles are determined randomly and the value of the objective function is calculated for each particle. The weights w_1, w_2 and w_3, which are the parameters set at the beginning, represent the importance of the HB (best position), GP (good particle) and BP (bad particle) equilibrium positions, respectively. Determining these equilibrium positions created by using these weights is the next step of the algorithm. In this section, a function called the descending function (D) is defined to show the effect of damping ratio, which is one of the most important factors affecting the vibration motion, on the motion.

The equation for this function is given in Equation 1. One of the initial parameters of the algorithm, α, refers to the constant used in the definition of the descending function. With the definition of this function, the new positions of the particles are determined. In the determination of these new positions, it is checked whether the BP position will be neglected by using the p parameter, which is one of the initial parameters. This control is done by accepting the w_3 parameter as zero if the p parameter is less than the randomly generated number. The equations for determining the new position of the particles are given in Equation 2.

$$D = \left(\frac{Number\ of\ iterations}{Maximum\ Number\ of\ Iterations}\right)^{-\alpha} \quad (1)$$

$$NP = w_1[D.A.rand1 + HB] + w_2[D.A.rand2 + GP] + w_3[D.A.rand3 + BP]$$

$$A = w_1(HB - PP) + w_2(GP - PP) + w_3(BP - PP) \quad (2)$$

w_1+w_2+w_(3)=1

NP in Equation 2 represents the new position of the particle, PP represents the current position of the particle.

In the step before testing the stopping criterion for the algorithm, the particles that violate the boundary are reconstructed by using the harmony search base approach to determine the boundary violations that may occur due to the position change. After this process is done, the stopping criterion is tested and if the criterion is met, the algorithm is completed (Kaveh and Ilchi Ghazaan 2017).

The most important issue in the use of optimization algorithms is the appropriate creation of the fitness function that expresses the problem. There are various fitness functions used in the literature. Examples of these are ISE (integral square error), IAE (integral absolute error), ITAE (integral time absolute error) and ITSE (integral time square error) fitness functions (Gyongyosi 2020).

The IAE fitness function integrates the absolute values of the measured errors. Similarly, the ISE fitness function operates by integrating the squares of the errors. Equations of these fitness functions are given in Equation 3 and Equation 4, respectively.

$$IAE = \int_0^t |e(t)|dt \quad (3)$$

$$ISE = \int_0^t e^2(t)dt \quad (4)$$

The ITAE fitness function is the evaluation of the operations performed in the IAE fitness function with a time constraint. Similarly, the ITSE fitness function operates by evaluating the ISE fitness function with a time constraint. You can see the equations of these functions in Equation 5 and Equation 6, respectively.

$$ITAE = \int_0^t t|e(t)|dt \quad (5)$$

$$ITSE = \int_0^t te^2dt \quad (6)$$

3. Results and Discussion

In this section, the procedures used to create the mathematical model of the designed Single DoF helicopter system are explained. The system identification method was used to determine the appropriate transfer function for the system. First of all, the necessary data was collected by applying unit step input to the system. Afterwards, filtering was applied to these data and the data set was obtained.

The Vibrating Particle System algorithm was used to determine the parameters of the transfer function. The five different transfer function models were defined by varying the number of poles and zeros. The ideal values of the poles and zeros in these transfer functions were determined by four different fitness functions and the ideal values were obtained with the proposed algorithm. The optimizations were made to determine the optimum values of the number of iterations, α, w1, w2, w3, p parameters, which are the initial parameters of the algorithm. In order to find the appropriate values of the parameters, the algorithm was run with different parameter values. As a result of these processes, optimum values were determined. These values were determined as 100, 0.3, 0.2, 0.2, 0.6, 0.2, respectively. The initial parameters of the VPSA was determined according to similar studies used VPSA in the literature. As a result of the optimization processes, the accuracy rates of the transfer functions determined according to the real system behavior were obtained. During this process, the MAPE (mean absolute percentage error) value was used as the performance criterion. The mathematical expression for this performance criterion is given in Equation 7.

$$MAPE = \frac{100\%}{n}\sum_{t=1}^{n}\left|\frac{e_t}{y_t}\right| \quad (7)$$

The times and accuracy values of the optimization operations performed using four different fitness functions for five different transfer functions are presented by comparing them in Table 1.

Table 1: Comparative optimization results

Transfer Functions	Pole Number	Zero Number	Fitness Function	Transfer Function	Accuracy %	Time
TF-1	p=2	z=0	ISE	$\frac{88.58}{3.25s^2+3.35s+2.46}$	97.410	307.12
			IAE	$\frac{34.05}{0.24s^2+1.14s+0.84}$	92.234	313.12
			ITSE	$\frac{89.90}{1.83s^2+3.72s+2.46}$	95.951	301.42
			ITAE	$\frac{91.38}{2.69s^2+4.28s+2.55}$	93.947	339.1
TF-2	p=2	z=1	ISE	$\frac{0.97s+81.66}{s^2+3.93s+2.06}$	94.713	297.63
			IAE	$\frac{0.60s+79.89}{s^2+4.53s+2.35}$	85.105	298.88
			ITSE	$\frac{0.75s+81.96}{s^2+1.85s+2.15}$	92.306	305.46
			ITAE	$\frac{5.48s+78.20}{s^2+3.05s+2.17}$	93.653	302.55
TF-3	p=3	z=0	ISE	$\frac{69.82}{s^3+1.76s^2+1.77s+2.02}$	75.407	245.76
			IAE	$\frac{95.35}{s^3+2.81s^2+4.35s+2.50}$	98.612	247.44
			ITSE	$\frac{97.26}{s^3+3.65s^2+5.20s+2.42}$	93.969	253.66
			ITAE	$\frac{97.53}{s^3+3.30s^2+5.31s+2.73}$	91.698	244.93
TF-4	p=3	z=1	ISE	$\frac{98.34s+2.15}{s^3+79.05s^2+7.45s+5.03}$	94.705	294.87
			IAE	$\frac{66.89s+2.35}{s^3+92.97s^2+6.11s+5.23}$	92.615	274.96
			ITSE	$\frac{10.98s+2.43}{s^3+91.75s^2+3.30s+3.81}$	97.239	262.90
			ITAE	$\frac{92.87s+2.26}{s^3+82.56^2+5.39s+5.20}$	98.082	255.51
TF-5	p=3	z=2	ISE	$\frac{5.98s^2+2.86s+1.36}{s^3+46.03s^2+45.78s+3.72}$	94.365	288.18
			IAE	$\frac{12.44s^2+3.02s+1.16}{s^3+35.10s^2+44.26s+3.18}$	94.998	277.96
			ITSE	$\frac{31.60s^2+3.77s+1.51}{s^3+92.88s^2+49.06s+12.76}$	86.225	271.08
			ITAE	$\frac{39.06s^2+2.41s+1.48}{s^3+59.49s^2+41.78s+7.12}$	89.650	287.07

At the same time unit step responses of the obtained transfer functions were compared with the real system response. A total of four graphs are presented for each fitness function, showing the compatibility of transfer functions with the real system response.

Figure 5 shows the comparison of the unit step responses of the transfer functions determined according to the ISE fitness function with the real system response. As can be seen from the Table 1, accuracy rates were between 75.407% (ISE, TF-1) and 97.41% (ISE, TF-3). Similar to the results in the Table 1, graphically, TF-3 transfer function gave the best result, and TF-1 transfer function gave the worst result.

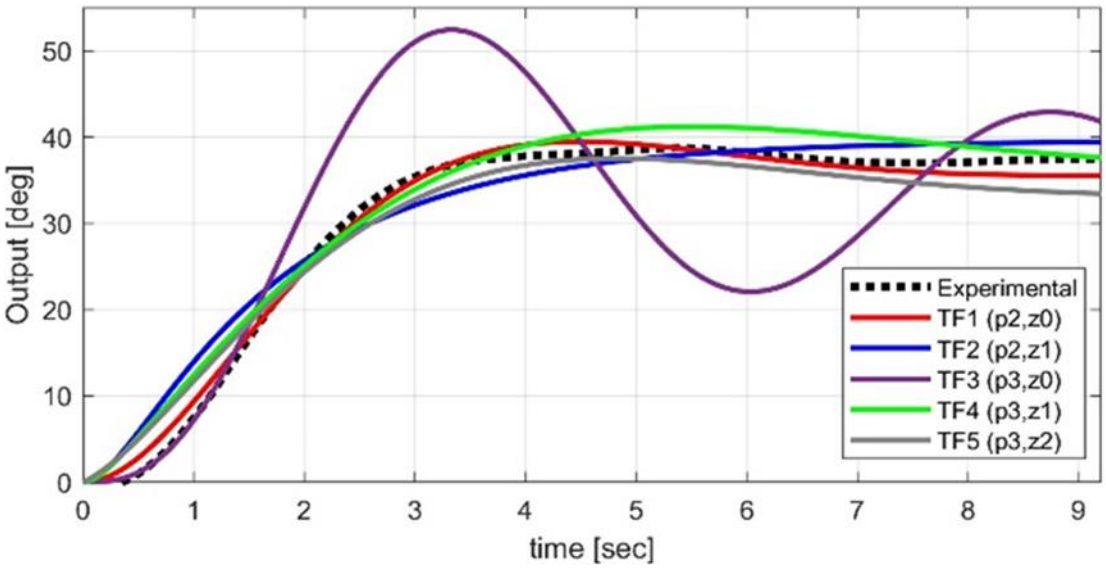

Fig 5: Comparison of the time response of five different transfer functions with the real system response for the ISE fitness function

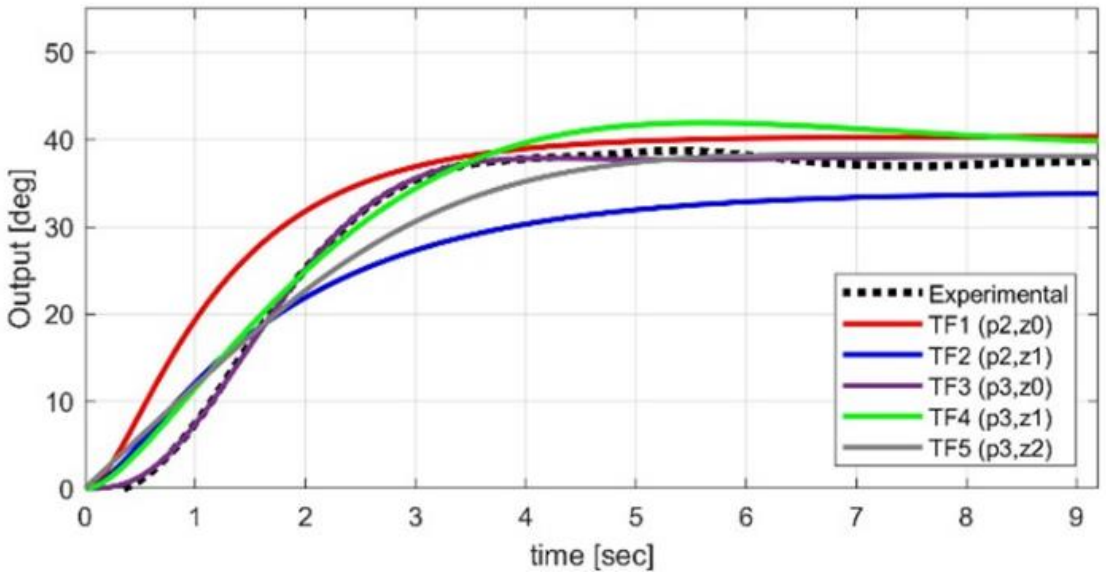

Fig 6: Comparison of the time response of five different transfer functions with the real system response for the IAE fitness function

Figure 6 shows the comparison of the unit step responses of the transfer functions determined according to the IAE fitness function with the real system response. As can be seen from the Table 1, accuracy rates were between 85.105% (IAE, TF-2) and 98.612% (IAE, TF-3). Similar to the results in the Table 1, graphically, TF-3 transfer function gave the best result, and TF-2 transfer function gave the worst result.Figure 7 shows the comparison of the unit step responses of the transfer functions determined according to the ITSE fitness function with the real system response. As can be seen from the Table 1, accuracy rates were between 86.225% (ITSE, TF-5) and 97.239% (ITSE, TF-4). Similar to the results in the Table 1, graphically, TF-4 transfer function gave the best result, and TF- transfer function gave the worst result.

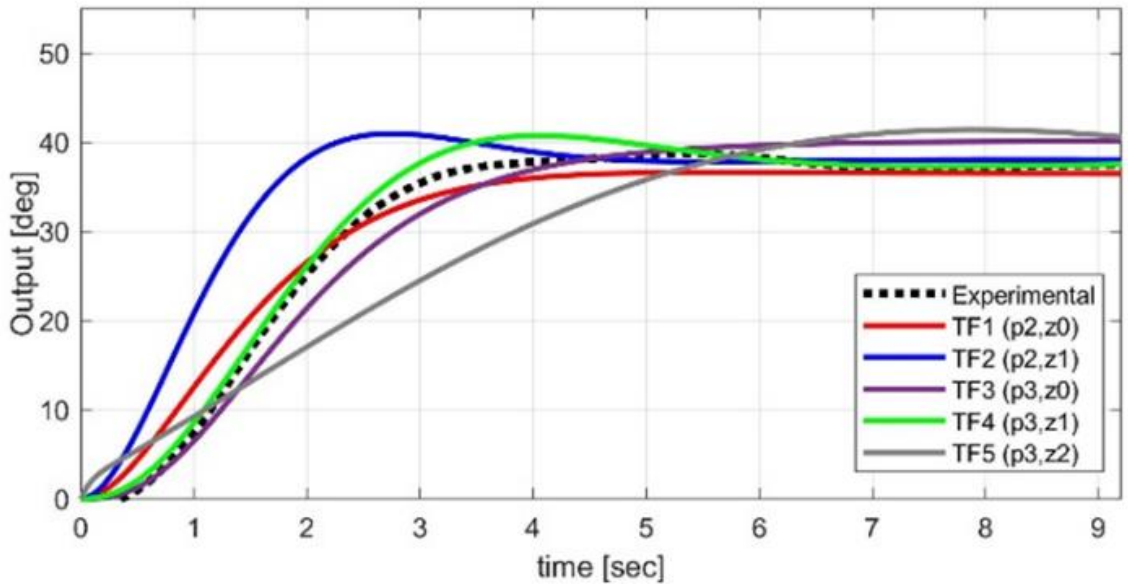

Fig 7: Comparison of the time response of five different transfer functions with the real system response for the ITSE fitness function

Figure 8 shows the comparison of the unit step responses of the transfer functions determined according to the ITAE fitness function with the real system response. As can be seen from the Table 1, accuracy rates were between 89.650% (ITAE, TF-5) and 98.082% (ITAE, TF-4). Similar to the results in the Table 1, graphically, TF-4 transfer function gave the best result, and TF-5 transfer function gave the worst result.

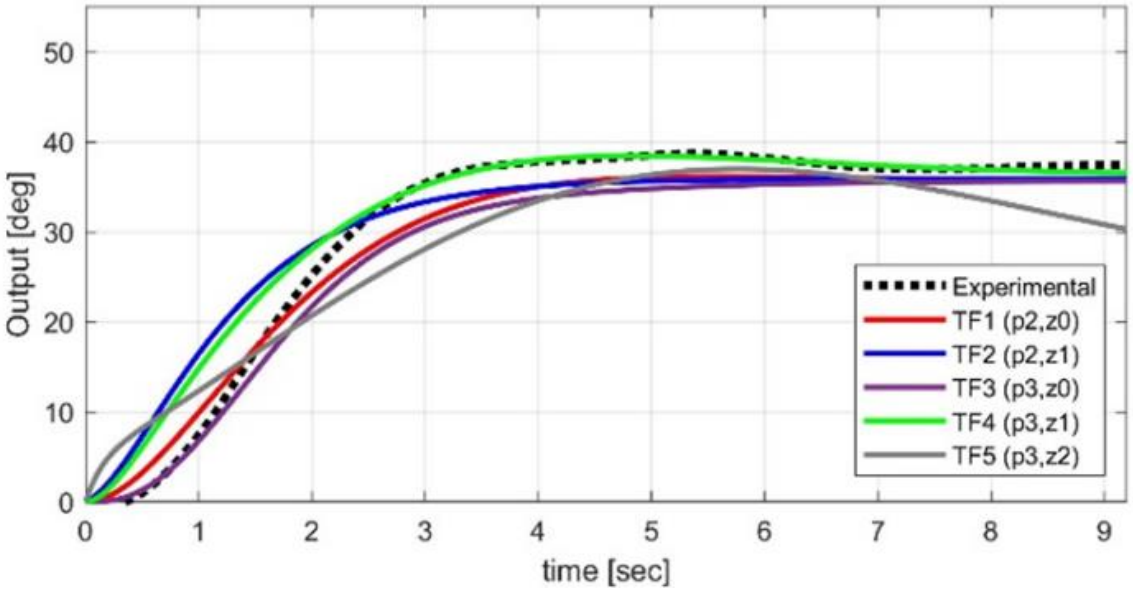

Fig 8: Comparison of the time response of five different transfer functions with the real system response for the ITAE fitness function

When the comparative results obtained were examined, it was seen that the TF-3 transfer function determined according to the IAE fitness function with an accuracy value of 98.612% could provide the most compatible answer with the real system behaviour. The lowest accuracy value was observed to be 75.407% in the TF-3 response determined according to the ISE fitness function.

4. Conclusion

The system identification process using experimental data can provide modelling that can meet the real system dynamics with high accuracy in cases where mathematical modelling cannot be done or the model cannot be verified. The success criterion of the system identification process is accepted as the accuracy ratio of the proposed model with the real model response.

In this study, an experimental set of a Single-DoF Copter system was created and transfer functions that could model the system dynamics with the highest accuracy were investigated using a metaheuristic method. Five different transfer functions have been proposed, in which the zero and pole values are optimized and adjusted by the Vibrating Particle System algorithm. A total of four different fitness functions, namely ISE, IAE, ITSE and ITAE, were used to adjust a total of five different transfer functions with different zero and pole values. The unit step response applied to the system was used to verify the transfer functions. The accuracy values of the transfer function models obtained as a result of the optimization processes were evaluated using the MAPE performance criterion.

Unit step responses of transfer functions and real system responses are presented comparatively in tables and graphs. When the numerical results were examined, it was seen that the TF-3 transfer function with an accuracy value of 98.612%, determined according to the IAE fitness function, provided the real system dynamics at the highest rate. It has been observed that the proposed method can successfully obtain a transfer function model that can represent the system dynamics of an experimental Single-DoF Copter with high accuracy. It is anticipated that this approach can be used to predict transfer functions and nonlinear models in different systems and is a method open to development.

Nomenclature

ARX	: Auto Regressive with Exogeneous Inputs
ARMAX	: Auto Regressive Moving Average with Exogenous Variable Models
BP	: Bad Particle
CIO	: Combined Input-Output
DC	: Direct Current
DOF	: Degree of Freedom
ESC	: Electronic Speed Controller
GP	: Good Particle
BP	: Best Position
ISE	: Integral Square Error
IAE	: Integral Absolute Error
ITSE	: Integral Time Squared Error
ITAE	: Integral Time Absolute Error
MAPE	: Mean Absolute Percentage Error
MIMO	: Multiple Input Multiple Output
NARX	: Non-Linear Autoregressive Exogenous
OE	: Output Error
PI	: Proportional Integral
PRBS	: Pseudo Random Binary Sequence
PWM	: Pulse Width Modulation
SAS	: Stability Augmentation System
SISO	: Single Input Single Output
UAV	: Unmanned Aerial Vehicle
VPSA	: Vibrating Particle System Algorithm

CRediT Author Statement

Kübra Çiftçi: Conceptualization, Methodology, Software, Writing – Original Draft, Writing – Review & Editing, Resources. **Muhammet Arif Şen:** Conceptualization, Methodology, Software, Writing – Original Draft, Writing – Review & Editing. **Hasan Huseyin Bilgic:** Conceptualization, Methodology, Software, Writing – Original Draft, Writing – Review & Editing, Supervision

References

Almufti, S., (2022). Vibrating Particles System Algorithm: Overview, Modifications and Applications. Icontech International Journal [online], 6 (3), 1–11. Available from: https://icontechjournal.com/index.php/iij/article/view/226.

Altan, A. and Hacioglu, R., (2017). İnsansız Hava Aracı Üzerinde Bulunan 3 Eksenli Yalpa Sisteminin Dış Bozucu Altında Modellenmesi. In: 2017 25th Signal Processing and Communications Applications Conference, SIU 2017. Institute of Electrical and Electronics Engineers Inc.

Bogdanski, K. and Best, M. C., (2017). A new structure for non-linear black-box system identification using the extended Kalman filter. Proceedings of the Institution of Mechanical Engineers, Part D: Journal of Automobile Engineering, 231 (14), 2005–2015.

Doğa Okcu, I. and Leblebicioğlu, K., (2022). Kapalı Döngü Test Verisi Kullanarak Helikopter Dinamik Sistem Tanımlaması. Fırat Üniversitesi Uzay ve Savunma Dergisi, 1 (1), 422–429.

Ebrahimi, B. and Barzamini, F., (2021). Aircraft System Identification Using Parametric Approaches and Intelligent Modeling. In: 2021 IEEE Aerospace Conference (50100). 1–12.

Fahmi Pairan, M., Syafiq Shamsudin, S. and Fadhli Zulkafli, M., (2020). Neural Network-Based System Identification for Quadcopter Dynamic Modeling: A Review. Journal Of Advanced Mechanical Engineering Applications [online], 1 (2), 20–33. Available from: http://penerbit.uthm.edu.my/ojs/index.php/jamea.

Fidan, Ş. and Erkan, E., (2023). Boost Konvertörün Black-Box Sistem Tanımlama Yöntemi ile Transfer Fonksiyonunun Elde Edilmesi ve Parçacık Sürü Algoritması Tabanlı PI Kontrolör Tasarımı [online]. Available from: http://as-proceeding.com/.

Fidan, S., Sevim, D. and Erkan, E., (2022). System Identification and Control of High Voltage Boost Converter. In: IEEE Global Energy Conference, GEC 2022. Institute of Electrical and Electronics Engineers Inc., 25–31.

Geluardi, S., Nieuwenhuizen, F. M., Venrooij, J., Pollini, L. and Bülthoff, H. H., (2018). Frequency Domain System Identification of a Robinson R44 in Hover. Journal of the American Helicopter Society [online], 63 (1), 1–18. Available from: https://search.ebscohost.com/login.aspx?direct=true&db=asn&AN=128077292&site=eds-live.

Gyongyosi, L., (2020). Objective function estimation for solving optimization problems in gate-model quantum computers. Scientific Reports [online], 10 (1), 14220. Available from: https://doi.org/10.1038/s41598-020-71007-9.

Hoffer, N. V., Coopmans, C., Jensen, A. M. and Chen, Y., (2014). A survey and categorization of small low-cost unmanned aerial vehicle system identification. Journal of Intelligent and Robotic Systems: Theory and Applications, 74 (1–2), 129–145.

Ivler, C. M., Rowe, E. S., Martin, J., Lopez, M. J. S. and Tischler, M. B., (2021). System identification guidance for multirotor aircraft: Dynamic scaling and test techniques. Journal of the American Helicopter Society, 66 (2), 1–16.

Kaveh, A. and Ilchi Ghazaan, M., (2017). Vibrating particles system algorithm for truss optimization with multiple natural frequency constraints. Acta Mechanica, 228 (1), 307–322.

Kaveh, A., Kaveh, A. and Ilchi Ghazaan, M., (2017). A new meta-heuristic algorithm: vibrating particles system. Scientia Iranica [online], 24 (2), 551–566. Available from: https://scientiairanica.sharif.edu/article_2417.html.

Nugroho, L. and Akmeliawati, R., (2018). Comparison of black-grey-white box approach in system identification of a flight vehicle. Journal of Physics: Conference Series [online], 1130 (1), 012024. Available from: https://dx.doi.org/10.1088/1742-6596/1130/1/012024.

De Oliveira, E. C. L., de Araujo, J. P. L., da Silva Silveira, A., Silva, O. F., Vidal, J. F. and de França Silva, A., (2019). Quadrotor Black-Box System Identification Using Metaheuristics.

Özcan, A. B. and Caferov, E., (2022). Frequency Domain Analysis of F-16 Aircraft in a Variety of Flight Conditions. Journal, 03 (01), 21–34.

Pehlivan, K. and Akuner, C., (2020). Quadrotor Test Düzeneği Tasarımı ve Uygulaması. International Periodical of Recent Technologies in Applied Engineering, 2 (1), 15–24.

Saengphet, W., Tantrairatn, S., Thumtae, C. and Srisertpol, J., (2017). Implementation of system identification and flight control system for UAV. In: 3rd International Conference on Control, Automation and Robotics (ICCAR). 678–683.

Salameh, I. M., Ammar, E. M. and Tutunji, T. A., (2015). Identification of quadcopter hovering using experimental data. In: 2015 IEEE Jordan Conference on Applied Electrical Engineering and Computing Technologies (AEECT). 1–6.

Sanatel, Ç., (2020). Uzun Kısa Süreli Bellek Tabanlı Sistem Tanıma ve Uyarlamalı Kontrol. İstanbul Teknik Üniversitesi, İstanbul .

Sayll, A., Erden, F., Tüzün, A., Baykara, B. and Aydemir, M., (2023). A folding wing system for guided ammunitions: mechanism design, manufacturing and real-time results with LQR, LQI, SMC and SOSMC. Aeronautical Journal.

Simmons, B. M., (2021). System Identification for eVTOL Aircraft Using Simulated Flight Data. In: AIAA SCITECH 2022 Forum [online]. American Institute of Aeronautics and Astronautics. Available from: https://doi.org/10.2514/6.2022-2409.

Somov, Y., Somova, T. and Rodnishchev, N., (2021). Identification and Stochastic Optimizing the UAV Motion Control in Turbulent Atmosphere. Journal, 02 (02), 57–63.

Ťapák, P. and Huba, M., (2018). One Degree of Freedom Copter. In: Moreno-Díaz, R., Pichler, F., and Quesada-Arencibia, A., eds. Computer Aided Systems Theory – EUROCAST 2017. Cham: Springer International Publishing, 91–98.

Tugal, H., Okumuş, H. I. and Tugal, H., (2010). Bir Hava Isıtma Sisteminin Optimum Modellenmesi. In: Electrical, Electronics and Computer Engineering [online]. Available from: https://www.researchgate.net/publication/251987598.

Wei, W., Tischler, M. B. and Cohen, K., (2017). System identification and controller optimization of a quadrotor unmanned aerial vehicle in hover. Journal of the American Helicopter Society, 62 (4).

Yu, Y., Tang, P., Song, T. and Lin, D., (2020). A two-step method for system identification of low-cost quadrotor. Aerospace Science and Technology [online], 96, 105551. Available from: https://www.sciencedirect.com/science/article/pii/S1270963819309368.

Yuan, W. and Katupitiya, J., (2011). A time-domain grey-

box system identification procedure for scale model helicopters. In: Proceedings of the 2011 Australasian Conference on Robotics and Automation.

Zaloğlu, M., Fïdan, Ş. and Erkan, E., (2023). Meta-Heuristik Optimizasyon Algoritmalarının Sistem Tanımlama Problemine Uygulanması ve Performans Karşılaştırması. In: 2nd International Conference on Engineering, Natural and Social Sciences [online]. Konya. Available from: http://as-proceeding.com/://www.icensos.com/.

International Journal of Aviation Science and Technology

Research Article

Battery Technologies to Electrify Aviation: Key Concepts, Technologies, and Figures

María Zamarreño Suárez[1*], Francisco Pérez Moreno[2], Raquel Delgado-Aguilera Jurado[3], Rosa María Arnaldo Valdés[4], Víctor Fernando Gómez Comendador[5]

[1] *Department of Aerospace Systems, Air Transport and Airports, School of Aerospace Engineering, Universidad Politécnica de Madrid (UPM), 28040 Madrid, Spain*
maria.zamsuarez@upm.es- 0000-0002-1563-8694
[2] *Department of Aerospace Systems, Air Transport and Airports, School of Aerospace Engineering, Universidad Politécnica de Madrid (UPM), 28040 Madrid, Spain*
francisco.perez.moreno@upm.es - 0000-0003-2650-8358
[3] *Department of Aerospace Systems, Air Transport and Airports, School of Aerospace Engineering, Universidad Politécnica de Madrid (UPM), 28040 Madrid, Spain*
raquel.djurado@upm.es- 0000-0002-6479-4714
[4] *Department of Aerospace Systems, Air Transport and Airports, School of Aerospace Engineering, Universidad Politécnica de Madrid (UPM), 28040 Madrid, Spain*
rosamaria.arnaldo@upm.es- 0000-0001-6639-6819
[5] *Department of Aerospace Systems, Air Transport and Airports, School of Aerospace Engineering, Universidad Politécnica de Madrid (UPM), 28040 Madrid, Spain*
fernando.gcomendador@upm.es - 0000-0003-0961-2188

Abstract

Aviation is undergoing a paradigm shift to become a more sustainable industry. Priorities include reducing fossil fuel consumption, cutting carbon dioxide and other emissions, and developing new technologies. One of the major enabling technologies is the electrification of aircraft. Batteries are a key part of this revolutionary concept. This paper aims to provide key insights into battery technology and its potential to electrify aviation. Therefore, it proposes a comprehensive presentation of this technology following a detailed research process. Five different topics are addressed. The first is a general overview of the chemistry of electrochemical cells, the basic element of batteries. This is followed by a presentation of some of the most relevant previous work in this topic, highlighting their contributions and their main outcomes to be considered in further research. The main performance metrics used to compare the different batteries are presented next. For each of them, the definition, and related requirements that batteries used in electric aviation must meet are included. The paper then analyzes the possibilities for battery use in aviation and identifies some key challenges that need to be overcome to scale-up this technology. Finally, some battery technologies, their current uses, and their potential for further progress toward a more sustainable aviation are presented in detail.

Keywords

Electric Aviation,
Batteries,
Emerging Technologies,
Sustainability,
Environmentally Friendly Aviation

Time Scale of Article

Received 6 November 2023
Revised to 10 December 2023
Accepted 12 December 2023
Online date 30 December 2023

1. Introduction

One of the current priorities of the aviation industry is sustainability. Currently, the main propulsion system for commercial aircraft are turbofan engines, and they are directly involved in many of the environmental impacts caused by aviation (Ranasinghe et al., 2019). This type of engine produces several environmentally harmful emissions. The most important emission is carbon

*: Corresponding Author María Zamarreño Suárez, maria.zamsuarez@upm.es
DOI: 10.23890/IJAST.vm04is02.0205

dioxide (CO2), a greenhouse gas. However, other emissions, such as nitrogen oxides, hydrocarbons, sulfur oxides, and contrails, are also associated with aircraft.

In particular, emission reduction strategies could be divided into two distinct categories: technological innovations and the development of interventions to influence behavioral change (Gössling and Dolnicar, 2023). All improvements related to propulsion systems, that is, the development of new propulsion technologies and the replacement of fossil fuels with Sustainable Aviation Fuels (SAF), fall into the first category. Other measures to offset emissions or reduce the number of flights fall into the second category.

The focus of this paper is on a specific case of the first category, namely the use of battery technology as an enabling technology for a more-electric aviation. Electric aviation involves the use of new propulsion technologies. The benefits of electric aviation have been analyzed in several studies.

In particular, the authors of (Moua et al., 2020), after analyzing various prototypes, present as the main advantages of all-electric aircraft a reduction in noise of around 17%, a reduction in greenhouse gas emissions of around 80%, and a reduction in operating costs and pilot training of around 70%. However, to scale-up the use of this technology and overcome some of its major limitations, an international effort is needed to develop new technologies. This study is of great interest because it analyzes different prototypes of short-range aircraft. For each of them, the main characteristics are analyzed, and the study concludes with some interesting recommendations. One of the most interesting aspects is the great contribution that this type of aircraft could make to serving small communities.

Depending on how energy for flight is stored, three different approaches can be distinguished in electric aviation: battery, turboelectric, and hybrid electric (Epstein and O'Flarity, 2019). This previous relevant study is of great interest as it presents the main characteristics of each of these architectures. At a general level, it identifies five key challenges for electric propulsion, namely weight, efficiency, heat rejection, reliability, and cost.

For battery technology to reach its full potential in electric aviation in the coming years, several limitations must be overcome. Today, the technology with the greatest potential for commercialization is lithium-ion batteries. However, this technology also presents several challenges. One of the main concerns is the thermal stability. Therefore, it is necessary to continue developing various research to determine techniques for monitoring battery temperature, as well as optimal battery management systems. An example of this type of study is (Yetik and Karakoc, 2022a) where the authors investigate the effects of cooling a system of 15 prismatic batteries connected in series using air and alumina nanofluids. Currently, the use of massive data analysis and machine learning techniques is a tool with great potential for application in this field. For example, in (Yetik and Karakoc, 2021) a study is carried out that focuses on the thermal stability of different materials as elements of lithium-ion batteries using artificial neural networks techniques. Thermal stability is one of the critical safety issues for the certification of batteries for use in aviation. For this reason, research efforts should be directed towards improving their thermal stability.

Due to the great potential of the use of this technology, there are many international projects that address the assessment of battery technology and try to define different roadmaps to evaluate its development in the coming years.

An example of these roadmaps is (Battery 2030+ project, 2023). This is the result of the Battery 2030+ project, which presents a long-term vision beyond the 2030 horizon. This roadmap has been regularly updated to reflect the latest developments in this well-researched field of innovation. This initiative is a major project at the European level, integrating contributions from different sectors. Contributions from a total of 24 countries and various stakeholders have been considered in the preparation of the updated version of the roadmap. One of the most interesting aspects is the research areas related to batteries covered by the roadmap. These include research into new materials, the integration of smart functionalities into the battery, manufacturability, and recycling.

Specifically, the work presented in this paper is part of the Environmentally Friendly Aviation for All Classes of Aircraft (EFACA) project. This project is co-funded by the European Commission through the Horizon Europe program. The aim of the project is to promote a more environmentally friendly aviation sector and the development of new technologies using electric and hybrid thermoelectric propulsion systems (EFACA project, 2023). To this end, it is divided into several work packages (WPs), each focusing on one of the emerging technologies that will change the world of aviation. Figure 1 shows some details of the project.

In the EFACA project, WP6 is dedicated to the study of battery power for small, short-range aircraft. This category includes a new disruptive concept, the so-called urban air mobility (UAM). The work presented in this paper is framed within this WP, which takes as its starting point an assessment of the current state of batteries, their possibilities, and limitations. As mentioned above, the development of electric aviation in general and battery technology in particular is a cutting-edge topic. The scalability of this technology would be a breakthrough because of its contribution to reducing dependence on fossil fuels and the reduction in greenhouse emissions.

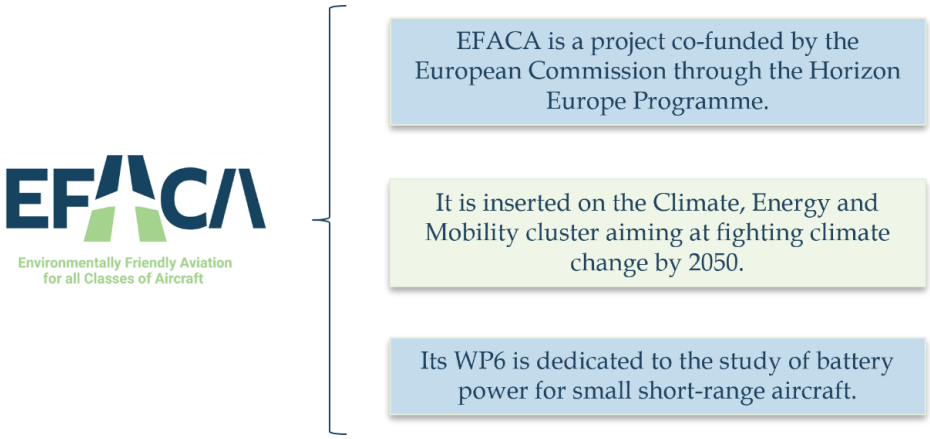

Fig. 1. Key ideas regarding the Environmentally-Friendly Aviation for All Classes of Aircraft (EFACA) project. The information included in the figure has been obtained from (EFACA project, 2023).

1.1. Originality and objectives of the present study

The originality of the present study is that it integrates an overview of the possibilities of using batteries in aviation. At the same time, it provides a list of the main battery performance metrics that will determine their use in aviation. Additionally, it provides an overview of the batteries used in aviation over the last decades and includes the most promising current and emerging technologies that will advance the concept of electric aviation.

The aim of this paper is to introduce a very complex subject, on which a great deal of literature has been published in recent years, for new researchers in the field or for those who, even if they have considerable knowledge of chemistry or technology, are interested in learning about the applications of this technology in the world of aviation.

To this end, the paper provides a general overview of the subject, from the most general concepts, defining the elements of the electrochemical cell, to the most detailed ones, reviewing the different technologies.

The aim is to present all these concepts in a general, but at the same time visual, manner. For this reason, figures and diagrams have been included to illustrate the main concepts highlighted in the paper.

Interesting previous studies are listed in the different sections of the paper. In addition, a list of 10 previous works is proposed in Section 3.2, which are useful references to extend the information on the key concepts presented in this paper. The order of the previous work included follows the outline in which some of the most important concepts are presented in this paper.

The main objective of the paper is to answer five research question. The questions have been formulated to cover the main aspects of the state-of-the-art in the use of batteries in aviation. These questions are as follows.

- What is the main element of batteries and what are their basic components?
- What list of previous works could be of interest to other researchers to present an overview of this technology, its main characteristics, and applications?
- What are the main parameters to consider for the use of batteries in aviation?
- What are the main advantages of this technology in aviation? On the other hand, what are the main challenges to overcome?
- Is it possible to present a chronological overview of the application of batteries in aviation, considering not only past experience but also future developments?

To answer the aforementioned research questions, the remainder of the paper is structured as follows. Section 2. Method presents the structure of the research developed, as well as the main expected results of each of the stages. Section 3. Results presents the outcomes of the five stages of the methodology, focusing on presenting the key concepts of battery technology in aviation. Finally, Section 4. Conclusions and future work, presents the main conclusions of the work carried out, and outlines relevant future works.

2. Method

The methodology followed in the study was to identify certain key areas to present the basic concepts of battery technology and its potential for use in aviation. The first step was to identify these key areas to properly answer the five research questions previously stated. A chronological process was then followed to address them, considering how they would be of the greatest interest to a researcher who was not familiar with the subject but was interested in learning about it. Figure 2 shows an outline of the different stages of the study. Furthermore, the stages described in the diagram correspond to the structure of the following sections of this paper.

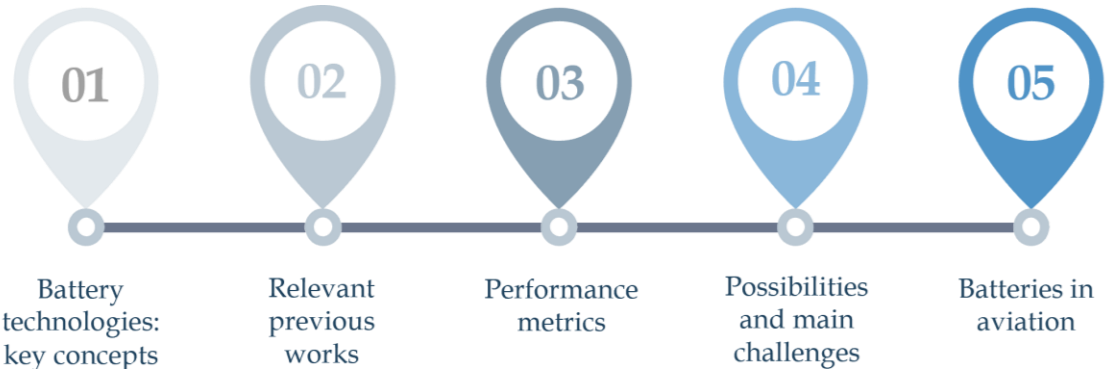

Fig. 2. Methodology followed in the study: from the key concepts of battery technologies to their use in aviation.

The first stage of the study was to define the basic concepts of a battery, in particular its basic element, the electrochemical cell. These are general aspects related to the chemistry of the cell and are common to the use of batteries in aerospace and other industries.

Battery technologies and their application in aviation are a currently well-researched topic. For this reason, many papers have been published, some of them very specific. However, it is difficult to identify certain key references that need to be read and understood before moving on to more specific topics. For this reason, it was considered relevant that one of the outcomes of the study was a set of 10 references that address key topics and can be used as a starting point before conducting further research.

There are many battery options available on the market and in development. To decide which battery is best for each application, it is necessary to compare some parameters, such as the energy density or the number of life cycles. Therefore, it was essential to include in the study an overview of these parameters and some reference values.

As mentioned in Section 1. Introduction, electric aviation has significant potential to achieve sustainability in air transport. However, to realize the full potential of battery technologies, several limitations need to be overcome. To identify the directions in which research needs to move forward, this paper identifies some of the main limitations of battery use.

Finally, the last step of the methodology was to present a chronological view of the use of batteries in aviation. First, those batteries that belong to the low-energy density category, which, although not used in electric aviation, constitute a precedent of great relevance. Then, lithium-ion batteries are included as the most promising technology in electric aviation today, and, finally, this overview presents other options currently under development to replace lithium in these batteries and limit some of their problems.

Section 3. Results is divided into five different subsections, each presenting the research results of the five stages presented and described in the methodology.

3. Results and Discussion

In this section, the answers to the five research questions considered in the study are presented in a structured and detailed manner. To this end, the research findings are divided into five different subsections, following the order in which the questions were presented.

The approach taken in this section starts with a presentation of the main elements of an electrochemical cell and continues in depth, ending with an overview of the different types of batteries that have been used or may have interesting applications in aviation.

3.1. Key concepts of battery technology

This first subsection answers the first research question. Electrochemical cells are the main element of batteries. Within these cells there are different elements that have important functions for the correct functioning of the battery.

Batteries, by definition, are electrical energy storage devices that convert chemical energy into electrical energy and can store this energy for long periods of time (Gabbar et al., 2021). The basic element of batteries is the electrochemical cell, in which chemical energy is converted into electrical energy by a reduction and oxidation (redox) reaction.

The basic structure of an electrochemical cell consists of two active materials that are used as electrodes and an electrolyte that facilitates the reaction between the cathode and the anode. The anode, cathode, electrolyte, and separator are the main elements of the electrochemical cell (Winter and Brodd, 2004). Figure 3 shows schematically the main elements of an electrochemical cell and a definition of each. The diagram shows the structure of an electrochemical cell, indicating the position of the cathode and anode and the type of reaction that takes place in each. The direction of motion of the electrons is also shown. Below the diagram, the definitions of the main elements of the electrochemical cell are presented.

In a very simplified form, batteries used in aviation consist of a series of electrochemical cells connected in series until the desired voltage is reached. They are also made up of several additional coating elements, wiring, and other elements necessary to protect them from undesirable phenomena, such as thermal runaway. The combination of all of these elements is called a battery pack.

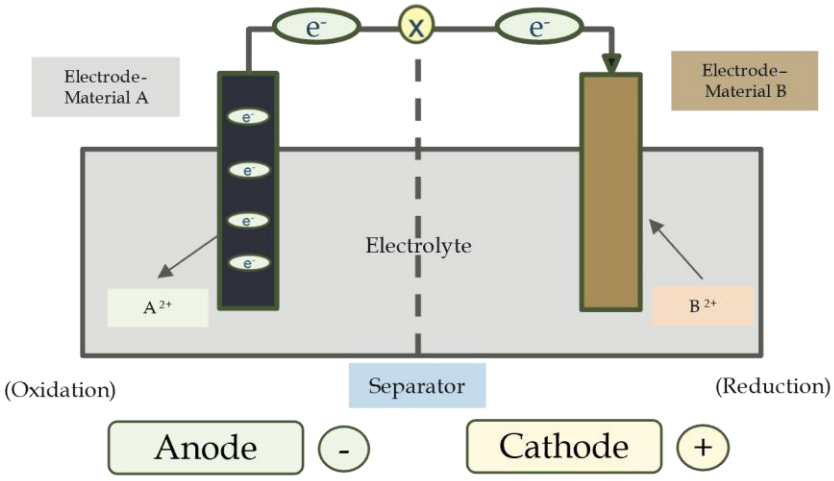

Anode	The electrode where oxidation occurs is called the anode and is negatively charged. Oxidation, i.e., the loss of electrons, takes place at the anode.
Cathode	The electrode where reduction occurs is called the cathode and is positively charged. The reduction, i.e., the gain of electrons, takes place at the cathode.
Electrodes	The electrodes are usually made of two different materials. Together they form the active material of the battery.
Electrolyte	The electrolyte is not part of the active material. Its function is to facilitate the reaction between anode and cathode through ionic conduction.
Separator	The separator is a physical barrier between the electrodes. They must be permeable to ion movement. One of their main functions is to prevent short circuits from occurring.

Fig. 3. Representation and description of the fundamental elements in an electrochemical cell. For the definition of the elements included in the figure, the main reference was (Winter and Brodd, 2004).

The electromotive force of the cell is generated by the movement of the electrodes from the anode to the cathode. In primary batteries, once the redox reaction is complete, the battery must be replaced. If the battery is rechargeable, also known as a secondary battery, this reaction can be reversed by connecting the battery to an external power source, which causes the electrodes to return to the anode and restart the reaction. Batteries of interest in electric aviation are secondary batteries.

3.2. Getting an insight into battery technology: previous relevant works

This subsection contains a list of relevant previous work. It has been included to answer the second research question, which relates to a body of previous work that could serve as a reference for other researchers. The aim is to identify several contributions that support the main concepts presented in this paper.

The aim of this paper is to explain the basic characteristics of the use of batteries as an aircraft propulsion technology. Although these concepts will be explained progressively in the sections below, it is worth giving an overview at this point to justify the interest of the references that will be presented and to help build the global vision that will be explained later.

The use of battery technology in aviation can be divided into three stages. The first corresponds to the use of low-energy density batteries used in aircraft with conventional propulsion systems. This group includes lead-acid, nickel-cadmium (Ni-Cd), and nickel-metal hydride (NiMH) batteries. Later came lithium-ion batteries (LIBs), which are used in the technology industry and in other electric vehicles.

Although lithium-ion batteries are currently the most promising option for electric aviation, they face some limitations. As a result, much research and investment are currently being made to develop batteries that

overcome the limitations of lithium-ion batteries. Some of these new batteries are already commercially available, but most are still in development.

Given the number of different batteries and the maturity of each, the research papers published on this topic are very heterogeneous. Although some provide comprehensive and detailed reviews of certain types of batteries, others present experimental results of new chemistries under development.

As a result, it is not easy for a new researcher in the field to get a comprehensive overview of the current state-of-the-art. Following detailed research, this subsection aims to overcome this limitation by presenting 10 relevant previous studies that can serve as a general reference on the key concepts and developments of battery technology.

This selection is based on an extensive prior review of papers and previous work. A total of 10 contributions were selected as a compromise from a list that was not overly extensive but included references of great interest that focused on the key concepts discussed in this paper.

These 10 papers are presented in Table 1. Each row of the table contains a different reference, the title of the publication, and the main topic addressed.

In addition to including these papers, the aim is to summarize their main contributions, to identify certain sections of their content that are of great relevance, and to identify methodologies and models of interest to be considered in further research.

The order in which they are presented in Table 1 corresponds to the structure of this paper, with the first references of a more general nature and the latter more specific to the different types of batteries.

Table 1. List of previous relevant works: reference in the study, title, and main topic addressed.

Reference	Title of the publication	Topic
(Schmidt-Rohr, 2018)	How Batteries Store and Release Energy: Explaining Basic Electrochemistry	General insights into cell electrochemistry
(Barzkar and Ghassemi, 2020)	Electric Power Systems in More and All Electric Aircraft: A Review	Electric power systems in more and all-electric aircraft
(Tariq et al., 2017)	Aircraft Batteries: Current Trend Towards More Electric Aircraft	Comparison of batteries used in aviation
(Bills et al., 2020)	Performance Metrics Required of Next-Generation Batteries to Electrify Commercial Aviation	Specific energy calculation for regional, narrow-body and wide-body aircraft
(Deng, 2015)	Li-ion: Basics, Progress and Challenges	General concepts of lithium-ion batteries
(Shen et al., 2021)	Advanced Electrode Materials in Lithium Batteries: Retrospect and Prospect	Review of electrode materials used in lithium-ion batteries
(Shahid and Agelin-Chaab, 2022)	A Review of Thermal Runaway Prevention and Mitigation Strategies for Lithium-Ion Batteries	Key ideas regarding thermal runaway in lithium-ion batteries
(Gao et al., 2022)	High-Energy Batteries: Beyond Lithium-Ion and Their Long Road to Commercialization	Detailed review of different battery alternatives to overcome the disadvantages of lithium-ion batteries
(Takada, 2013)	Progress and Prospective of Solid-State Lithium-Ion Batteries	Review on lithium-ion solid-state batteries
(Kühnelt et al., 2022)	Structural Batteries for Aeronautic Applications – State of the Art, Research Gaps and Technology Development Needs	Review on the use of batteries with dual functionality: energy storage and structural support

The first paper included in the table above is (Schmidt-Rohr, 2018). It presents the general electrochemical concepts of how batteries store energy. It also explains some key concepts that, as the author points out, are often missing from general descriptions of how cells work. A general summary of the ideas contained in the study is given in the 'Implications for Teaching' section. Of particular interest to electric aviation is the section of the paper devoted to lithium-ion batteries, which explains some of their key electrochemical characteristics.

To understand the changes to be introduced by electric aviation in terms of propulsion systems, it is essential to understand electrical power systems. For an overview of this, a great previous work is (Barzkar and Ghassemi, 2020). It explains in detail the different architectures of

electrical power systems. Also of great interest is the section of the paper entitled 'Towards All-Electric Aircraft'. In this section, additional weight of the aircraft and the development of batteries are listed as some of the main challenges that electric aircraft will have to overcome. Future research on this topic will need to evaluate these limitations.

The study published in (Tariq et al., 2017) is a good complement to the work mentioned above. When selecting a battery for electric aviation, it is of great interest to establish comparisons between the parameters of the different types. This study presents a comparison between lithium-ion, lead-acid, and nickel-cadmium batteries. It also includes a compilation table of different batteries used in aircraft throughout history. From a more quantitative point of view, the methodology proposed in the study is relevant to the cost and weight factors of nickel-cadmium and lithium-ion battery systems. This methodology distinguishes between two aspects. On the one hand the batteries and on the other hand the charger, the coating and the sensing circuits. This methodology may be of interest to other researchers who wish to develop a similar analysis with other types of batteries.

The two papers mentioned above present an overview of the use of batteries in electric aviation. The authors in (Bills et al., 2020) present the calculation of the specific energy required at the pack level to power three categories of aircraft: regional, narrow-body, and wide-body. The methodology used for the calculation is explained in detail and is accompanied by graphs and diagrams that may be of great interest to researchers. The results of the study show that, considering current developments, only next-generation battery chemistries would be able to meet all the requirements to power small regional aircraft.

As mentioned above, the commercially available batteries with the greatest potential for use in electric aviation are lithium-ion batteries. The author of (Deng, 2015) presents the basic principles of how these batteries work and reviews the characteristics of their main elements, including the cathode, anode, electrolyte, and separator. Although the reference may be outdated in terms of future predictions, it may be of great interest to other researchers to understand the basic concepts behind lithium-ion batteries and their main components.

In the general category of lithium-ion batteries, there are many different batteries depending on the cathode and anode components. The work published in (Shen et al., 2021) provides a detailed and comprehensive review of the different electrode materials used in these batteries. It distinguishes between different categories of electrodes, from the first designs, through those currently on the market, to promising materials with the aim of increasing the specific energy. In addition to its detailed review, this paper is of great interest because of the diagrams and graphs it contains, which clearly show the structure of the different materials used in the electrodes.

(Shahid and Agelin-Chaab, 2022) provides a detailed review of the risk of thermal runaway in lithium-ion batteries, including the mechanisms that initiate thermal runaway, how it propagates, and a characterization of the gases emitted from the battery. The paper explains that thermal runaway can occur as a result of various forms of mechanical, chemical, or electrical abuse of the battery. In addition to a detailed review of this phenomenon, the paper presents numerical and mathematical models for predicting thermal runaway based on previous studies. These models can be of great interest to other researchers. Finally, various strategies to prevent and mitigate thermal runaway are presented. In particular, a summary of thermal runaway prevention strategies based on previous work is shown in a table. The paper points out that one of the ways to prevent thermal runaway is to have an adequate thermal management system in place.

To the best of the authors' knowledge, (Gao et al., 2022) is the most comprehensive study focusing on the investigation of other types of batteries beyond lithium-ion to overcome their main limitations. This review proposes other active ions beyond lithium to address the cost issue of LIBs. If the aim is to increase the capacity of LIBs, conversion electrodes are proposed. Finally, to address the safety issue, beyond-liquid electrolyte batteries are proposed to avoid the high flammability problems of LIBs. For each of these categories, the different options on the market or in development, their advantages and disadvantages, and the state-of-the-art are presented. It is an excellent reference for the development of future work, combining general considerations with more specific electrochemical and manufacturing details. It also discusses the long road to commercialization of many of these innovative batteries, pointing out that there are sometimes significant differences between the theoretical performance results obtained in the laboratory and the large-scale manufacturing of these batteries. The final conclusion from all of the work presented is that lithium-ion batteries are currently the best performers in terms of energy density, cycle life, and cost. However, higher capacity alternatives are expected to co-exist with or surpass them in the 2020s.

As mentioned above, one of the solutions to overcome the safety problems of lithium-ion batteries lies in research into solid-state batteries, where the electrolyte is solid. A review of this technology is presented in (Takada, 2013). As this is a reference published several years ago, the expected developments may not be up to date. However, it is included as a relevant previous work to understand the possibilities of this technology, which

is necessary for the development of more complex batteries. The main advantages of this technology listed in the paper are the simplification of the safety mechanism of lithium-ion batteries, the possibility of simplifying the battery structure, and the possibility of incorporating new materials in the electrodes of the batteries.

Previous work has been included to highlight developments around the primary function of batteries, which is energy storage. However, there are developments in the use of batteries in aviation that aim to combine this traditional function with a complementary load-bearing function. These batteries are known as structural batteries and are the focus of (Kühnelt et al., 2022). Their advantage is that they are designed to compensate for additional weight restrictions imposed by the use of batteries in aircraft. These batteries are characterized by parameters related to their ability to store energy and also to support loads. As a conclusion of the review, it is recommended that future research address certain limitations of these batteries, focusing on materials, their integration with aircraft, testing methods, and performance monitoring.

This section presented an overview of the 10 previous relevant publications and some recommendations for further research based on them. Additionally, relevant previous studies will be cited in other sections of the paper to provide figures or more specific information on the characteristics of different types of batteries.

3.3. How to compare batteries: performance metrics

In this subsection, the main performance metrics of batteries are presented to answer the third research question. These are a series of parameters that characterize the behavior of batteries and are very useful for comparing their performance and applicability in electric aviation.

Many batteries have already been commercialized and many others are currently in development. To select the best option for each application, batteries are characterized by several key parameters, referred to by many authors as performance metrics. Although the list is extensive, the six most relevant are included in this section. First, a definition of each of them is presented and then the requirements to be met by batteries that can be used in electric aviation are specified.

The performance metrics considered are six: energy density, power density, service temperature, charging capacity, cycle life, and weight.

- Energy density. This parameter represents the amount of energy stored by the battery per unit of mass. It is considered the fundamental parameter in battery selection. The achievement of ever higher specific energy values motivates the development and research of new types of batteries. It is measured in Wh/kg.

- Power density. This parameter represents the battery's ability to deliver power quickly when required. It is measured in W/h.

- Service temperature. This parameter quantifies the temperature ranges in which the battery can operate safely. Temperature ranges are usually expressed differently for charging and discharging. It is measured in °C. According to several studies, for example (Yetik and Karakoc, 2022b), the parameter that most affects the performance, lifetime, safety, and cost of batteries is their operating temperature.

- Charging capacity. For rechargeable batteries, a parameter of great importance is their charge capacity, which quantifies the time it takes for the battery to recharge.

- Cycle life. This parameter represents the number of charge and discharge cycles that a battery can withstand without significantly affecting its performance.

- Weight. Weight is a fundamental parameter in aircraft design. It is also very important for batteries, as their additional weight can severely limit the range of the aircraft and the payload that can be carried. When evaluating the weight of a battery, it is necessary to consider not only the weight of the electrochemical cells but also the weight of the coatings and other additional systems required for the battery to function properly.

These parameters have been selected as the most relevant for the selection of batteries for aircraft use. However, the list of parameters to be considered to explain the specifications of a battery is much longer. An example of these specifications can be found in (MIT Electric Vehicle Team, 2008). After a general presentation of the concepts associated with performance metrics, Figure 4 presents their specific requirements for the use of batteries as a propulsion system for electric aircraft.

The performance metrics presented in this section are essentially technical, related to the design and configuration of electrochemical cells and battery packs. However, to compare and select batteries for different aeronautical applications, it is essential to consider some additional parameters.

The first of these refers to the materials used in the battery design. Some promising battery options contain rare earth elements, the extraction of which may have a significant impact or pose a problem for the scalability of the technology. In this context, it is important to consider the safety and environmental impacts of the battery throughout its life cycle, from the extraction of raw materials to recycling at the end of its service life.

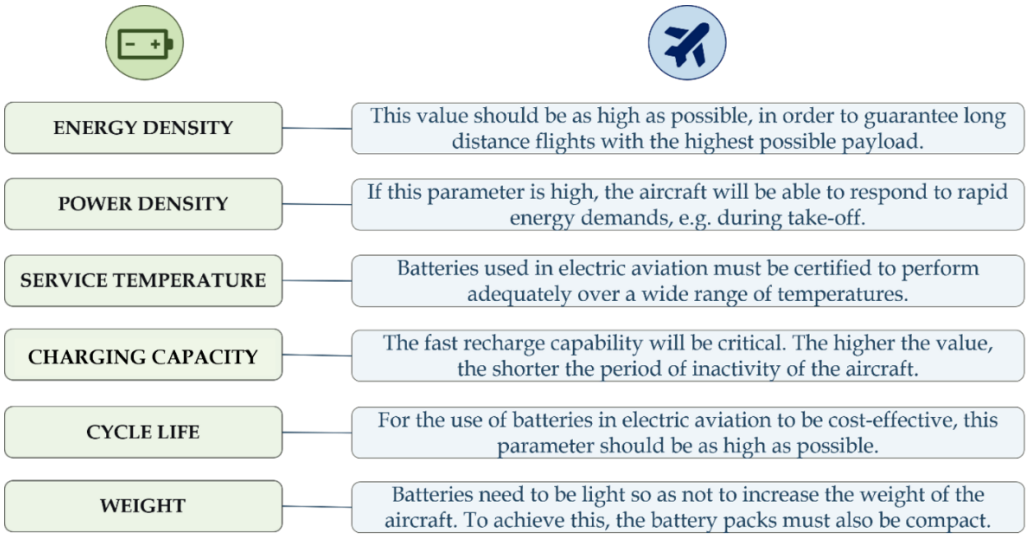

Fig. 4. Key performance metrics of batteries to be met for their use in electric aviation: energy density, power density, service temperature, charging capacity, cycle life, and weight.

3.4. Possibilities and limitations of the use of batteries in electric aviation

The fourth research question posed at the beginning of this paper related to the opportunities and main challenges of using batteries in aviation. After presenting the chemistry of batteries at the cell level and the main performance metrics used to characterize and compare them, this subsection summarizes the main opportunities and challenges for the use of batteries in aviation.

As mentioned in previous sections, the great potential of batteries in aviation is that they are an enabling technology for more-electric and all-electric aircraft. Using this propulsion technology, it is possible to reduce dependence on fossil fuels, limit the noise impact of operations, and reduce in-flight emissions compared to other propulsion technologies.

Figure 5 presents an overview of the potential of batteries in aviation electrification. The upper part of the figure highlights the main rationale for the electrification of aviation and the objectives to be achieved, such as reducing greenhouse gases, eliminating dependence on fossil fuels, and reducing environmental impact. In the lower part of the figure, the two approaches that consider the application of battery technologies to achieve this are presented. These two alternatives are the direct use of battery technologies and their use in collaboration with other technologies in hybrid-electric configurations.

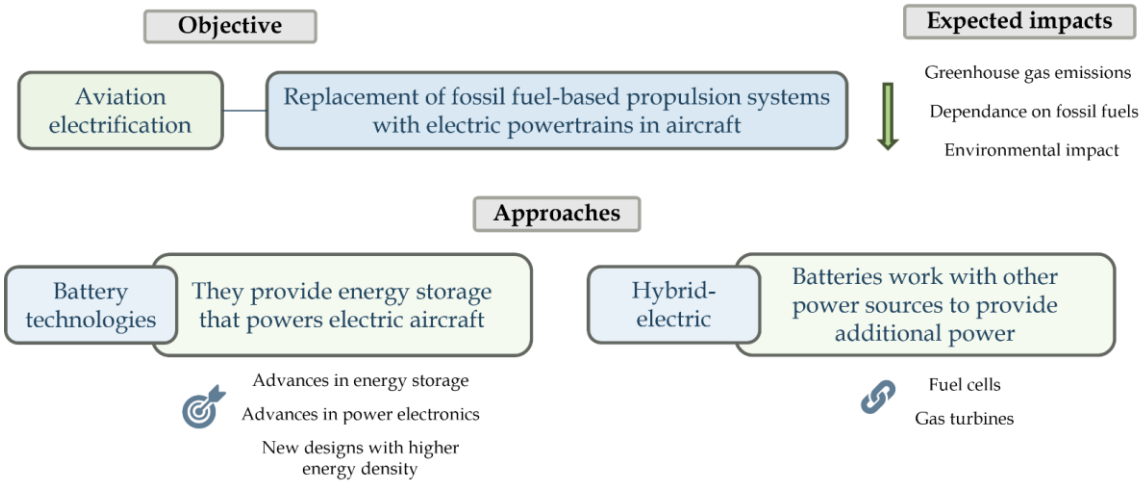

Fig. 5. Possibilities of battery technologies for electric aviation: objective, expected impacts and approaches.

Batteries themselves can be used as a propulsion technology. Scaling-up of this technology will require innovation in several areas. These include advances in energy storage, power electronics, and new chemistries of batteries to achieve higher energy densities.

There is also an intermediate option, hybrid-electric propulsion, in which batteries work with other energy systems to provide electric power. In these cases, batteries could work in conjunction with fuel cells or gas turbines.

The use of batteries in aviation represents a great opportunity and a breakthrough towards greener aviation. However, this technology will have to overcome several challenges. Although each type of battery has its own limitations, some general aspects are presented in this subsection.

These challenges are shown schematically in Figure 6. These challenges can be grouped into two categories. The first group of challenges is related to battery design. These include achieving sufficient energy densities, achieving designs that are sufficiently light, thermally stable, with high cycle life, or preventing thermal runaway. A second category of challenges relates to the difficulties in scaling-up the use of batteries as a propulsion system. Challenges related to maintenance, raw materials used and other impacts on the battery life cycle are included in this category.

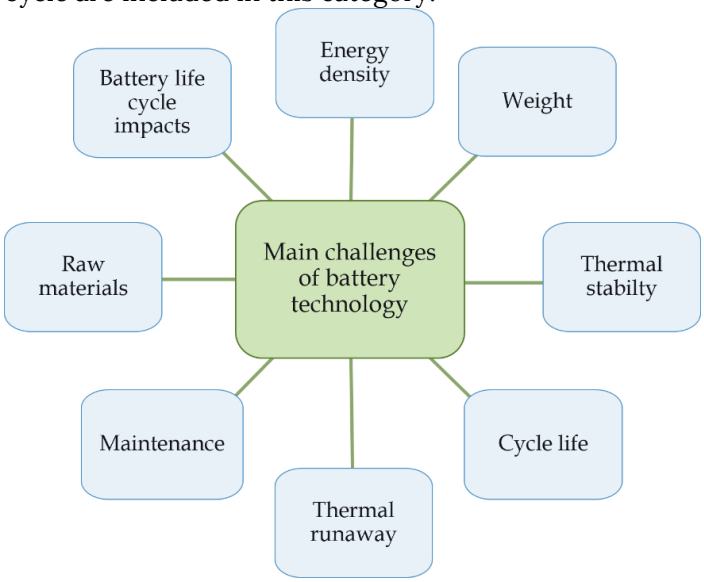

Fig. 6. Main challenges of battery technologies related to their design (energy density, weight, thermal stability, cycle life and thermal runaway) and the scalability of this technology (maintenance, raw materials, and battery life cycle impacts).

The most limiting performance metric in terms of the distance the aircraft can fly and the payload it can carry is energy density. Therefore, it is not surprising that it is the most important factor in battery selection. The trend in research is towards higher energy density batteries. A fundamental aspect to consider is that high values of this parameter are often obtained at a theoretical level. In practice, however, these values are significantly reduced during the manufacturing process compared to laboratory studies.

Another key constraint is weight. As in the case of an aircraft, batteries should be as light as possible. The problem is that weight is often the trade-off to solve other problems. For example, additional materials can be included in the battery pack to mitigate overheating. Therefore, while improving safety, this increases the overall weight of the pack, in turn limiting the range and payload of the aircraft.

Another important challenge is thermal stability. One of the specific requirements for batteries to be used in aviation is the wide range of temperatures to which the aircraft is exposed during flight. These temperature changes can affect battery performance and alter the chemical reactions involved. It is important to monitor the temperature of the batteries to ensure that they function properly. If the limits of the battery's operating temperature range are exceeded, the battery life may be shortened. Additionally, undesirable situations, such as fire, may occur (Yetik, 2020).

As mentioned above, batteries of interest for electric aircraft applications are rechargeable batteries. For their use in aviation to be cost-effective, they must be able to withstand a large number of charge and discharge cycles. As will be seen below, some of the most promising compositions (e.g., lithium-sulfur or lithium-air) present certain recharging limitations, which result in shorter life cycles than desired.

The fundamental safety issue with some batteries is thermal runaway. Specifically, this is a major problem in lithium-ion batteries. This is a process associated with overheating of one of the electrochemical cells as a result of various triggers. If this first stage is not controlled, the cell separator will degrade, making the problem worse and extending it to other cells connected in series in the battery (Shahid and Agelin-Chaab, 2022). In the third stage, the electrolyte burns, which can lead to explosions. For this reason, it is very important to develop mathematical models that address the propagation of thermal runaway and to design mitigation measures to be implemented during the first stage of this phenomenon.

Maintenance will be a key element to ensuring battery safety. To this end, it will be essential to establish procedures for monitoring the state of charge of batteries and implement battery management systems (BMS) that evaluate key battery parameters to schedule maintenance tasks accordingly.

The raw materials needed for battery manufacturing are a major challenge. Some solutions with great potential require the use of rare earth elements. This is associated with an increase in environmental impact and in the energy used to manufacture batteries. Another related issue is the availability of some of these materials. Lithium is an example. For this reason, alternative materials must be sought for their design. A third issue related to raw materials is the political or social conflicts that arise from their extraction. An example of this challenge is the mining of cobalt. These issues apply not only to the materials used in the manufacturing of the electrochemical cell but also to the battery management systems and the battery pack.

There are several environmental impacts throughout the battery life cycle. These range from mining for some of the raw materials to recycling at the end of its service life. Modeling and trying to mitigate these impacts are two of the major challenges in scaling-up the use of this technology.

A major challenge that combines the above is the certification of these new propulsion architectures. Standards and certification procedures will need to adapt to these technological developments. Although progress has been made in recent years, many challenges remain. In addition to the technical certification of the battery life cycle itself, certification of other elements of the system, such as infrastructure or personnel, will be required. A previous work of great interest in this aspect is (Yildiz, 2022). It provides a detailed review of the progress made in the certification of electrical aircraft architectures. It also identifies various limitations of current standards and some gaps that need to be addressed. An example of this is the certification process for large aircraft with electric architectures. In addition, this study proposes a new definition of common unit to simplify the hybrid electric propulsion architecture of commercial aircraft, with a positive impact on the certification process.

3.5. Battery technology in aviation: past, present, and future

The previous sections have provided an overview of the use of batteries in aviation, including relevant studies and an analysis of their performance metrics, possibilities, and challenges. This section aims to integrate all the above and provide an overview of the specific batteries used in aviation, including the past, present, and expected future technologies used. The chronological overview of the use of batteries in aviation presented in this section allows the fifth and final research question to be answered. This chronological overview ranges from the first batteries used in aviation a few decades ago to new developments with great potential for the electrification of aviation.

Figure 7 shows the categorization of the batteries that will be presented in this section: low-energy density batteries, lithium-ion batteries, and beyond-lithium-ion batteries. The three categories shown in the diagram, from left to right, correspond to the chronological development of the three types of batteries described. Low-energy density batteries have been used in aircraft throughout the 20th century. Lithium-ion batteries emerged in the 1990s to revolutionize the technology industry and are now being used in electric vehicles. Beyond-lithium-ion batteries are currently under development to overcome the drawbacks of lithium-ion batteries. Most of the batteries in this group are still in the development stage or have been commercialized on a very small scale.

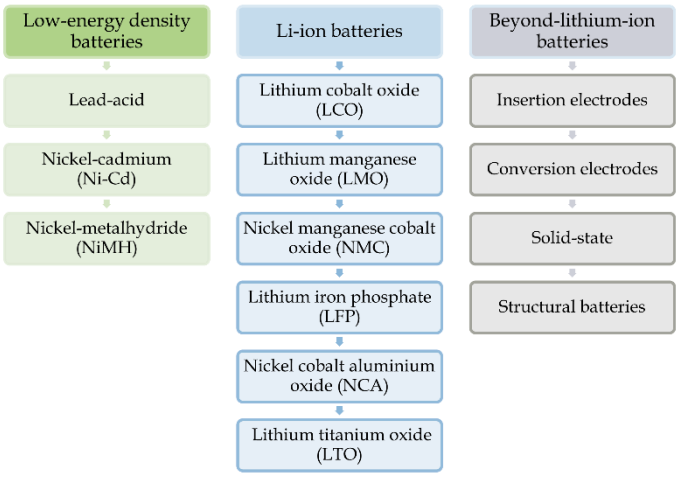

Fig. 7. Overview of batteries used in aviation over the years and those under development for future use: low-energy density batteries, lithium-ion batteries, and beyond-lithium-ion batteries.

The first batteries to be considered are those with low-energy density. This category includes batteries that are not suitable for use in electric aircraft but have been used regularly in aircraft with conventional propulsion systems.

The first group in this category is lead-acid batteries. They have low specific energy values but high specific power, which is useful for starting engines. This was their main application before they were replaced by Ni-Cd and lithium-ion batteries.

The second category is Ni-Cd batteries, which became commercially available in the 1950s. They can operate at higher charge and discharge rates than the former. However, they are more expensive and have a lower specific power. They have been used in aviation as the main aircraft battery for engine ignition, auxiliary power units, and emergency power ("Aircraft Batteries," 2023).

The latest batteries in this category are nickel-metal-hydride batteries, which were introduced in the late 1980s. They are more expensive than lead-acid batteries but have comparatively higher values for specific energy, specific power, cycle life, and, most importantly, recyclability ("Aircraft Batteries | SKYbrary Aviation Safety," n.d.).

A comparison of some key performance metrics has been made based on the information consulted in (Liu et al., 2018). Lead-acid batteries have an energy density of 30-50 Wh/kg and between 200 and 400 cycle life. Nickel-cadmium batteries have a specific energy of 45-80 Wh/kg and 500-1000 cycle life. Finally, NiMH batteries have a specific energy of 60-120 Wh/kg and 300-500 cycle life.

Lithium-ion batteries were introduced in the 1990s to improve performance in terms of energy density. Their operation is explained in detail in (Deng, 2015). The main idea is as follows. These batteries consist of a cathode and an anode connected by an electrolyte containing lithium ions. The battery is assumed to be assembled in

a discharged state. During the charging process, the electrodes are connected externally to an electrical source. The electrodes are released at the cathode and move externally towards the anode. Lithium ions move in the same direction, but inside the battery. The discharge process is the opposite.

These batteries have been used in most modern generations of commercial aircraft. The most famous example is its use in the Boeing 787 and the overheating problems that these batteries have suffered (Williard et al., 2013). They are also the frontrunners for use in electric aircraft in the coming years. There are many studies that present the development of hybrid aircraft using lithium-ion batteries for different uses and applications (Farsi and Rosen, 2023).

Within the lithium-ion battery category, there are different batteries with different characteristics. Figure 7 shows the main types. The first five are named after the abbreviations of their cathode materials. The last one is found in the carbon-based anode material options. The performance metrics of each type vary considerably. As an example, specific energy and cycle life values are presented for comparison with low-energy density batteries. In ("Batteries in a Portable World," 2017) it was reported that the energy density and cycle life values for the different cathode material alternatives are as follows. LCO batteries have specific energies between 150 and 200 Wh/kg and between 500 and 1000 cycle life. For LMO the values are specific energies between 100 and 150 Wh/kg and between 300 and 700 cycle life. For NMC, the values are higher, with specific energies between 150 and 220 Wh/kg and between 1000 and 2000 cycle life. LFPs have specific energies between 90 and 120 Wh/kg and more than 2000 cycle life. Finally, NCAs have energy densities between 200 and 280 Wh/kg and 550 cycle life. Of the anode options, LTOs have the advantage of a much longer cycle life. According to ("All About Batteries, Part 12", 2015), their specific energy is between 50 and 80 Wh/kg, but the number of cycles increases to between 3000 and 7000. All cycle life values are at 80% battery depth of discharge (DOD).

However, in view of the large-scale scalability of battery technologies expected in the coming years, lithium-ion batteries have some drawbacks. These include insufficient specific energy, the price of lithium, problems with material depletion, and safety problems due to short circuits or overheating that can lead to thermal runaway. For this reason, alternatives to lithium-ion batteries have been extensively researched in recent years. Some of these alternatives are presented below.

To replace lithium, the first option is to keep the working principle of lithium-ion batteries but substitute the lithium with other materials with similar properties in the periodic table. These are so-called insertion-electrode batteries with ions other than lithium. These ions include magnesium (Mg), aluminum (Al), sodium (Na), zinc (Zn), potassium (K), and calcium (Ca). (Gao et al., 2022) provides a detailed review of each of these options, analyzing their advantages and limitations from an electrochemical point of view. In summary, sodium ions are the most similar to lithium ions. However, apart from cost savings, they have the same problems as lithium-ion batteries. As demand for lithium-ion batteries increases, the relative price of lithium-ion batteries decreases, so the advantage is less significant.

Another alternative is the use of conversion electrode batteries. Unlike insertion-electrode batteries, conversion electrode batteries undergo significant structural changes in the electrode materials during the redox reaction. Within this group, there are two main promising battery types: lithium-sulfur (Li-S) batteries and lithium-air batteries.

Li-S batteries have undergone significant development during the 2010s, with important progress made at the laboratory level (Zhao et al., 2020). These batteries have theoretical potential to improve current lithium-ion batteries by about five to six times in terms of specific energy and specific capacity (Arote, 2022).

Another chemistry with great potential is lithium-air batteries. According to (Ding et al., 2023), the development of these solid-state batteries with a very high energy density would allow their use in electric vehicles for long-distance travel.

Some of the key previous works cited in Section 3.2 present these batteries as one of the most promising technologies. For example, (Barzkar and Ghassemi, 2020) points out that the specific energy of jet fuel is 12000 Wh/kg. For comparison, the equivalent figure for lithium-ion batteries is 250 Wh/kg, so further research is needed on higher energy density alternatives. Li-air batteries with a specific energy of 2000 Wh/kg are mentioned as potential batteries for use in electric propulsion systems.

Additionally, in the study on the performance metrics required to power different types of aircraft included in (Bills et al., 2020), Li-air batteries are presented as those whose progress could make it possible to power small regional aircraft, for which the average specific energy requirement has been set at 600 Wh/kg-pack.

The development of some of these batteries, such as the Li-S and lithium-air batteries mentioned above, is also dependent on the development of solid electrolytes. Current requirements for batteries used in electric aviation require larger batteries, an application for which solid-state batteries are essential. Furthermore, because their electrolyte is solid, they have other advantages, such as no electrolyte leakage, no vaporization problems, and longer cycle life, as well as increased safety due to the elimination of electrolyte flammability problems (Takada, 2013).

Compared to other novel configurations under study, structural batteries are cutting-edge technology. The idea is to reduce the extra weight associated with the use of batteries so that they fulfill a dual function: energy storage and structural bearing. In this case, in addition to the standard performance metrics, others are used to characterize the load-bearing function of batteries. Among these, Young's modulus is beginning to be considered as the most representative (Kühnelt et al., 2022).

As outlined in this section, there are many battery developments with potential applications in aviation. At present, lithium-ion batteries are the most promising in the short term, but future development of other alternatives, particularly those based on conversion electrodes, could represent a major leap forward in terms of the scalability of this technology.

Throughout this subsection, the main characteristics of each type of battery have been presented according to their chemical composition and main properties. As a final remark, it is of interest to highlight some ideas on the characteristics presented.

- For many batteries currently under development, the values obtained in the various studies and tests are theoretical or can only be obtained under laboratory conditions. For industrial production, therefore, the values of the parameters may be affected.
- When choosing one type of battery over another, it is necessary to consider the whole system. Depending on the configurations used, some batteries that present lower values for some parameters at the cell level can improve their performance. In addition to the cell-level components, the battery pack consists of several additional elements. Examples include the cooling system, isolation components, or electrical connections.
- Although some battery configurations present better characteristics than others, it will be necessary to consider more than just technical aspects for future development. Examples of these parameters have been mentioned in previous sections of the paper. Examples include the use of rare earth materials, the availability of materials used in their manufacturing, safety considerations, certification, or the environmental impact of the battery life cycle.

4. Conclusions and Future Work

The aviation industry has a strong commitment to sustainability. Electrification of aviation is one of the most innovative approaches to achieve this. Batteries are presented as an enabling technology for this paradigm shift. This paper presents an overview of the use of batteries in aviation, covering five fundamental topics.

First, a general overview of the chemistry behind an electrochemical cell, the basic element of the battery, is presented. The important elements at cell level are the electrodes, the electrolyte, and, if present, the separator. It is within these cells that redox reactions occur.

With so many battery technologies under development, the literature on the subject is extremely large and heterogeneous. This can be a problem for new researchers in the field. Therefore, as part of this work, 10 key papers have been identified to provide an overview of the use of batteries in aviation. Their main contributions have been explained, and recommendations for other authors have been included.

As the existing batteries are many and varied, it is necessary to define a set of performance metrics to compare them and select the most suitable for each application. These performance metrics have been defined in the paper and their requirements for batteries to be used in electric aviation have been indicated.

The potential of this technology is linked to a reduced environmental impact and dependence on fossil fuels. However, to scale it up, several constraints need to be overcome. Eight of these have been presented and analyzed: energy density, weight, thermal stability, cycle life, thermal runaway, maintenance, raw materials, and battery life cycle impacts

Finally, considering all these concepts, an overview of the batteries used in aviation has been presented, divided into three different groups. The first group consists of low-energy density batteries, which have been used for various purposes throughout the 20th century. Lithium-ion batteries are the main batteries that will be used in electric aviation in the coming years. However, important work is being done to develop safer, lower cost or higher specific energy alternatives. These include other insertion-electrode batteries, conversion electrode batteries, solid-state batteries, and structural batteries. The development of these latter prototypes will undoubtedly be essential to scale-up the technology and achieve a more sustainable aviation.

Future work will be directed towards further investigation of each of the battery types and finding detailed information on their performance metrics. Developing a complete a comparison between them as possible will be the ultimate objective.

In later stages of the research, a detailed study will be necessary that involves the evaluation of the battery system as a whole. In this first stage of research, a classification of batteries has been made based on their electrochemistry. However, to select the best batteries to be used in different types of aircraft, it will be necessary to consider other important elements of the system beyond the electrochemical cell. These include: the battery management system, the electrical connections, the isolation system, the location of the batteries within the aircraft, or the redundancy systems that will need to be implemented in the event of battery failure.

Nomenclature

Al	: Aluminium
BMS	: Battery Management System
Ca	: Calcium
CO2	: Carbon Dioxide
DOD	: Depth of Discharge
EFACA	: Environmentally Friendly Aviation for All Classes of Aircraft
K	: Potassium
LCO	: Lithium Cobalt Oxide
LFP	: Lithium Iron Phosphate
LIBs	: Lithium-Ion Batteries
Li-S	: Lithium-Sulfur Batteries
LMO	: Lithium Manganese Oxide
LTO	: Lithium Titanium Oxide
Mg	: Magnesium
Na	: Sodium
NCA	: Nickel Cobalt Aluminum Oxide
NMC	: Nickel Manganese Cobalt Oxide
Ni-Cd	: Nickel-Cadmium
NiMH	: Nickel-Metal-Hydride Batteries
SAF	: Sustainable Aviation Fuels
S	: Sulfur
UAM	: Urban Air Mobility
WP	: Work Package
Zn	: Zinc

CRediT Author Statement

María Zamarreño Suárez: Conceptualization, Methodology, Investigation, Data Curation, Visualization, Writing-Original Draft. **Francisco Pérez Moreno**: Methodology, Data Curation, Visualization, Writing – Review and Editing. **Raquel Delgado-Aguilera Jurado**: Data Curation, Visualization, Writing – Review and Editing. **Rosa María Arnaldo Valdés**: Conceptualization, Supervision, Funding Acquisition, Writing – Review and Editing. Víctor **Fernando Gómez Comendador**: Supervision, Project Administration, Fundinc Acquisition, Writing – Review and Editing.

References

Aircraft Batteries, (2023). . Aircraft Systems. URL http://www.aircraftsystemstech.com/2017/06/aircraft-batteries.html (accessed 11.5.23).

Aircraft Batteries | SKYbrary Aviation Safety [WWW Document], n.d. URL https://skybrary.aero/articles/aircraft-batteries (accessed 11.5.23).

Arote, S.A., (2022). Fundamentals and perspectives of lithium–sulfur batteries, in: Lithium-Ion and Lithium–Sulfur Batteries: Fundamentals to Performance. IOP Publishing. https://doi.org/10.1088/978-0-7503-4881-2ch3

Barzkar, A., Ghassemi, M., (2020). Electric Power Systems in More and All Electric Aircraft: A Review. IEEE Access 8, 169314–169332. https://doi.org/10.1109/ACCESS.2020.3024168

Batteries in a Portable World: A Handbook on Rechargeable Batteries for Non-Engineers, Fourth Edition by Isidor Buchmann: new (2017) 4th. | My Books Store [WWW Document], 2017.

Battery 2030+ project, (2023). B-2030-Science-Innovation-Roadmap-updated-August-2023.pdf.

Bills, A., Sripad, S., Fredericks, W.L., Singh, M., Viswanathan, V., (2020). Performance Metrics Required of Next-Generation Batteries to Electrify Commercial Aircraft. ACS Energy Lett. 5, 663–668. https://doi.org/10.1021/acsenergylett.9b02574

Deng, D., (2015). Li-ion batteries: basics, progress, and challenges. Energy Science & Engineering 3, 385–418. https://doi.org/10.1002/ese3.95

Ding, Y., Li, Y., Wu, Z.-S., (2023). Recent advances and challenges in the design of Li–air batteries oriented solid-state electrolytes. Battery Energy 2, 20220014. https://doi.org/10.1002/bte2.20220014

EFACA project, (2023). EFACA – Environmentally Friendly Aviation for all Classes of Aircraft. URL https://efaca.eu/ (accessed 11.1.23).

Epstein, A.H., O'Flarity, S.M., (2019). Considerations for Reducing Aviation's CO2 with Aircraft Electric Propulsion. Journal of Propulsion and Power 35, 572–582. https://doi.org/10.2514/1.B37015

Farsi, A., Rosen, M.A., (2023). Performance analysis of a hybrid aircraft propulsion system using solid oxide fuel cell, lithium ion battery and gas turbine. Applied Energy 329, 120280. https://doi.org/10.1016/j.apenergy.2022.120280

Gabbar, H.A., Othman, A.M., Abdussami, M.R., (2021). Review of Battery Management Systems (BMS) Development and Industrial Standards. Technologies 9, 28. https://doi.org/10.3390/technologies9020028

Gao, Y., Pan, Z., Sun, J., Liu, Z., Wang, J., (2022). High-Energy Batteries: Beyond Lithium-Ion and Their Long Road to Commercialisation. Nano-Micro Lett. 14, 94. https://doi.org/10.1007/s40820-022-00844-2

Gössling, S., Dolnicar, S., (2023). A review of air travel behavior and climate change. WIREs Climate Change 14, e802. https://doi.org/10.1002/wcc.802

Kühnelt, H., Beutl, A., Mastropierro, F., Laurin, F., Willrodt, S., Bismarck, A., Guida, M., Romano, F., (2022). Structural Batteries for Aeronautic Applications—State of the Art, Research Gaps and

Technology Development Needs. Aerospace 9, 7. https://doi.org/10.3390/aerospace9010007

Liu, X., Li, K., Li, X., (2018). The Electrochemical Performance and Applications of Several Popular Lithium-ion Batteries for Electric Vehicles - A Review, in: Li, K., Zhang, J., Chen, M., Yang, Z., Niu, Q. (Eds.), Advances in Green Energy Systems and Smart Grid, Communications in Computer and Information Science. Springer Singapore, Singapore, pp. 201–213. https://doi.org/10.1007/978-981-13-2381-2_19

MIT Electric Vehicle Team, (2008). A Guide to Understanding Battery Specifications. Retrieved from: http://web.mit.edu/evt/summary_battery_specifications.pdf

Moua, L., Roa, J., Xie, Y., Maxwell, D., (2020). Critical Review of Advancements and Challenges of All-Electric Aviation, in: International Conference on Transportation and Development 2020. Presented at the International Conference on Transportation and Development 2020, American Society of Civil Engineers, Seattle, Washington (Conference Cancelled), pp. 48–59. https://doi.org/10.1061/9780784483138.005

Ranasinghe, K., Guan, K., Gardi, A., Sabatini, R., (2019). Review of advanced low-emission technologies for sustainable aviation. Energy 188, 115945. https://doi.org/10.1016/j.energy.2019.115945

Schmidt-Rohr, K., (2018). How Batteries Store and Release Energy: Explaining Basic Electrochemistry. J. Chem. Educ. 95, 1801–1810. https://doi.org/10.1021/acs.jchemed.8b00479

Shahid, S., Agelin-Chaab, M., (2022). A review of thermal runaway prevention and mitigation strategies for lithium-ion batteries. Energy Conversion and Management: X 16, 100310. https://doi.org/10.1016/j.ecmx.2022.100310

Shen, X., Zhang, X.-Q., Ding, F., Huang, J.-Q., Xu, R., Chen, X., Yan, C., Su, F.-Y., Chen, C.-M., Liu, X., Zhang, Q., (2021). Advanced Electrode Materials in Lithium Batteries: Retrospect and Prospect. Energy Material Advances 2021. https://doi.org/10.34133/2021/1205324

Takada, K., (2013). Progress and prospective of solid-state lithium batteries. Acta Materialia 61, 759–770. https://doi.org/10.1016/j.actamat.2012.10.034

Tariq, M., Maswood, A.I., Gajanayake, C.J., Gupta, A.K., (2017). Aircraft batteries: current trend towards more electric aircraft. IET Electrical Systems in Transportation 7, 93–103. https://doi.org/10.1049/iet-est.2016.0019

Williard, N., He, W., Hendricks, C., Pecht, M., (2013). Lessons Learned from the 787 Dreamliner Issue on Lithium-Ion Battery Reliability. Energies 6, 4682–4695. https://doi.org/10.3390/en6094682

Winter, M., Brodd, R.J., (2004). What Are Batteries, Fuel Cells, and Supercapacitors? Chem. Rev. 104, 4245–4270. https://doi.org/10.1021/cr020730k

Yetik, O., (2020). Thermal and electrical effects of basbars on Li-Ion batteries. International Journal of Energy Research 44, 8480–8491. https://doi.org/10.1002/er.5533

Yetik, O., Karakoc, T.H., (2022a). A study on lithium-ion battery thermal management system with Al2O3 nanofluids. International Journal of Energy Research 46, 10930–10941. https://doi.org/10.1002/er.7893

Yetik, O., Karakoc, T.H., (2022b). Thermal and electrical analysis of batteries in electric aircraft using nanofluids. Journal of Energy Storage 52, 104853. https://doi.org/10.1016/j.est.2022.104853

Yetik, O., Karakoc, T.H., (2021). Estimation of thermal effect of different busbars materials on prismatic Li-ion batteries based on artificial neural networks. Journal of Energy Storage 38, 102543. https://doi.org/10.1016/j.est.2021.102543

Yildiz, M., (2022). Initial airworthiness requirements for aircraft electric propulsion. Aircraft Engineering and Aerospace Technology 94, 1357–1365. https://doi.org/10.1108/AEAT-08-2021-0238

Zhao, M., Li, B.-Q., Zhang, X.-Q., Huang, J.-Q., Zhang, Q., (2020). A Perspective toward Practical Lithium–Sulfur Batteries. ACS Cent. Sci. 6, 1095–1104. https://doi.org/10.1021/acscentsci.0c00449